

Heat in anaerobic digestion

Temperature inhibition and heat transfer integration with anaerobic digestion modelling

Sjoerd Heegstra



Heat in anaerobic digestion

Temperature inhibition and heat transfer integration with anaerobic digestion modelling

by

Sjoerd Heegstra

Student Name	Student Number
S.H. Heegstra	5281717

to obtain the degree of Master of Science
at the Delft University of Technology,
to be defended publicly on November 22, 2022 at 13:00.

Assessment committee

Chair:	R.E.F. Lindeboom
2 nd assessor:	M.K. de Kreuk
3 rd assessor:	L.C. Rietveld

Daily supervisors

P.C. Chafra
A. Moradvandi

Preface

This thesis culminates the two years of my master's education in environmental engineering. Looking back on it now, it has been one of the most challenging but enriching experience of my life. For the past 10 months, I have been obsessed with anaerobic digestion, modelling and lab work, which has all led to this report. Many days were filled with finding a single wrong character in my code or redoing the same experiment over and over in the lab, but I have enjoyed it tremendously. I'm therefore deeply grateful to everyone who was a part of this process, both professionally and personally.

First I want to thank my thesis committee, Ralph Lindeboom, Merle de Kreuk and Luuk Rietveld, for all the guidance you've given me over the course of this project. I think every student feels lost at the beginning of their thesis project, but you were always able to navigate me to the next milestone. Thank you Ralph, for all your expertise, enthusiasm and encouragement during our meetings. I always left your office with more excitement and certainty about my work, which helped tremendously in seeing the value. Thank you too Merle, for the in-depth feedback and interest in the project. Furthermore, I really appreciated all the work you do for the entire master program, and your ability to still always find time for every individual students. Thank you Luuk, for your critical observations and suggestions throughout the entire process. They have helped me to stay focused on viable subjects and the practical implications of the research, and to round up the whole project into something worthwhile for both me and La Trappe.

But the biggest thanks go to my daily supervisors, Ali Moradvandi and Pamela Chafra. You were always available for my endless questions and uncertainties, and your help has made this whole thesis possible. I can not thank you enough for your guidance and warmth. Thank you Pamela, for all your patience with me in the lab. As a student of covid times, I have never done a Hach test before starting this thesis, and you have helped me to gain confidence in my own work, and showed me how to teach myself new skills as well. Thank you Ali, for your open door policy, both during the creation of my model as well as with the writing of this report. You have helped me more than you know, as often when I got stuck, I would prepare some questions to ask you, but by writing these questions out I already found solutions. Classic rubber duck debugging, but knowing that you were just down the hall helped me feel supported and less alone at these times and in the whole project.

A huge thank you to all my fellow students from the Dispuut, who I have had the pleasure of meeting in the past two years. I truly feel blessed with the friendships I've developed here. Thank you for getting me through the hardest period of my life, with lockdown, a broken wrist and a house where I did not feel at home. You guys have kept me going where I would otherwise have broken down. Furthermore, the past months at the afstudeerhok have made something which many students dread into a truly enjoyable experience, and I do not jest when I say that I will miss these times. I also want to thank my family and girlfriend, who have supported me through the whole process, and were kind enough to act interested when I had another rant about how cool I thought my model was. I'm so fortunate to have you in my life.

With the finishing of this thesis, I truly feel like I'm ending the chapter of my early life, and start a new phase as an adult. I think this project has helped me feel more responsible, professional and capable, and it is with this attained feeling that I am ready for whatever comes next.

*Sjoerd Heegstra
Delft, November 2022*

Summary

Interest in biogas has increased due to natural gas shortages and the energy transition. Most digesters in the EU have internal heating for process stability. Unheated reactors could potentially lower costs, but have decreased kinetics due to low operational temperatures, especially in winter. This raises the question how seasonal temperature fluctuations affect biogas production. If this effect could be incorporated in current models such as the Anaerobic Digestion Model no.1 (ADM1), scenarios could be compared to investigate when heating is worthwhile.

In this thesis, an extension is created to the ADM1 in Python to predict the operational temperature and its effects on the anaerobic digestion process. To lower the stiffness of the ADM1, different pH calculation methods were compared. These methods and the used Python version of the model were validated by digestion of the Benchmark Simulation Model 2 (BSM2) ADM1 influent. It was found that the combination of the Differential Algebraic Equation (DAE) with the Radau numerical solving method produced the smallest errors with the lowest computational burden.

A heat-transfer model was included, which calculates bulk liquid temperature as a function of weather data, digester design and some operational factors. A One-At-a-Time (OAT) sensitivity analysis showed the dependence of yearly temperature fluctuations on several design and operational parameters.

The calculated operational temperature is coupled to the ADM1 through several temperature inhibition functions for biochemical processes. Furthermore, the dependency of the liquid-gas transfer coefficient was investigated. It was found that this last step in biogas production could potentially become rate-limiting at temperatures lower than 30 °C, but this result was not validated.

The coupled heat transfer - ADM1 model is used to study the case of an unheated fixed-dome reactor for the co-digestion of spent wort and Waste Activated Sludge (WAS) of the La Trappe brewery in the Netherlands. The influent substrate concentrations were determined by a biochemical fractionation procedure, and the model was able to simulate methane production curves found in Biochemical Methane Potential (BMP) experiments. Simulations of digestion for the La Trappe case showed seasonality in biogas production, increasing in summer and decreasing in winter. The extent of the effect was found to be dependent on substrate composition, with lipid-rich substrates being affected more than carbohydrate- or protein-rich substrates. Furthermore, the simulation showed seasonality in rate-limiting step, with hydrolysis in summer and methanogenesis in winter. This caused the pH to lower with winter, and it was found that higher base dosage is needed in colder winters to prevent acidification. Higher influent temperatures improved process stability, lowered amounts of base needed and increased biogas production.

Furthermore, the relation between temperature and volume showed that washout of methanogens and consequent VFA accumulation is dependent on the absolute temperature inhibition function for acetoclastic methanogens. Simulation of the digestion of BSM2 influent showed that the maximum Organic Loading Rate (OLR) increased with temperature till 30 °C, but decreased above this point as free ammonia inhibition starts to limit methanogenic metabolism. For La Trappe, OLR determines the needed base dosage, allowing smaller volumes if more base is added. Lastly, internal heating with the produced biogas was investigated, and optimal heating for biogas production was found.

The found results from the model were used to assess the costs and benefits of several design and operational options for the digester at La Trappe. This digester will be used in future research for validation of the model.

Contents

Preface	i
Summary	ii
Nomenclature	v
1 Introduction	1
1.1 Anaerobic degradation process	1
1.2 Temperature dependency	2
1.3 Household reactors	3
1.4 Problem statement	4
1.5 La Trappe as a case-study	4
1.6 Research question	5
2 Background literature	6
2.1 ADM1	6
2.1.1 Biochemical reactions	6
2.1.2 Physico-chemical reactions	7
2.1.3 pH calculation	8
2.2 Developed models for integration of temperature with anaerobic digestion	9
2.2.1 Temperature effects in anaerobic digestion	9
2.2.2 Literature review	10
2.2.3 Vilms-Pedersen heat transfer model	11
3 Materials & Methods	13
3.1 Heat transfer model	13
3.1.1 Simulation of yearly temperature fluctuation at La Trappe	13
3.1.2 Heat transfer model sensitivity analysis	14
3.2 ADM 1 Model	15
3.2.1 pH calculation	15
3.2.2 Simplifications	15
3.2.3 Temperature's effects on ADM1	15
3.3 Sludge characterisation	18
3.3.1 Sample collection	18
3.3.2 Chemical analysis	18
3.3.3 Biochemical methane potential test	18
3.3.4 Biochemical fractionation	19
3.4 Calibration and simulation	20
3.4.1 BMP simulation	20
3.4.2 Design and operation	20
4 Results and discussion	22
4.1 ADM1 model modifications	22
4.1.1 pH calculations	22
4.1.2 Absolute temperature inhibition	24
4.1.3 Liquid - gas transfer coefficient	27
4.2 Heat transfer model and dynamic temperature inhibition	28
4.3 Sludge Characterisation	34
4.3.1 Chemical analysis	34
4.3.2 Biochemical methane potential test	35
4.3.3 Biochemical fractionation	36
4.4 Calibration and simulation	37

4.4.1	BMP calibration	37
4.4.2	Simulations	37
5	Conclusion and recommendations	46
5.1	Conclusion	46
5.2	Recommendations	47
5.2.1	La Trappe design	47
5.2.2	Further research	49
	References	51
A	ADM1 Petersen matrix	58
B	Simplifications	63
C	Code metadata	65
D	Biochemical fractionation for high sCOD substrate	66
E	Other considerations for La Trappe	67

Nomenclature

Abbreviations

Abbreviation	Definition
ADM1	Anaerobic Digestion Model No. 1
AMPTS	Automatic Methane Potential Test System
BMP	Biochemical Methane Potential
BSM2	Benchmark Simulation model No. 2
COD	Chemical Oxygen Demand
CSTR	Continuously-fed Stirred Tank Reactor
DAE	Differential Algebraic Equation
dODE	Differentiated ODE
EPS	Extracellular Polymeric Substance
EU	European Union
HRT	Hydraulic Retention Time
IWA	International Water Association
KNMI	Koninklijk Nederlands Meteorologisch Instituut
LHV	Lower Heating Value
MNR	Metabolic Network Reactor
OAT	One-At-a-Time
ODE	Ordinary Differential Equation
OLR	Organic Loading Rate
PE	Polyethylene
PVC	Polyvinyl-chloride
PyADM1	Python implementation of ADM1
sCOD	Soluble Chemical Oxygen Demand
SS	Suspended Solids
TAN	Total Ammonia Nitrogen
tCOD	Total Chemical Oxygen Demand
TKN	Total Kjeldahl Nitrogen
tN	Total Nitrogen
tP	Total Phosphorus
TS	Total Solids
VFA	Volatile Fatty Acid
VS	Volatile Solids
WAS	Waste Activated Sludge
WWTP	Wastewater Treatment Plant

Symbols

Symbol	Definition	Unit
A	Area of each side of the cubical digester	m^2
C_{sub}	Specific heat capacity of the substrate	$J kg^{-1} K^{-1}$
CH_4_{burned}	Amount of CH_4 burned to keep the substrate at the operational heating temperature	m^3
E	Elasticity of the solvent	$N m^{-2}$
f_d	Biodegradable fraction of the total COD	

Symbol	Definition	Unit
B_0	Ultimate methane potential	$\text{N mL CH}_4 \text{ kg}^{-1}$
h_{i-j}	Convective heat transfer coefficient of i to j	$\text{W m}^{-2} \text{ K}^{-1}$
I_i	Inhibition factor of process i	
$K_{H,i}$	Henry's coefficient of gas i	$\text{kmol m}^{-3} \text{ d}^{-1}$
$K_{A,B,i}$	Acid-base kinetic rate coefficient of i	$\text{kg COD m}^{-3} \text{ d}^{-1}$
$K_{a,i}$	Acid-base equilibrium coefficient of i	
$K_{S,i}$	Half-saturation constant of process i	kg COD m^{-3}
$k_{1,2}$	Synthetic and degradative process coefficients of the Arrhenius equation	
$k_{dis,hyr}$	First-order coefficient for disintegration or hydrolysis	d^{-1}
k_p	Pipe resistance coefficient	$\text{m}^3 \text{ d}^{-1} \text{ bar}^{-1}$
$k_{m,i}$	Monod kinetic coefficient of process i	d^{-1}
k_{La}	Volumetric liquid-gas transfer rate coefficient	d^{-1}
k_{opt}	Optimum value of the kinetic parameter under study	d^{-1}
L_c	Characteristic length of the geometry	m
k_l	Overall liquid mass transfer coefficient	m d^{-1}
M_N	Molar mass of nitrogen	g mol^{-1}
Nu	Nusselt number	
$p_{gas,i}$	Partial gas pressure of gas i	bar
p_{atm}	External (atmospheric) pressure	bar
Pr	Prandtl number	
Q_i	Heat transfer with transfer process i to the substrate	J
Q_{solar}	Incoming solar irradiance as measured by a weather institute	$\text{J m}^{-2} \text{ d}^{-1}$
q_i	Flow of i	$\text{m}^3 \text{ d}^{-1}$
$Q_{CON, i-sub}$	Convective heat transfer from source i to the substrate	J
R	Universal gas coefficient	$\text{bar mol}^{-1} \text{ K}^{-1}$
$R_{CNV/CND,i-j}$	Convective or conductive resistance to heat transfer from i to j	$\text{m}^2 \text{ KW}^{-1}$
Re	Reynolds number	
S_i	Concentration of substrate i	kg COD m^{-3}
$S_{gas,i}$	Concentration of i in the gas phase	kg COD m^{-3}
S_{i-}	Concentration of the conjugated base of i	kg COD m^{-3}
$S_{in,i}$	Concentration of substrate i in the influent flow	kg COD m^{-3}
$S_{liq,i}$	Concentration of gas i in the liquid phase	kg COD m^{-3}
s_{hg}	Constant which represents the temperature change which would half the microbial growth	K
$T_{influent}$	Temperature of the influent entering the reactor	K
T_{op}	Operational bulk liquid temperature in the reactor and of the substrate leaving the reactor	K
T_{min}	Minimal temperature for microbial activity according to the cardinal temperature equation	K
T_{opt}	Optimal temperature for microbial activity according to the cardinal temperature equation	K
T_{max}	Maximum temperature for microbial activity according to the cardinal temperature equation	K
T_a	Temperature to which the acetogenic methanogens are attuned to	K
T_{Heater}	Temperature boundary below which heating will be applied	K
U	Overall heat transfer coefficient	$\text{W m}^{-2} \text{ K}^{-1}$
V_i	Volume of i in the reactor	m^3
v	Air viscosity	m s^{-1}

Symbol	Definition	Unit
X_i	Concentration of particulate i	kg COD m ⁻³
$X_{in,i}$	Concentration of particulate i in the influent	kg COD m ⁻³
α_i	Synthetic and degradative exponents of the Arrhenius equation	
Δx	Depth of the digester wall	m
ϵ_i	Radiative heat emmissivity of element i	
η	Absorptivity of the cover	
λ_i	Thermal conductivity of i	W m ⁻¹ K ⁻¹
$\rho_{dis,hyd}$	First-order rate coefficient	kg COD m ⁻³ d ⁻¹
$\rho_{m,i}$	Monod kinetic rate coefficient of i	kg COD m ⁻³ d ⁻¹
$\rho_{i,liq-gas}$	Transfer rate of gas i from the liquid phase to the gas phase	kg COD m ⁻³ d ⁻¹
ρ_{sub}	Density of the digester substrate	kg m ⁻³
$\nu_{i,j}$	Rate coefficient of component i in process j	kg COD m ⁻³
ν	Kinematic viscosity of the fluid	m ² s ⁻¹
σ	Stefan-Boltzmann constant	J d ⁻¹ m ⁻² K ⁻⁴
σ_t	Interfacial surface tension of the solvent	N m ⁻¹
σ_{shock}	Parameter controlling the growth disturbance due to temperature shock	
τ_a	Adaptation time for microbes to attune to new temperatures	d

Introduction

Biogas is a small but important part for the energy sector, and the EU is aiming to grow its share due to the energy transition and recent gas shortages [48]. Since 2018, worldwide biogas production is 59.3 billion m³/y, which is equivalent to 1.36 EJ [103]. This is 0.8 % of all primary renewable energy produced worldwide [47]. More than half of the production is found in Europe, where the main production takes place in heated industrial anaerobic digesters. The second largest producer of biogas is Asia, where unheated small-scale household anaerobic digesters form a large part of the producers. In China alone, 40 million household anaerobic digesters exist, producing more than 75 % of the nations biogas [62]. Moreover, the use of anaerobic digesters to provide energy to people living in poor rural areas in the tropics or subtropics has been suggested in a large number of studies [71, 31, 14, 27, 8, 92]. In many countries in the global south, small-scale digesters are therefore promoted as a sustainable technology for treating manure and other wastes, while generating a renewable energy source and effluent digestate, which can be used as a fertilizer [99]. This can be especially convenient for resource-constraint communities, which are not connected to a central power grid.

1.1. Anaerobic degradation process

The anaerobic degradation of organic matter is a complex system of reactions performed by several groups of micro-organisms. It proceeds in four consecutive reactions: hydrolysis, acidogenesis, acetogenesis and methanogenesis, as shown in Figure 1.1a. Before these steps take place, complex organic material is broken down into proteins, carbohydrates, lipids and inert material within the disintegration process step.

During hydrolysis, enzymes convert these undissolved macro components into soluble compounds, like amino acids, sugars, alcohols and fatty acids. Hydrolysis is often the rate-limiting step for the overall digestion process, especially for influent with high amounts of particulate solids. Important parameters that influence the conversion rate are the suspended solids (SS) to chemical oxygen demand (COD) ratio, temperature and extracellular enzyme concentration. When this step is rate-limiting, it determines reactor volumes of anaerobic digesters. Pre-treatment, either physical, chemical or in combination, can accelerate this step[101].

Acidogenesis is the conversion of amino acids into sugars and the oxidation of higher fats into smaller volatile fatty acids (VFAs), lactate and ethanol. Acidogenesis is often the fastest conversion step, with the highest $-\Delta G_0$ of all anaerobic conversions. Because of the high bacterial growth rates of this group, and the acidity of the produced VFAs, anaerobic reactors are prone for sudden pH shifts. This lower pH causes inhibition of methanogens, which will be less able to convert the acidic acetate into methane. This causes a positive feedback cycle, resulting in acidification of the substrate. This phenomenon can occur if influent concentrations are too high, which is called overloading. A schematic overview of the positive feedback cycle is given in Figure 1.1b

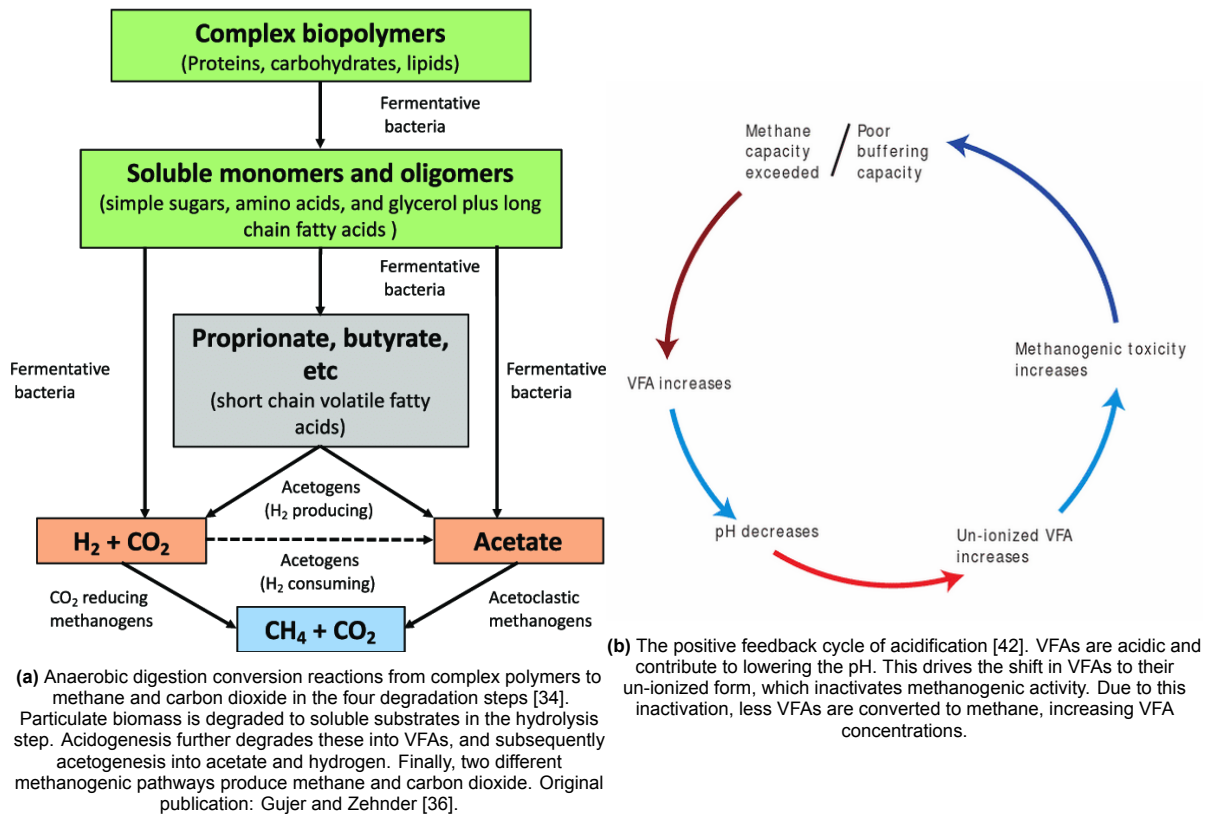


Figure 1.1: Flowcharts of the anaerobic degradation process (a) and the positive feedback of acidification (b).

Two different pathways exist for acetogenesis. In the proton-reducing pathway, VFAs and small soluble organic molecules are metabolized, producing acetate, hydrogen gas and carbon dioxide. During homoacetogenesis, hydrogen gas and carbon dioxide are metabolized, and acetate is produced. Most acetate in anaerobic digesters is produced with the proton-reduction pathway, and the most important substrates are propionate and butyrate, but also lactate, ethanol and methanol are converted. However, these acetogenic bacteria are inhibited by hydrogen (H_2), which they produce themselves. They therefore form a mutualistic bond with methanogenic bacteria, which are hydrogen consuming. This creates a certain range of hydrogen concentration in anaerobic digesters for both species to survive. This hydrogen concentration is maintained in stabilised digesters, because of the effective uptake of hydrogen by methanogens.

The last step is methanogenesis, in which two pathways exist as well. Aceticlastic methanogens metabolize acetate and hydrogenotrophic methanogens metabolize carbon dioxide and hydrogen, both producing methane. This is often found to be the rate limiting step after hydrolysis step. Generally, 70 % of the produced methane originates from acetate, while the rest is produced from hydrogen. The growth rate of aceticlastic methanogens is low, with a typical doubling time of several days. This causes the long start-up time of anaerobic digesters. Hydrogenotrophic bacteria have higher growth rates, which give anaerobic systems more stability under various operating conditions.

1.2. Temperature dependency

Typically biogas production is considered in three main temperature ranges (psychrophilic 15-20 °C, mesophilic 30-45 °C and thermophilic 50-65 °C) [82]. A general relation between the absolute growth rates of the methanogens in these ranges and their relation to temperature can be mesophilic, and mesophilic species have higher absolute growth rates and methane production than psychrophilic species [80, 46]. This effect is lessened when looking at net growth, as decay rates are affected by temperature as well. Nevertheless, thermophilic digestion has the increased metabolic rates as the advantage, but decreased process stability and high energy input requirements as the disadvantages [60].

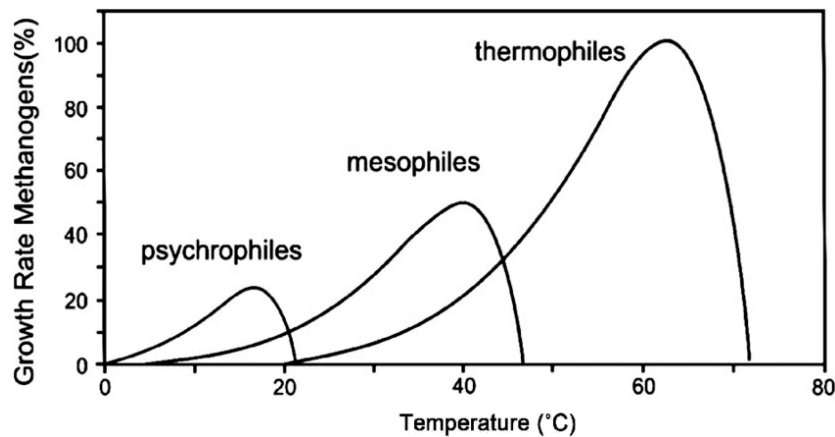


Figure 1.2: Relative growth rates of different methanogenic species with temperature [97].

Apart from the absolute temperature, the change in temperature over time should be limited as well. It is common knowledge among digester operators that temperature fluctuations should remain below $0.5\text{ }^{\circ}\text{C d}^{-1}$ in order to not cause biomass inactivation and decreased biogas production [46]. This is the main reason why most industrial digesters contain temperature regulation in colder regions. Furthermore, if temperature drops below psychrophilic temperatures ($<15\text{ }^{\circ}\text{C}$) for a longer time, all biogas producing biomass becomes dormant, and reactors often need a long time to regain former biogas production levels [21].

1.3. Household reactors

In addition to operational temperature, the anaerobic digestion process is dependent on many other factors, such as pre-treatment, substrate composition and HRT. These influence the design of the reactor, just like technical, economical, legislative and social factors. Due to the wide variety of cases, numerous reactor designs exist. This makes it difficult to categorize anaerobic digesters, but when considering small scale domestic application, three most used designs can be defined. These include the tubular bag digester, the floating drum digester and the fixed-dome reactor [25].

Tubular bag digesters are sealed tubular PVC or PE bags, often referred to as balloons. They are mostly implemented in South America and are successful due to their low cost and easy implementation and operation. Floating drum digesters consist of an underground digester with a movable gas drum floating on the bulk liquid. As gas is collected in the gas drum, it will rise due to the increased pressure, and it will fall if gas is removed from the drum. This gives constant gas pressure and a visible inventory of the amount of gas in the digester. However, since the increase in the number of digesters in China, it has been observed that the fixed-dome design is the most used design approach, allowing for an affordable and reliable solution for the domestic household market with low maintenance [8]. In India, a switch is made from the floating drum design to the fixed dome (Austin and Morris, 2012).

Because of the masonry required for construction of these reactors, and the variable load they need to be able to handle depending on the user, no standard design of a fixed-dome digester exists. However, prefabricated reactors are increasingly produced, and have advantages like the lower production costs, improved quality assurance and lower environmental impacts [25]. A schematic design of a typical fixed-dome reactor is shown in Figure 1.3. Many variations on the design exist, but all use the same principles. Biodegradable waste is introduced to the reactor through an inlet pipe. Because of the low area exposed to the atmosphere, the reactor becomes anaerobic. The microbial community in the digester produces gases, which builds up pressure in the dome, pushing the sludge down. At the top of the dome, a gas pipe is installed for gas extraction. A removal outlet opposite of the inlet is present with an overflow system. Furthermore, an outlet pipe is present to pump heavier sludge from the bottom of the reactor out directly. This outlet pipe is not always present.

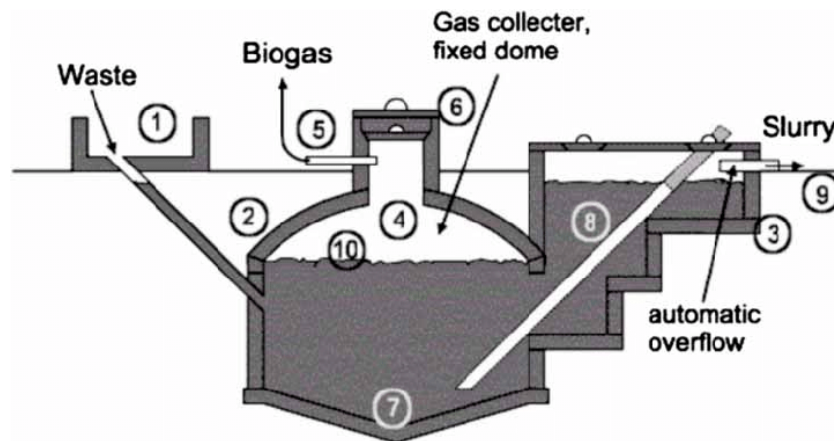


Figure 1.3: Schematic overview of a fixed dome anaerobic digester. 1. Mixing tank with inlet pipe and sand trap. 2. Digester. 3. Compensation and removal tank. 4. Gasholder. 5. Gas pipe. 6. Entry hatch, with gas tight seal. 7. Accumulation of thick sludge. 8. Outlet pipe. 9. Reference level. 10. Supernatant scum, broken up by varying level. [52]

1.4. Problem statement

Even though the merits are well understood, the wide-spread implementation of household fixed-dome anaerobic digesters in developing countries is still a slow-moving process [27]. One of the constraints which causes the delay in implementation of anaerobic digestion in developing countries is found in the low biogas production [63]. Because of the low production, the economic incentive decreases and no longer meets the user's expectations. The decrease in production is partially caused by process instability [4]. The performance of a digester is adversely affected by sub optimal temperatures and by temperature fluctuations [78]. In basic fixed-dome reactors, no control technology is present to regulate operating temperature. This reduces the production of biogas of fixed-dome digesters especially in countries with large seasonal temperature fluctuations. In Bangladesh for example, it was found that a fixed-dome anaerobic digester had a decrease in biogas production of 47.85 % between autumn and winter [110].

Recommendations have been made to increase biogas production quantity and quality in small-scale household digesters [101]. Several of these recommendations are centered around the increase and stabilisation of digester temperature, with for example insulation. Another proposal is the inclusion of heaters powered with renewable energies such as solar, wind or the produced biogas [107]. However, it is important to understand the effects of temperature and temperature fluctuations on the biogas production process, as to understand which recommendations are effective in which context. A model is therefore needed to simulate the effect of these measures on the anaerobic digestion process. As temperature changes as a function of environmental conditions, a thermal balance model of the digester is needed in order to predict the temperature of the bulk liquid in the digester. This can subsequently be linked to an anaerobic digestion model such as the Anaerobic Digestion Model No. 1 (ADM1) to model the effect of the temperature on biogas production.

1.5. La Trappe as a case-study

At the WWTP of the La Trappe brewery and the connected monastery Koningshoeve in Tilburg, Netherlands, anaerobic digestion is proposed as a wastewater treatment step. At the moment, the spent wort, a sugary waste product from the brewing process, is discharged to the WWTP and sludge from this WWTP is directly applied as fertilizer on nearby farmland. However, their affiliated monastery in Uganda successfully started digesting their organic waste streams in an unheated household fixed-dome digester, which inspired the Dutch monastery to utilize the same technology. This hypothetical unheated fixed-dome digester could therefore be used to investigate the effects of seasonal temperature fluxes on the digestion process stability. The intention is to feed the digester with the spent wort stream from the brewery. This 72 °C stream contains high concentrations of hydrolysed carbohydrates, and its biochemical composition is variable depending on which of the twelve types of La Trappe beer was brewed

in the given batch. This thesis therefore focused on the digestion at mesophilic temperatures, as it was assumed that thermophilic digestion would suffer from process instability due to fluctuations in the substrate concentrations and in the operational temperature [50, 105]. It was assumed that the spent wort is readily biodegradable, and that methanogenesis will therefore be the rate limiting step for digestion, possibly causing acidification. In the hope to set the mean rate limiting step to hydrolysis, co-digestion with a less-readily biodegradable COD source is investigated, therefore preventing acidification. This other substrate is the Waste Activated Sludge (WAS) stream which originates from the WWTP. This WWTP has a Metabolic Network Reactor (MNR), which is an activated sludge treatment step where plants grow on top of the reactors, with their roots hanging in the wastewater stream. These plant roots allow for better biomass retention times. The whole reactor is covered by a greenhouse, which is kept at 27 °C. The MNR is followed by dissolved air flotation and gravity belt thickening. Around 1 m³ of wort and 1 m³ of belt-thickened sludge is produced in the brewery and WWTP per day. The WAS coming from the belt thickener is assumed to be less readily biodegradable compared to the wort stream. These two streams can therefore be co-digested for process stability. As the monks request for innovative but frugal solutions, a similar fixed-dome reactor design as the Ugandan reactor is considered. However, as seasonal temperature fluctuations in the Netherlands are substantial, a heat management strategy is needed for the digester.

1.6. Research question

The following research question is to be answered in this thesis:

How will seasonal temperature fluctuation influence the biogas production in a frugal digester in a cold climate, using La Trappe as an example?

The goal of this thesis is to create a coupled heat transfer and anaerobic digestion model capable of simulating the effects of temperature on the anaerobic digestion processes for the La Trappe case. The heat transfer model will calculate the operational temperature of the bulk liquid in the digester as a function of weather data from the KNMI. Influent concentrations for the co-digestion of the wort and sludge of La Trappe will be determined with a biochemical fractionation method for ADM1 input variables. The created model will be used to simulate different design and operational strategies for biogas production. A schematic representation of the situation is shown in Figure 1.4.

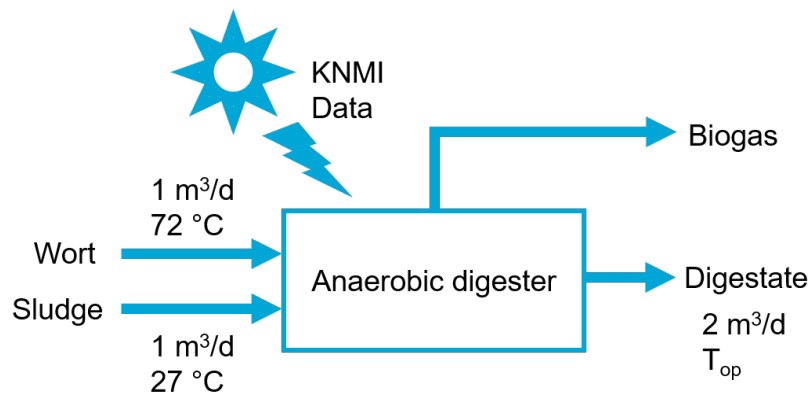


Figure 1.4: Schematic overview of the situation at La Trappe as modelled in this thesis. A mixture of 1 m³ of wort and 1 m³ of sludge are proposed as the daily influent to the digester, which will be exposed to the Dutch climate as represented with data from the Dutch weather institute KNMI. The heat transfer model will simulate the effect of ambient conditions on the bulk liquid temperature, and the coupled extended ADM1 will simulate the effect of this temperature on the biogas production.

2

Background literature

2.1. ADM1

The Anaerobic Digestion Model No. 1 was developed by the IWA Task Group for Mathematical Modeling of Anaerobic Digestion, and was released in 2002 [11]. This model has since its release had many modifications and extensions, but has never been revised completely, due to its general applicability and accuracy. In the model, differential equations track the state of 35 concentrations over 28 reactions which describe the anaerobic digestion process, and the full Petersen matrix with all reactions in Appendix A. The processes can be divided into bio-chemical and physico-chemical processes.

One of the generally accepted and adopted modifications came from Rosen and Jeppsson [85], which modified the ADM1 for its integration in the BSM2. The BSM2 simulates a full WWTP, and the modified ADM1 is used in this model to digest the primary sludge and WAS of this WWTP. The steady-state composition of this influent are generally used for validation of ADM1 extensions, and their input characteristics can be found in the paper of Rosen and Jeppsson [85]. The modifications for BSM2 integration and the steady-state influent concentrations for validation have also been used in this thesis. Concentrations are given in kg COD m^{-3} , which is the amount of oxygen in kg needed to fully oxidize the organic matter present in 1 m^3 of water. The units for inorganic carbon and nitrogen are in moles as they have no COD. For gas flow, conversions are made from pressure in bar to $\text{m}^3 \text{ d}^{-1}$.

2.1.1. Biochemical reactions

The biochemical processes consists of the disintegration, hydrolysis, acidogenesis, acetogenesis and methanogenesis reactions, as well as the decay of cell mass. These reactions are sequential and irreversibly implemented. The rates of these processes are determined with first-order and Monod-type kinetic equations, as shown in (2.1) and (2.2), respectively. It should be highlighted that X_i is used for particulate matter or microbial cells, and S_i for soluble matter only.

$$\rho_{\text{dis/hyd}} = k_{\text{dis/hyd}} X_{\text{dis/hyd}} \quad (2.1)$$

$$\rho_{m,i} = \mu_{m,i} X_i \frac{S_i}{S_i + K_{S,i}} \prod I_i \quad (2.2)$$

The inhibition factors I_i lower the outcome of rate equations and slow down the overall digestion process. Inhibition factors are biological and therefore only influence the Monod kinetics, not the disintegration and hydrolysis steps, nor the physico-chemical equations. In the BSM2 implementation of the ADM1, the choice was made for Hill inhibition functions, which have been used in this study as well. There are eight different inhibition functions in the ADM1, three based on pH, three based on dissolved hydrogen gas, and two on inorganic nitrogen concentration. Figure 2.1 shows the inhibition functions over pH or concentration. Processes are uninhibited if their respective inhibition functions have value 1. For uninhibited digestion, high enough concentrations of inorganic nitrogen (S_{IN}), low

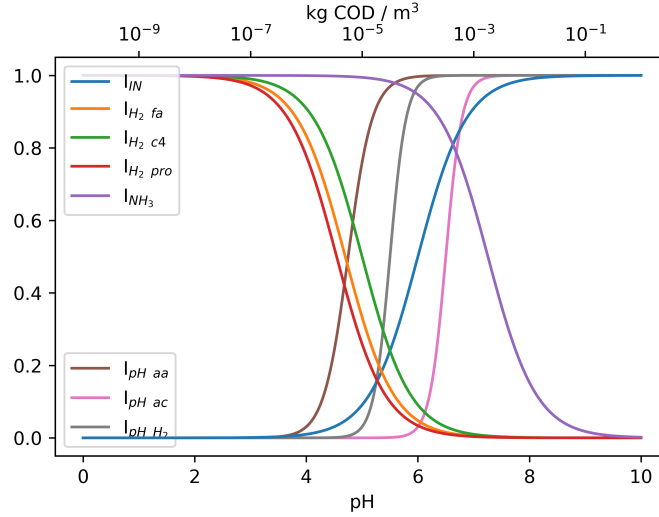


Figure 2.1: The inhibition functions in the original ADM1. The pH inhibition functions follow the lower x-axis, while the hydrogen and inorganic nitrogen based functions follow the upper x-axis.

concentrations of hydrogen gas and free ammonia, and a pH of at least 7 have to be present in the bulk liquid. For more details on inhibition functions in anaerobic digestion and its implementation in the ADM1, the reader is referred to Chen, Cheng, and Creamer [24] and Rosen and Jeppsson [85].

Once the rates are calculated for a single time-step, the change in a state can be found by multiplying the rates times their weights, and correcting for in- and outflow. In the Petersen matrix in Appendix A, the weights of each reaction are displayed. The change in concentration for each state in the liquid phase can be calculated with (2.3). This formulation does assume that volume and flow rate are constant over time.

$$\frac{dS_{liq,i}}{dt} = \frac{q_{inluent} S_{inluent,i}}{V_{liq}} - \frac{q_{inluent} S_{liq,i}}{V_{liq}} + \sum_{j=1}^{26} \rho_j \nu_{i,j} \quad (2.3)$$

2.1.2. Physico-chemical reactions

The physicochemical processes consist of the acid-base association reactions, as well as the gas solubility reactions in the bulk liquid. They are equilibrium reactions, and are therefore reversible. The rates of these equations is determined by acid-base kinetics and Henry's law. The acid-base reactions follow the form of (2.4), while the gas equations are depicted in (2.5) and (2.6).

$$\frac{dS_{i-}}{dt} = -\rho_{A,i} = -k_{A,B,i}(S_{i-}(K_{a,i} + S_{H^+}) - K_{a,i}S_i) \quad (2.4)$$

$$\begin{aligned} \rho_{T,H_2} &= k_L a (S_{liq,H_2} - 16 K_{H,H_2} p_{gas,H_2}) \\ \rho_{T,CH_4} &= k_L a (S_{liq,CH_4} - 64 K_{H,CH_4} p_{gas,CH_4}) \\ \rho_{T,CO_2} &= k_L a (S_{liq,CO_2} - K_{H,CO_2} p_{gas,CO_2}) \end{aligned} \quad (2.5)$$

$$\frac{dS_{gas,i}}{dt} = -\frac{S_{gas,i} q_{gas}}{V_{liq}} + \rho_{T,i} \frac{V_{liq}}{V_{gas}} \quad (2.6)$$

The partial pressures of each gas are found with the ideal gas law, and the factors 16 and 64 are used for the conversion of kg COD to kmol for hydrogen and methane, respectively. There are two different ways to calculate the gas flow, assuming variable or steady head space pressure. Both these methods assumes that the reactor head space is saturated with water vapour pressure. The partial pressure of water vapour is dependent on temperature as shown in (2.7). Following from this, the variable pressure can be calculated with (2.8), while for the steady pressure calculation, (2.9) can be

used. The steady pressure calculation is used for the BSM2 integration and in this thesis unless stated otherwise.

$$p_{\text{gas},H_2O} = 0.0313 \exp\left(5290 \left(\frac{1}{2980} - \frac{1}{T_{\text{op}}}\right)\right) \quad (2.7)$$

$$q_{\text{gas}} = \frac{R T_{\text{op}}}{p_{\text{atm}} - p_{\text{gas},H_2O}} V_{\text{liq}} \left(\frac{\rho_{T,H_2}}{16} + \frac{\rho_{T,CH_4}}{64} + \rho_{T,CO_2} \right) \quad (2.8)$$

$$\begin{aligned} q_{\text{gas}} &= k_p (p_{\text{gas}} - p_{\text{atm}}); \\ p_{\text{gas}} &= p_{\text{gas},H_2} + p_{\text{gas},CH_4} + p_{\text{gas},CO_2} + p_{\text{gas},H_2O} \end{aligned} \quad (2.9)$$

2.1.3. pH calculation

In the revision of the ADM1 by Rosen and Jeppsson [85], two methods are suggested to calculate the hydrogen ion and dissolved hydrogen gas concentration, the Ordinary Differential Equation (ODE) method and the Differential Algebraic Equation (DAE) method. The DAE method was invented in order to lower the stiffness of system. Using the implementation with the DAE equations, it is assumed that processes with higher rates are instantaneous, which from the perspective of the slower processes holds true. The DAE implementation was chosen in the original PyADM1, disregarding the ODE system. In this work, the ODE has again been added to the model, as well as the differentiated balance equation (dODE) method proposed by Thamsiriroy and Murphy [95]. In all methods, the charge balance as shown in (2.10) is assumed.

$$S_{\text{Cat}^+} + S_{\text{NH}_4^+} + S_{\text{H}^+} - S_{\text{HCO}_3^-} - \frac{S_{\text{Ac}^-}}{64} - \frac{S_{\text{Pr}^-}}{112} - \frac{S_{\text{Bu}^-}}{160} - \frac{S_{\text{Va}^-}}{208} - S_{\text{OH}^-} - S_{\text{An}^-} = 0 \quad (2.10)$$

Here, S_{Cat^+} and S_{An^-} represent metallic ions and are included to represent strong bases and acids, respectively. The denominators for organic acids convert the kg COD concentration to charge.

In the ODE implementation, this balance is used to calculate the unknown S_{H^+} concentration by rearranging the terms in an algebraic equation as shown in (2.11)

$$\begin{aligned} S_{\text{H}^+} &= -\frac{\Theta}{2} + \frac{1}{2} \sqrt{\Theta^2 + 4K_W} \\ \Theta &= S_{\text{Cat}^+} + S_{\text{NH}_4^+} - S_{\text{HCO}_3^-} - \frac{S_{\text{Ac}^-}}{64} - \frac{S_{\text{Pr}^-}}{112} - \frac{S_{\text{Bu}^-}}{160} - \frac{S_{\text{Va}^-}}{208} - S_{\text{OH}^-} - S_{\text{An}^-} \\ S_{\text{NH}_4^+} &= S_{\text{IN}} - S_{\text{NH}_3} \\ S_{\text{CO}_2} &= S_{\text{IC}} - S_{\text{HCO}_3^+} \end{aligned} \quad (2.11)$$

In practicality, it was found that the ODE suffers from high stiffness, which is problematic for use in the BSM2 framework. Therefore, two different DAE versions have been created (DAE_{pH} and DAE_{pH,S_{H₂}) [85]. In this paper, only the DAE_{pH,S_{H₂} is used. In this method, the differential equation of the pH and S_{H_2} states are approximated by an implicit algebraic equation, which is solved numerically with the Newton-Raphson method. With this method, the value at the next iteration step is calculated using (2.12). The reader is referred to the Appendix Rosen and Jeppsson [85] for the full equations of S_{H_2} and the gradient of the algebraic equation.}}

$$\begin{aligned} S_{\text{H}^+,k+1} &= S_{\text{H}^+,k} - \frac{E(S_{\text{H}^+,k})}{dE(S_{\text{H}^+})/dS_{\text{H}^+}|_{S_{\text{H}^+,k}}}; \\ E(S_{\text{H}^+,k}) &= S_{\text{cat}^+,k} + S_{\text{NH}_4^+,k} + S_{\text{H}^+,k} - S_{\text{HCO}_3^-,k} - \\ &\quad \frac{S_{\text{Ac}^-,k}}{64} - \frac{S_{\text{Pr}^-,k}}{112} - \frac{S_{\text{Bu}^-,k}}{160} - \frac{S_{\text{Va}^-,k}}{208} - \frac{K_W}{S_{\text{H}^+,k}} - S_{\text{An}^-,k} \end{aligned} \quad (2.12)$$

Lastly, the dODE uses the chain rule to differentiate the charge balance equation after rearrangement of the terms. This method eliminates the need for the conjugated base states, reducing the number of states in the ADM1 by 5. The formula can be found (2.13).

$$\begin{aligned}
\frac{dS_{H^+}}{dt} &= \frac{A}{B}; \\
A &= \frac{dS_{an^+}}{dt} + \frac{K_{a,IN}}{(K_{a,IN} + S_{H^+})} \frac{dS_{IN}}{dt} + \frac{K_{a,CO_2}}{(K_{a,CO_2} + S_{H^+})} \frac{dS_{IC}}{dt} + \frac{1}{64} \frac{K_{a,ac}}{(K_{a,ac} + S_{H^+})} \frac{dS_{ac}}{dt} + \\
&\quad \frac{1}{112} \frac{K_{a,pro}}{(K_{a,pro} + S_{H^+})} \frac{dS_{pro}}{dt} + \frac{1}{160} \frac{K_{a,bu}}{(K_{a,bu} + S_{H^+})} \frac{dS_{bu}}{dt} + \\
&\quad \frac{1}{208} \frac{K_{a,va}}{(K_{a,va} + S_{H^+})} \frac{dS_{va}}{dt} - \frac{dS_{IN}}{dt} - \frac{dS_{cat^+}}{dt} \\
B &= 1 + \frac{K_{a,IN}S_{IN}}{(K_{a,IN} + S_{H^+})^2} + \frac{K_{a,CO_2}S_{IC}}{(K_{a,CO_2} + S_{H^+})^2} + \frac{1}{64} \frac{K_{a,ac}S_{ac}}{(K_{a,ac} + S_{H^+})^2} + \\
&\quad \frac{1}{112} \frac{K_{a,pro}S_{pro}}{(K_{a,pro} + S_{H^+})^2} + \frac{1}{160} \frac{K_{a,bu}S_{bu}}{(K_{a,bu} + S_{H^+})^2} + \frac{1}{208} \frac{K_{a,va}S_{va}}{(K_{a,va} + S_{H^+})^2} + \frac{K_w}{S_{H^+}}
\end{aligned} \tag{2.13}$$

It should be highlighted that the ODE implementation uses algebraic equations, and the DAE uses algebraic equations solved with a numerical method. This makes their naming confusing. The dODE provides the actual ordinary differential equation. However, as the ODE and DAE implementations as explained above are referenced in a number of studies with these abbreviations, it was chosen to not deviate from these.

2.2. Developed models for integration of temperature with anaerobic digestion

2.2.1. Temperature effects in anaerobic digestion

To model the effects of temperature on anaerobic digestion, it is important to understand how temperature influences different processes within the overall anaerobic degradation process. In the ADM1 modified by Rosen and Jeppsson [85], operational temperature was already used to calculate the acid-base equilibrium constants of water (K_w), carbon dioxide (K_{a,CO_2}) and inorganic nitrogen ($K_{a,IN}$). Furthermore, the Henry constants of carbon dioxide, methane and hydrogen have been linked to temperature, as well as the dependency of water vapour pressure on temperature. This was all done using the van 't Hoff's equation. It is therefore assumed that the aforementioned gases behave as ideal gases [16]. Additionally, it was stated in both the original ADM1 report as well as in the revisions of Rosen and Jeppsson [85] that for more well-fitted modelling of temperature dependency, biochemical parameters values should be described as functions of temperature as well [11].

Hinshelwood proposed that the effect of temperature on microbial activity is composed of a synthetic and degradative process [43]. Below the optimum temperature range, the synthetic process is increased more than the degradative with temperature, increasing biological activity. If the temperature is higher than the optimum however, the degradative processes become more substantial with increasing temperature, lowering microbial activity. This effect can be comprehended as an inhibition function, where for uninhibited process rates, the temperature should be at the optimal value. For each other temperature, the rate of the metabolic activity will be lowered. This effect can be modelled the using a double Arrhenius equation, as written in (2.14) [76].

$$I_{temp} = k_1 \exp(\alpha_1(T_{op} - T_{opt})) - k_2 \exp(\alpha_2(T_{op} - T_{opt})) \tag{2.14}$$

Another method to simulate a similar relation is the cardinal temperature equation, which is normally used to describe plant growth, but proposed as a model for microbial activity by Rosso, Lobry, and Flandrois [86], shown in (2.15). Donoso-Bravo et al. [28] found the parameters T_{min} , T_{opt} and T_{max} for this equation for hydrolysis, acidogenesis and methanogenesis, using starch, glucose and acetic acid as substrates. Acidogenesis was excluded from this study.

$$I_{temp} = \frac{(T_{op} - T_{max})(T_{op} - T_{min})^2}{(T_{opt} - T_{min})[(T_{opt} - T_{min})(T_{op} - T_{opt}) - (T_{opt} - T_{max})(T_{opt} - T_{max})(T_{opt} + T_{min} - 2T_{op})]} \tag{2.15}$$

2.2.2. Literature review

Over the years, many models have been created to simulate the effect of temperature on biogas production. These models either consist of heat transfer models, anaerobic digestion models, or combined models. The heat transfer models all used thermal balances to determine the bulk liquid temperature of the anaerobic digestion reactor. This temperature state is then linked to gas production, either with simplified relations or in combined models by influencing parameters in an anaerobic digestion model with relations as shown in (2.14) and (2.15) or similar.

Calise et al. [18] performed a literature review summarizing all mathematical temperature models for digesters. The potential integration with the anaerobic digestion process was also discussed. The most relevant findings are summarised as follows together with other relevant studies.

A heat transfer model of unheated fixed-dome digesters buried in the ground has been made by Terradas-III et al. [94]. In this research, three states were defined, for the heat in the cover, the heat in the biogas and the heat in the bulk liquid. These findings were used with simple exponential relations to couple temperature to biogas production. Bandgar et al. [10] made a heat transfer model of a household floating drum digester and experimentally validated the predicted values. The model consisted of two states, for the heat in the bulk liquid and the biogas. A strong relation between the measured solar irradiance and the biogas production was observed in the experiment. Vilms Pedersen et al. [98] made a similar temperature model, but only with one state for the bulk liquid temperature. This model was validated without need of calibration in two different scenarios, but was not linked to biogas production.

Mathematical models of digesters utilizing solar heat have also been made to analyse their capability to optimize biogas production. Modelling and validation of heat transfer in anaerobic digesters covered by greenhouses indicated increased temperatures, allowing processes to operate in regions which normally would be too cold for unheated digesters [39]. Adouani et al. [2] combined a thermal model with the ADM1 to investigate possible strategies to mitigate substrate variability. The thermal model was re-used from an earlier study [45]. Using a step function to determine the effect of temperature on k_m , a link was found between the maximal reaction rate and climatic conditions. Axaopoulos et al. [9] modelled solar collectors, which delivered energy to the digester using heat exchangers in Greece. Furthermore, the heat collectors were used as the top cover of the model to add an extra insulation layer. The model used similar heat transfer equations and biogas production relations as the model of Terradas-III et al. [94]. The influence of direct absorption of irradiation for buried anaerobic digesters with a glass top has been modelled as well [61]. This study simplified the ADM1 in order to couple it to temperature.

An anaerobic digester was modelled containing a heat exchanger by Calise et al. [20]. A heat transfer model was made containing the heating system's and the digesters' thermal balance equations. This was used to investigate how different parameters would influence gas yield. The anaerobic digestion model 1 (ADM1) was used for analysis of the kinetic and biological features of the process. The biological activity was linked to temperature using Arrhenius' equations, but no details are given on the used constants or method of implementation. In a subsequent research, Calise et al. [19] used this model in order to investigate the effect of concentrating photovoltaic/thermal collectors and a biomass heating system to supply an anaerobic digestion plant with both electricity and heat. In addition, a biogas upgrading process was added, which converts biogas with between 40 % to 65 % methane concentrations to biomethane with 95 % methane purity. Furthermore, an energy and economic model were added, which considered capital and operating costs of the overall plant. A payback period lower than 3 years was found for a hypothetical case in Naples. The model was however not validated.

Lastly, Bergland, Dinamarca, and Bakke [15] combined a heat transfer model with the ADM1 to simulate the digestion of cow manure at 25, 30 and 35 °C. The model compared different sets of literature data to simulate the change in growth parameters with change in temperature. The model was validated and the combination of the most accurate relation between temperature and growth parameters at these different temperatures was concluded.

2.2.3. Vilms-Pedersen heat transfer model

As mentioned above, Vilms Pedersen et al. [98] made a heat transfer model to simulate the effect of meteorological conditions on the bulk liquid temperature of an unheated digester. In Figure 2.2, a schematic representation of the model is shown. In this model, the influence of solar irradiance, atmospheric heat radiance, air temperature convection, soil temperature convection and influent and effluent advection are taken into account. This results in the balance equation as shown in (2.16), which is used to calculate the bulk liquid temperature in the reactor at a given moment.

$$\rho_{\text{sub}} C_{\text{sub}} V_{\text{sub}} \frac{dT_{\text{op}}}{dt} = Q_{\text{ADV}} + Q_{\text{RAD}} + Q_{\text{IRR}} + \sum Q_{\text{CON}, i-\text{sub}} \quad (2.16)$$

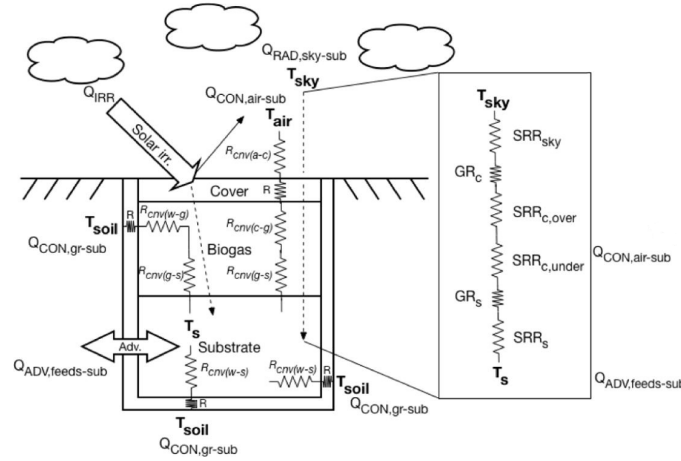


Figure 2.2: Diagram showcasing the different heat sinks and sources and resistances of the heat balance model [98]. The amount of resistance terms are shown per pathway. Each heat transfer process has one pathway, except the convection-conduction process, which has four pathways. These four conduction pathways originate in the air, the soil next to the vertical wall at biogas height, the soil next to the vertical wall at bulk liquid height and the soil under the floor of the digester.

Irradiance

The heat transfer from solar irradiance Q_{IRR} can be calculated using the solar irradiance as measured by weather institutes, the area of the digester which receives solar irradiance and the absorptivity of irradiance of the cover, as formulated in (2.17). In the model, the digester is assumed to be a cube where only the ceiling is exposed to irradiance. The area exposed to solar irradiance can therefore be calculated from the reactor volume for each simulation.

$$Q_{\text{IRR}} = Q_{\text{solar}} A \eta \quad (2.17)$$

Advection

The heat transfer from advection is determined by the difference in temperature between the influent and the bulk liquid, and can be calculated as written in (2.18). It should be highlighted that it is presumed that the volume of the bulk liquid does not change over time.

$$Q_{\text{ADV}} = q_{\text{influent}} \rho_{\text{sub}} C_{\text{sub}} (T_{\text{influent}} - T_{\text{op}}) \quad (2.18)$$

Convection and conduction

The convective and conductive heat transfer are modelled as heat transfer resistances in series, where convection is the process of heat transfer among different phases i.e. gas, solid and liquid, while conduction is the process of heat transfer over the depth of solids, which in this case is the walls of the digester. These series of resistances are used to formulate the heat transition between the air and bulk liquid, as well as between bulk liquid and soil surrounding the buried digester.

A particular long series of resistances is modeled for heat exchange between ambient air and bulk liquid in the digester. First, there is convective resistance between the air and the cover. This convective resistance depends on wind speed, which influences the Reynolds number and consequently the Nusselt number of the air/cover interface. The convective heat transfer coefficient can be formulated by (2.19), (2.20) and (2.21).

$$h_{\text{air-cover}} = \frac{Nu\lambda}{L_c} \quad (2.19)$$

$$Nu = 0.037Re^{0.8} \sqrt[3]{Pr} \quad (2.20)$$

$$Re = \frac{vL_c}{\nu} \quad (2.21)$$

Here, the Nusselt number is calculated for a flat plate [22].

The resistance to the convective heat transfer is the inverse of the transfer coefficient, as written in (2.22). This is used in the convective heat transfer from ambient air to the digester, but also for the transfer from soil to digester walls, from walls to biogas, from biogas to bulk liquid and from walls to bulk liquid.

$$R_{\text{CNV},i-j} = \frac{1}{h_{i-j}} \quad (2.22)$$

The temperature pathway from air to bulk liquid is followed by conductive resistance. Conduction takes place over the depth of the digester walls. The resistance for conductive heat transfer is found with (2.23). For adding extra insulation, the same formula can be used and the total conduction of the digester wall and the insulation layer would be the sum of both individual resistances.

$$R_{\text{CND}} = \frac{\Delta x}{\lambda} \quad (2.23)$$

Once the heat is inside the reactor, convective resistances determines the heat exchange between cover and biogas, and between biogas and bulk liquid, which are again determined by (2.22). The overall heat transfer coefficient is calculated by summing the inverse of the resistances for the whole convection - conduction pathway, as written in (2.24). There are four different pathways of heat convection and conduction included which influence the bulk liquid temperature, as shown in Figure 2.2.

$$U = \frac{1}{\sum_{i=1}^n R_{\text{CNV},i} + R_{\text{CND}}} \quad (2.24)$$

The overall resistance is used to calculate the heat transfer through each pathway given by (2.25). Here, T_i is the temperature outside of the reactor where the series of resistances starts, e.g. the air or soil.

$$Q_{\text{CON},i-\text{sub}} = A U (T_i - T_{\text{op}}) \quad (2.25)$$

Radiative

Radiative heat transfer is calculated under the assumption that the digester cover acts as a radiation shield. The resistance to the radiative heat is calculated as a summation of the geometric resistance and the surface radiative resistance. The formulas used for calculating the radiative heat transfer from the sky to the bulk liquid are given in (2.26) and (2.27). Here, T_{sky} is the temperature of the sky found with (2.27) [93].

$$Q_{\text{RAD}} = \frac{\sigma(T_{\text{sky}}^4 - T_{\text{op}}^4)}{\frac{2}{A} + 2\frac{1-\epsilon_{\text{cover}}}{A\epsilon_{\text{cover}}} + \frac{1-\epsilon_{\text{sub}}}{A\epsilon_{\text{sub}}}} \quad (2.26)$$

$$T_{\text{SKY}} = 0.0552 T_{\text{air}}^{3/2} \quad (2.27)$$

3

Materials & Methods

In order to make accurate projections of the temperature and its influence on biogas production in the anaerobic digester at La Trappe, a heat transfer model based on the model of Vilms Pedersen et al. [98] as presented in chapter 2 is made. The heat transfer model is used to calculate the bulk liquid temperature, which is used in the ADM1. Several bio- and physico-chemical relations are used to link temperature and temperature fluctuations to biogas production. The influent states for the ADM1 for the sludge and wort of La Trappe have been determined using a biochemical fractionation method. The coupled heat transfer-ADM1 model is used to simulate the influence of temperature on biogas production. The model is however not calibrated or validated in the present work.

3.1. Heat transfer model

The Vilms-pedersen is used to predict the operational temperature under different climatic conditions. Changes to the model have been made:

- In the original model, Q_{solar} is based on the locations latitude and atmospheric pressure, but in the model used in this thesis, measured solar data from weather institutes is used [98].
- In the original model, a dampening coefficient based on the difference between the mean and actual air temperature is used to calculate the soil temperature over depth. However, for the Netherlands, measured soil temperatures over depth data from weather institutes have been used instead, as these were available.

3.1.1. Simulation of yearly temperature fluctuation at La Trappe

The model has been used to simulate the temperature of a digester in the Netherlands. Different heat transfer processes (e.g. convection or radiance) are compared to see which process contribute most to final operational bulk liquid temperature. The digester design parameters used in the heat transfer simulations are given in Table 3.1. The flow rate has been chosen based on the La Trappe case, and the volume was determined for a HRT of 20 days, as this was presumed sufficient for the wort, which is expected to be readily biodegradable. The walls at biogas height are assumed to be in contact with dry earth, while the walls surrounding the bulk liquid are assumed to be wet. The influence of adding an insulation layer of 2 cm of fiberglass to the digester wall is modelled as well. The wall thickness, insulation thickness and thermal conductivities have been taken from Metcalf and Eddy [67]. The model uses values for mean wind speed, solar irradiance, air temperature and ground temperature at one meter depth as inputs to calculate the temperature in the reactor. Weather data for the Netherlands taken from KNMI weather station de Bilt was deemed representative [54]. It should be highlighted that for the solar irradiance measurements of the KNMI, no shading objects are around the measuring device. It is therefore assumed that this will also be the case for the digester of La Trappe. The soil under the floor of the digester is assumed to be at a constant temperature set at the mean of the air temperature. The initial temperature is determined by running the model for one year, and taking the end value of the temperature at the end of the simulation. The constants for the heat transfer model as given in Table

3.2 were used, and were taken from Vilms Pedersen et al. [98].

Table 3.1: Design parameters used in the heat transfer model to simulate the La Trappe digester.

parameter	value	unit
Volume	40	m ³
Flow rate	2	m ³ d ⁻¹
Temperature influent	35	°C
λ_{cover}	1.2	W m ⁻¹ K ⁻¹
$\lambda_{\text{dry walls}}$	0.6	W m ⁻¹ K ⁻¹
$\lambda_{\text{wet walls}}$	1.2	W m ⁻¹ K ⁻¹
$\lambda_{\text{insulation}}$	0.04	W m ⁻¹ K ⁻¹
Thickness walls	0.3	m
Thickness insulation	0.02	m

Table 3.2: Constants used in the heat transfer model [98].

Parameter	Value	Unit
λ_{air}	0.026	W m ⁻¹ K ⁻¹
$h_{\text{sub-floor}}$	244.15	W m ⁻² K ⁻¹
$h_{\text{cover-walls}}$	2.15	W m ⁻² K ⁻¹
$h_{\text{gas-wall}}$	2.70	W m ⁻² K ⁻¹
$h_{\text{gas-sub}}$	2.20	W m ⁻² K ⁻¹
$h_{\text{sub-wall}}$	177.25	W m ⁻² K ⁻¹
$C_{\text{substrate}}$	4.179	J kg ⁻¹ K ⁻¹
ρ_{air}	1.205	kg m ⁻³
$\rho_{\text{substrate}}$	1000	kg m ⁻³
μ_{air}	1.82×10^{-5}	Pa s ⁻¹
σ	5.67037×10^{-8}	W m ⁻² K ⁻⁴
η	0.75	
ϵ_{cover}	0.75	
$\epsilon_{\text{substrate}}$	0.67	
Prandtl number	0.7	

3.1.2. Heat transfer model sensitivity analysis

To investigate the effect of weather conditions on operational temperature at different regions around the world, two other cases are compared. The weather cases are used to simulate conditions of an unheated digester in Norway and Uganda as well. Different heat transfer processes are compared among these cases as well.

For the Norwegian case, data for solar irradiance was taken from the World Radiation Data Centre [104], and for mean wind speed, air temperature and ground temperature from the Klima Service Senter[74]. For Uganda, monthly average reported in an United Nations Habitat report were used [72].

In order to investigate the sensitivity of the heat transfer model on design and operational parameters, a one-at-a-time (OAT) sensitivity analysis is done. In this analysis, several parameters are selected to vary over a certain range, in order to determine how fast the output of the model changes with different values of the selected parameter. The influence of volume, flow rate, and influent temperature are evaluated for the Dutch weather case, and the solar irradiance absorptivity factor η was investigated as well.

3.2. ADM 1 Model

The heat transfer model is used to calculate the operational temperature of the reactor. This is linked to the ADM1 model through several biochemical and physico-chemical relations. In addition, the three calculation methods for pH, as explained in chapter 2, have been included in the ADM1 and are validated against the BSM2 standard. Lastly, four simplifications of the complete model have been made.

3.2.1. pH calculation

The different methods for pH calculation, as described in chapter 2, are the Ordinary Differential Equation (ODE) [11, 85], the Differential Algebraic Equation (DAE) [11, 85] or the differentiated Ordinary Balance Equation (dODE) as proposed by Thamsiriroj and Murphy [95]. These three implementations are validated by simulation of the digestion of the initial and input values of the BSM2 at 35 °C for 200 days. This has been used as a standard for comparing implementations and extensions of the ADM1 [100]. All three methods are compared with two different numerical solver methods, the Radau and the DOP853 solvers of the SciPy python software package.

3.2.2. Simplifications

It was expected that coupling the temperature model to the ADM1 would increase the computational burden. In order to relieve the model of complexities in terms of number of parameters, four consecutive simplifications of the ADM1 have been made according to the method proposed in the article of Weinrich and Nelles [102]. However, calibration needed for adjusted parameter estimation were excluded due to the time frame for this thesis. The method and resulting simulations with these simplifications can be found in Appendix B

3.2.3. Temperature's effects on ADM1

Absolute temperature inhibition

In the research of Bergland, Dinamarca, and Bakke [15], three different sets of relations between temperature and growth parameters found in literature are compared [41, 28, 84]. These relations are validated for their accuracy in predicting the digestion of manure at three different temperatures. It was found that a combination of the relations, with relative values for kinetic parameters at temperatures as presented in Table 3.3, demonstrated the most accurate results. The validation data was attained from a manure digester in Norway operated at these temperatures.

In this thesis, instead of simulation at three distinct static temperatures, continuous functions for temperature inhibition in the form of (2.14) or (2.15) will be used. Therefore, the constants of the Arrhenius and cardinal equations should be found. In order to find the Arrhenius constants, a non-linear least-squares analysis is done through the points as presented in Table 3.3, using the SciPy software package in Python. As there are four parameters investigated for the Arrhenius equation (k_1 , k_2 , a_1 , a_2) and three data points available in Table 3.3, more data points are needed to do this analysis. It is, therefore, assumed that at 5 and 45 °C, all rates of mesophilic microbial activity will approximate 0. Therefore, it was presumed that the inhibition functions at these temperatures will have a value of 0.01. For the least-square-analysis through the five coordinates initial guess of parameter value for each reaction is provided using the values found in the double Arrhenius equation fitted through the

Table 3.3: Relative change in kinetic parameters for anaerobic digestion with temperature, taken from Bergland, Dinamarca, and Bakke [15]

Process	Temperature			Ref.
	25 °C	30 °C	35 °C	
Disintegration and hydrolysis (K_{dis} and K_{hyd})	0.48	0.74	1.00	[28]
Acidogenesis ($\mu_{m, su, aa, fa}$)	0.21	0.22	1.00	[28]
Acetogenesis ($\mu_{m, c4}$)	0.67	0.86	1.00	[84]
Acetogenesis propionate ($\mu_{m, pro}$)	0.70	0.90	1.00	[84]
Methanogenesis ($\mu_{m, h2}$ and $\mu_{m, ac}$)	0.48	0.70	1.00	[84]

methanogenic activity of *M. arboriphilus*, given in Pavlostathis and Giraldo-Gomez [76]. These values are 0.75, 0.14, 0.15 and 0.30 for k_1 , k_2 , a_1 and a_2 , respectively. The found function was used to produce 10.000 vectors over the temperature interval from 0 °C to 50 °C, and these vectors were normalized to the value 1, as they are to be used as inhibitions functions. The normalized vectors were curve fitted again to obtain the Arrhenius constants for the inhibition functions.

The cardinal temperature parameters T_{\min} , T_{opt} and T_{\max} for hydrolysis and methanogenesis are taken from Donoso-Bravo et al. [28]. The acidogenic values reported in this paper did not result in a representative graph, and was therefore not taken. Therefore, the least square analysis was done in the same manner as the Arrhenius equation for the unknown cardinal temperature parameters for acidogenesis and acetogenesis, except that the initial guess of parameter value is done with the parameters for hydrolysis found by Donoso-Bravo et al. [28]. The cardinal temperature equations did not require normalization, as the found relation already described the relation between values 0 and 1.

The found constants are used in their respective functions (2.14 and 2.15) in the model to determine the temperature inhibition factor for the given temperature of each time step. In the original ADM1, no inhibition for hydrolysis is yet present, as seen in (2.1). The term is therefore added to this equation, as shown in (3.1). The temperature inhibition term found for each respective Monod equation is added to the product term in (2.2)

$$\rho_{\text{hyd}} = k_{\text{hyd}} X_{\text{hyd}} I_{T,\text{hyd}} \quad (3.1)$$

In this research, the effect of temperature on the decay rate (K_d), the growth yield (Y) and half saturation (K_s) were disregarded because of the following reasons [15]:

- In the ADM1, the decay rate of biomass K_d has a constant small value. Because the scale of temperature fluctuations of this study is within the mesophilic range, the net temperature effect is assumed small and not altered.
- According to Monod [70], the growth yield remains a constant factor in the relation between substrate concentration and growth rate. This assumption is extended to temperature and was confirmed to vary non-significantly by batch experiments [15].
- In the original article of the ADM1, it was recommended that the temperature dependency for biochemical reactions was expressed through $\mu_{m,i}$. Therefore, the effect of temperature on K_S is disregarded.

Dynamic temperature inhibition

As stated in chapter 1, the change in temperature over time should be limited for digestion process stability, as micro-organisms have to adapt to new temperatures. Kovalovszki et al. [56] proposed an extension for the BioModel, which simulates the decrease in microbial activity when the change in temperature over time is high. This was used to simulate the influence of temperature shocks on acetoclastic methanogens only, as they are generally considered the microbial group most sensitive to temperature change [81]. A similar function is implemented in this model. The implementation adds a state to the heat transfer model which follows the change in temperature with a lag factor. This state simulates the temperature to which the microbes are attuned to. The formula is given in (3.2). Here T_a is the temperature to which the acetogenic methanogens are attuned to, and τ_a is an adaptation constant, that represent the amount of days the microbes need to attune to a new temperature.

$$\frac{dT_a}{dt} = \frac{T_{op} - T_a}{\tau_a} \quad (3.2)$$

The difference between the operational temperature and the attuned temperature is used to calculate an inhibition factor to adjust the growth parameters of the acetogenic methanogens with. The formula for the temperature shock inhibition factor is given in (3.3) and (3.4). Here, σ_{shock} is a bell shaped parameter controlling the growth disturbance due to deviation between the operational and attuned temperature and s_{hg} is a constant which represents the temperature change which would half

the microbial growth at a set temperature.

$$I_{\text{shock}} = \exp\left(-\frac{(T_{op} - T_a)^2}{2\sigma_{\text{shock}}^2}\right) \quad (3.3)$$

$$\sigma_{\text{shock}} = \left(-\frac{s_{hg}^2}{2 \ln 0.5}\right)^{0.5} \quad (3.4)$$

In this way, the temperature shock function is used to calculate the inhibition factor at each time step, which is consequently used in the product term for inhibition as depicted in (2.2). The effect of this inhibition factor is showcased in the Dutch weather case simulation. The reactor follows the design and operation as shown in Table 3.1, and the values for τ_a and s_{hg} were taken as the mean values used by Kovalovszki et al. [56] at 15 d and 3.5 °C, respectively. Furthermore, the sensitivity of the combination of τ and s_{hg} on I_{shock} is analysed for the same case.

Physico-chemical factors dependent on temperature

In the model used in this thesis, the temperature dependent parameters defined in Rosen and Jeppsson [85], which include K_w , K_{a,CO_2} , $K_{a,IN}$, K_{H,CO_2} , K_{H,CH_4} , K_{H,H_2} and p_{gas,H_2O} , are made dependent on temperature using Henry's law (3.5) and the van 't Hoff equation (3.6), assuming that the gases behave according to the ideal gas law.

$$S_{E,i} = K_{H,i} * p_i \quad (3.5)$$

$$\ln \frac{K_{H,i,x}}{K_{H,i,T}} = \frac{\Delta H^\circ}{R} \left(\frac{1}{T_T} - \frac{1}{T_x} \right) \quad (3.6)$$

Another physico-chemical factor which is dependent on temperature is the k_{La} as shown in (2.5). This coefficient stems from the two-film theory of gas transfer. If the desorption of a slightly soluble gas is controlled by the liquid film transfer rate, the rate of mass transfer at steady state can be calculated by (3.7) [59, 67]. This equation is used in the ADM1, with unit conversions from COD to mole, as can be seen in (2.5).

$$\rho_{i \text{ liq-gas}} = k_L \frac{A}{V} (S_i - S_{E,i}) = k_{La} (S_i - S_{E,i}) \quad (3.7)$$

Here, A is the area through which the gas is transferred to volume V , S_i is the actual concentration of gas i in the liquid bulk phase in kg COD m⁻³ and $S_{E,i}$ is the equilibrium concentration of gas i as given by Henry's law in kg COD m⁻³. $(S_i - S_{E,i})$ therefore represents the degree of supersaturation.

According to Metcalf and Eddy [67], the value of k_{La} depends on water quality, the temperature and the type of aeration and/or mixing. This constant is determined experimentally for every situation. Pauss et al. [75] found a k_{La} of 3.84 ± 0.48 and $2.16 \pm 0.24 \text{ d}^{-1}$ for hydrogen and methane respectively in a 26.75 L CSTR fed with synthetically produced sludge, operated at 35 °C and mixed with a möbius-ribbon like paddle at 400 rpm. This found value for k_{La} is in stark contrast with the standard k_{La} of the ADM1, which has a constant value of 200 d^{-1} .

A relation between temperature and k_{La} was found by Lee [58]. This relation is shown in (3.8), and uses a predetermined k_{La} at a set temperature to calculate its value at a different temperature.

$$k_{La,sub} = k_{La,T} \frac{(E\rho_{\text{sub}}\sigma_t)_x}{(E\rho_{\text{sub}}\sigma_t)_T} \left(\frac{T_x}{T}\right)^5 \quad (3.8)$$

To investigate the effect of temperature on the k_{La} , this 5th order relation between k_{La} and temperature is used to find the relation between the base k_{La} at 35 °C and the temperature at which the liquid-gas transfer rate could potentially be the rate limiting factor for methane production. This done for both the k_{La} of Pauss et al. [75] and the original ADM1 k_{La} . The sensitivity of k_{La} on methane production in the ADM1 is investigated as well. This is done by varying the k_{La} from 0 to 2 for the digestion of BSM2 influent in a digester with design parameters of Table 3.1 for a period of one year, and comparing methane production.

3.3. Sludge characterisation

Sludge characterisation to determine influent states for the ADM1 has been done according to the methods proposed by Arnell et al. [7]. This method is based on biochemical fractionation of the total COD. For this method, the amount of TS, VS, tCOD, sCOD, VFAs, proteins, lipids, Total Ammonia Nitrogen (TAN), and a Biochemical Methane Potential test (BMP) are needed.

3.3.1. Sample collection

Samples have been taken at the La Trappe brewery in Berkel-Enschot, the Netherlands. 3 L of thickened WAS with a 16 % solids content was taken from the 1 m³ collection container of the belt thickener. Two samples of 3 L of spent wort (blond and quadruple) were taken from the discharge pipe at the end of the wort production process cycle, where roughly 200 L of spent wort are discharged per cycle. Samples from the influent of the Metabolic Network Reactor (MNR) were taken over a 24 h period with an interval of one hour. These were homogenized to create a mean representative sample for the influent. The effluent of the MNR was sampled at mid-day by collection of 2 L from the last reactor of the MNR series, which processes around 150 m³ d⁻¹. Samples were cooled in a fridge at 5 celsius over a period of two months for analysis. This storage period is longer than preferred for experiments, and further degradation of the sample could have taken place during this time. This should be taken into account when conclusions are drawn from the given results.

3.3.2. Chemical analysis

The amount of total solids (TS) and volatile solids (VS) was analyzed using standard methods [6]. The total chemical oxygen demand (tCOD), soluble chemical oxygen demand (sCOD), total nitrogen (tN), ammonium (TAN) and phosphor (tP) were determined in triplicate using HACH kits. For the sCOD determination, samples were filtered through 45 µm glass fiber filters to retrieve the soluble fraction. For Volatile Fatty Acids (VFAs) analysis, samples were centrifuged at 10 000 rpm for five minutes and the supernatant was filtered through 45 µm glass fiber filters. Quantitative analysis was done in triplicate using Agilent Technologies 7890A GC system. Total Kjeldahl Nitrogen (TKN) was determined in triplicate using the Behr Labor-Technik Behrotest InKjel system. The resulting values for total nitrogen in g N kg⁻¹ substrate were converted to proteins in g COD kg⁻¹ substrate using (3.9). The amount of carbohydrates was determined in triplicate using the method of Dubois et al. [29] using a calibration curve made with glucose.

$$\text{proteins} \left[\text{g COD kg}^{-1} \right] = 6.25 \left[\frac{\text{g proteins}}{\text{g organicN}} \right] (\text{TKN} - \text{TAN}) 1.42 \left[\frac{\text{g O}_2}{\text{g proteins}} \right] \quad (3.9)$$

3.3.3. Biochemical methane potential test

A BMP test was done according to the standardized method as described in Holliger et al. [44], with the exception that instead of storage at room temperature, the inoculum was cooled at 5 °C for a period of two days before the test. This inoculum was taken from Harnaschpolder WWTP Continuously-fed Stirred Tank Reactor (CSTR) located in Delft, the Netherlands. This CSTR is fed with primary sludge and WAS and is operated at 35 °C. The inoculum had a tCOD concentration of 33.03 g kg⁻¹ sludge, and was used in a 2:1 ratio with substrate on g COD:g COD basis.

The test was done by using the Bioprocess control AMPTS2 system. 400 mL bottles were filled in triplicate with compositions shown in Table 3.4. The positive control was done with crystalline cellulose, and the amount added was both in grams cellulose as well as mL demiwater. The wort and sludge mixture sample consist of two parts sludge, one part blonde and one part quadruple spent wort on weight basis. The influent and effluent samples consists of the same ratio's, but five parts of either influent or effluent from the MNR were used for dilution. The ratio of substrate to demiwater were determined to attain a 7 g COD L⁻¹ final substrate concentration. Further preparation was done according to the procedure of the TU Delft waterlab [35]. The head space of the bottles was flushed for 1 minute with a gas composed of 70 % nitrogen and 30 % carbon dioxide. The bottles were placed in a 35 °C water bath and mechanically stirred every other minute at 10 rpm. The produced biogas was led through carbon dioxide absorption solutions filled with 3 M NaOH solution. The remaining methane gas was further led through a moisture filter and quantified in the Bioprocess control flow cell array with a 9 mL resolution.

Table 3.4: Different bottle compositions for the BMP tests.

Constituent	Unit	Blank	Positive	Wort and sludge	Influent	Effluent
substrate volume	mL	0	2.4	33.3	71.2	73.3
Inoculum volume	mL	169.5	169.5	169.5	169.5	169.5
Demi water	mL	223.8	221.4	190.6	152.6	150.6

3.3.4. Biochemical fractionation

For the fractionation of the tCOD to all the input states of the ADM1, the method proposed by Arnell et al. [7] was used. This method uses the results from the chemical analysis and the BMP test in COD balance equations to calculate unknown states. In this method, the first step is to determine the biodegradable fraction of the tCOD from the BMP test results, using (3.10).

$$f_d = \frac{B_0}{350 \text{ tCOD}} \quad (3.10)$$

The amount of particulate COD follows from the total and soluble COD according to (3.11).

$$\text{pCOD} = \text{tCOD} - \text{sCOD} \quad (3.11)$$

Now the inert fraction of the soluble and particulate parts can be calculated using (3.12) and (3.13).

$$S_I = \text{sCOD} * (1 - f_d) \quad (3.12)$$

$$X_I = \text{pCOD} * (1 - f_d) \quad (3.13)$$

The particulate biodegradable COD can be divided in proteins, lipids and carbohydrates by using (3.14), (3.15) and (3.16). Here, the used method deviates from the method proposed by Arnell et al. [7]. In the original procedure, the amount of carbohydrates is calculated by subtracting the amount of proteins and lipids from the biodegradable particulate COD. Here, the amount of lipids is calculated by subtracting the amount of proteins and carbohydrates. It is assumed that the biodegradability of each fraction is equal to the overall biodegradability f_d .

$$X_{ch} = C_{ch} f_d \quad (3.14)$$

$$X_{pr} = C_{pr} f_d \quad (3.15)$$

$$X_{li} = \text{pCOD} f_d - X_{ch} - X_{pr} \quad (3.16)$$

The soluble biodegradable COD is divided in seven states according to the VFA analysis and the fractionation as done above. The VFA concentrations of acetate, butyrate, propionate and valerate can be directly calculated from the VFA analysis and their COD conversion factors. The conversion factors used are 1.07, 1.51, 1.82 and 2.04 g COD g⁻¹ for acetate, propionate, butyrate and valerate, respectively. The amount of monosaccharides, amino acids and long-chain fatty acids is calculated with (3.17), (3.18) and (3.19).

$$S_{su} = (\text{sCOD} f_d - \text{tVFAs}) \frac{X_{ch}}{\text{pCOD} f_d} \quad (3.17)$$

$$S_{aa} = (\text{sCOD} f_d - \text{tVFAs}) \frac{X_{pr}}{\text{pCOD} f_d} \quad (3.18)$$

$$S_{fa} = (\text{sCOD} f_d - \text{tVFAs}) \frac{X_{li}}{\text{pCOD} f_d} \quad (3.19)$$

The soluble inorganic nitrogen content (S_{IN}) is calculated by (3.20).

$$S_{IN} = \frac{TAN}{M_N * 1000} \quad (3.20)$$

The rest of the influent state variables of the ADM1 are set to 0.

3.4. Calibration and simulation

3.4.1. BMP simulation

According to the method of Arnell et al. [7], the ADM1 can be used to simulate BMP tests to investigate the hydrolysis constants. To do this, the influent flow rate in the ADM1 is set to zero, and the volume is adapted to the size of the bottle. Furthermore, the initial state has to be set to the composition of the BMP test. For the substrate, the results of the biochemical fractionation are used. For the inoculum, the steady states output values of the BSM2 as presented in the work of Rosen and Jeppsson [85] are used. This file has non-zero entities for each state, enabling each function. It was deemed representative, as the BSM2 simulates the digestion of primary sludge and WAS of a municipal WWTP at mesophilic temperatures, which is similar to the Harnaspolder WWTP from where the inoculum of the experiments was collected. In order to make sure the BSM2 file is truly representative of the Harnaspolder inoculum, the blank bottle test is simulated first. The results of this simulation are compared with the blank test results from the experiment. Changes are made to the BSM2 file by converting particulate inert material (X_I) to particulate composite material (X_{xc}) to attain similar biodegradability for the inoculum. Once representative inoculum concentrations are found, the wort and sludge mixture bottle test will be simulated by summing the inoculum state concentrations with the concentrations of the wort and sludge mixture in the ratios used in the experiment. The simulated blank test is subtracted from the simulated wort and sludge mixture bottle test simulation, just as is done with the experimental results.

3.4.2. Design and operation

La Trappe

In order to predict biogas production at La Trappe, simulations are done for the digestion of the wort and sludge mixture as determined with the biochemical fractionation method and with concentrations based on literature. For these values, it is assumed that wort consists for 90% of carbohydrates [40], and the WAS from the MNR has similar concentrations as the BSM2 digester influent as presented in Rosen and Jeppsson [85]. The amount of base, represent by the concentration of cations, needed to prevent acidification is determined for both these substrates for the year 2021 is investigated. This found result is added to the influent concentration states and simulation of the operation of the digester as depicted in Table 3.1 and subjected to the Dutch weather conditions from 2000 till 2003 is done. Furthermore, the influence of increasing influent temperature from 35 °C to 45 °C is investigated for the literature based results.

Washout

The temperature coupled ADM1 model is to be used as an instrument to help in the design and operation of reactors prone to change in temperature. In the design process, a trade-off has to be made between efficiency and robustness. In an efficient design for biogas, the volume for a given influent flow is such that the HRT is just large enough that most of the biodegradable COD is converted to methane, without washing out the methanogenic species in the digester. However, in anaerobic digestion for VFA production, methanogenic washout can be necessary, and the HRT should be set to accomplish this. As stated before, the rates determining methanogenic metabolism are linked to temperature, and therefore, the final volume is important for preventing or stimulating washout. To showcase this dependency, the model will be used to depict methane production and VFA concentration over volume and temperature. For this simulation, the BSM2 influent will be used for digestion in a reactor with the design parameters as shown in Table 3.1. Because these will be steady-state simulations, the weather dependent heat transfer model is not used, but constant inhibition coefficients are calculated for simulation at each temperature.

Overloading

In the operation of an anaerobic digester, a common type of failure is acidification due to overloading. In order to see the capability of the model to simulate these situations, the relation between OLR, temperature and methane production is investigated. Therefore, the digestion of the BSM2 influent is simulated in a reactor with the design and operation as shown in Table 3.1, with an operational temperature varying from 20 to 40 °C. For the influent, the ratio's of the BSM2 influent are kept, but their total loading rate is varied from 1 to 20 kg COD m⁻³ d⁻¹.

Furthermore, the influence cation dosage and volume for the digestion of the literature based wort and sludge mixture at an influent temperature of 45 °C in a digester with the design and operation as shown in Table 3.1 and subjected to the Dutch weather conditions of 2021 is investigated. Lastly, the effect of the particular cold winter of the Netherlands of 2010 on biogas production for the similar case but with an influent temperature of 35 °C and with minimal base dosage is simulated.

Heating

In practicality, most industrial digesters are kept at a steady temperature of 35 °C. To keep a digester at this temperature requires external heating, especially in winter. In some designs, the internally produced biogas is used for this heating application, which lowers the net biogas production. A flowchart of how this kind of heating would alter biogas flow for the La Trappe case is shown in Figure 3.1. From a controllers perspective, this means that heating is activated once the digesters' temperature reaches, for example, 34.5 °C, and that the heating is stopped once the temperature is 35 °C again. This is often automated by a thermostat-like device in which this lowest temperature before heating is activated (T_{Heater}), is installed. Having a higher T_{Heater} will insure that in winter a higher absolute biogas production is attained, but more biogas is used for heating, which lowers the net biogas production. One can question if for maximizing the net biogas production, it would not be more beneficial to only activate heating at a lower temperature, and therefore operate the digester with a lower T_{Heater} . In order to investigate this, a simulation is done where biogas is burned for heating the bulk liquid if the temperature calculated with the heat transfer model is lower than the operationally minimal temperature T_{Heater} . The amount of methane burned in m^3 to keep the digester at T_{Heater} is calculated with the formula as depicted in (3.21), and subtracted from the totally produced methane. The lower heating value of methane is assumed to be $35.5 \times 10^6 \text{ J m}^{-3}$ [96].

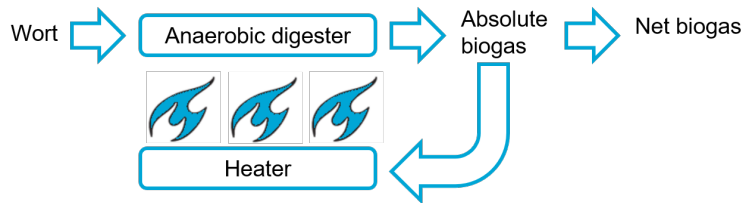


Figure 3.1: Flowchart showcasing the difference between absolute and net biogas production when biogas is used to heat the anaerobic digester.

$$CH_4_{burned} = \frac{(T_{Heater} - T_{op}) V_{sub} C_{sub} \rho_{sub}}{LHV_{CH_4}} \quad (3.21)$$

This formula is implemented with a loop which sets negative values to zero. For positive values of the equation, the change in temperature in the heat transfer model for the given time step is found with (3.22). This ensures that the calculated operational temperature for such a step is T_{Heater} .

$$\frac{dT}{dt} = T_{Heater} - T_{op} \quad (3.22)$$

To investigate the relation between the net biogas production and the operational heating temperature, the yearly biogas production of an anaerobic digester with the design and operation as in Table 3.1, fed with BSM2 and both compositions of the wort and sludge mixtures based on either the biochemical fractionation procedure or literature are subjected to the Dutch weather conditions of 2021 is simulated. The yearly net biogas production is found for operational heating temperatures varying from 20 to 40 °C.

4

Results and discussion

First the modifications made to the ADM1 are presented, as based on these results choices have been made on simulation settings later used. The functioning of the dynamic temperature inhibition function is presented together with the heat transfer model analysis, as this function can only be showcased under temperature fluctuations.

4.1. ADM1 model modifications

4.1.1. pH calculations

All three implementations of the pH calculation are run at steady state for validation. The attained concentrations of each state are compared to the standardized simulation results of the BSM2 used for validation. The absolute errors of each state with the original BSM2 steady state output for each pH implementation is shown in Table 4.1. The attained results with the DAE calculation method and the Radau solver are closest to the original BSM2 implementation, with the largest error of 6×10^{-7} for the particulate inert state (X_I).

According to the BSM2 report, this level of error validates the used method [12]. This was done with the lowest calculation time as well. This result is surprising, as it was stated that 'The choice between ODE and DAE is up to the user. If acceptable computation times can be achieved with the ODE implementation there is no other advantage to use DAE [85].' The results found here however, suggest that such an advantage does exist, as the DAE outputs do stay closer to the original outputs. The paper of Rosen and Jeppsson [85] does however not explicitly state which method they used in creation of the found standard steady state outputs for validation. The found errors are in addition even smaller than in the validation study of the PyADM1 [87]. This could be due to the change in solver method, from DOP853 to Radau, or by the change in data storage over simulation as can be found in the code in Appendix C. The Radau solver does give consistently more accurate results over all three pH calculation methods. Outcomes hindered by the stiffness of the system can be found in the results produced for the ODE and dODE pH calculation and the DOP853 solver method, where the values of hydrogen gas are overestimated by far. Based on these results the DAE implementation with the Radau solver was chosen to be used in all other simulations, unless stated otherwise.

Table 4.1: Comparison of different pH equation solving methods and numerical solvers. Absolute differences between the results of the simulation and the ADM1 benchmark model steady-state results for validation for each state are listed. Run times per simulation are given in seconds and the highest absolute difference, depicting the largest error, for each pH solving method and numerical solver are printed in bold.

Parameter Solver	ODE		DAE		dODE	
	DOP853	Radau	DOP853	Radau	DOP853	Radau
Runtime	5962	100	111	96	123	112
S_{su}	1.155 985	7.11×10^{-9}	2.98×10^{-10}	3×10^{-10}	1.155 977	2.19×10^{-9}
S_{aa}	0.322 508	2.45×10^{-9}	9.13×10^{-12}	7.2×10^{-12}	0.322 506	8.46×10^{-10}
S_{fa}	7.604 497	1.22×10^{-7}	5.24×10^{-10}	4.95×10^{-10}	7.604 497	2.06×10^{-8}
S_{va}	4.572 878	4.05×10^{-9}	1.2×10^{-11}	1.12×10^{-11}	4.572 878	1.84×10^{-9}
S_{bu}	5.907 456	8.73×10^{-9}	1.28×10^{-11}	1.31×10^{-11}	5.907 457	2.3×10^{-9}
S_{pro}	2.515 138	1.22×10^{-8}	4.54×10^{-10}	4.56×10^{-10}	2.515 14	3.54×10^{-9}
S_{ac}	10.0562	0.013 598	2.59×10^{-6}	5.5×10^{-8}	10.090 98	0.000 671
S_{H_2}	436.4686	6.61×10^{-14}	4.54×10^{-14}	4.48×10^{-14}	436.558	6.58×10^{-14}
S_{CH_4}	453.05	0.000 336	2.4×10^{-7}	4.17×10^{-13}	453.0349	0.000 189
S_{IC}	8.495 797	0.004 571	5.42×10^{-7}	1.07×10^{-8}	8.496 482	0.002 702
S_{IN}	0.130 226	3.17×10^{-6}	1.17×10^{-8}	1.22×10^{-8}	0.130 226	1.42×10^{-7}
S_I	0.740 734	1.76×10^{-5}	1.49×10^{-7}	1.55×10^{-7}	0.740 734	7.4×10^{-7}
X_{xc}	0.740 753	1.83×10^{-5}	3.69×10^{-9}	9.43×10^{-10}	0.740 753	8.94×10^{-7}
X_{ch}	0.007 371	1.82×10^{-7}	3.78×10^{-11}	9.49×10^{-12}	0.007 371	8.89×10^{-9}
X_{pr}	0.007 371	1.82×10^{-7}	3.78×10^{-11}	9.43×10^{-12}	0.007 371	8.89×10^{-9}
X_{li}	0.011 056	2.73×10^{-7}	5.67×10^{-11}	1.42×10^{-11}	0.011 056	1.33×10^{-8}
X_{su}	0.030 622	2.71×10^{-6}	9.6×10^{-9}	1.05×10^{-8}	0.030 623	1.26×10^{-7}
X_{aa}	0.065 808	2.01×10^{-6}	1.13×10^{-9}	1.77×10^{-9}	0.065 808	9.99×10^{-8}
X_{fa}	0.235 892	2.14×10^{-6}	1.69×10^{-9}	9.98×10^{-10}	0.235 892	1.09×10^{-7}
X_{C_4}	0.424 778	8.68×10^{-7}	7.5×10^{-10}	4.72×10^{-10}	0.424 778	4.43×10^{-8}
X_{pro}	0.130 163	4.19×10^{-7}	3.18×10^{-9}	3.32×10^{-9}	0.130 163	1.76×10^{-8}
X_{ac}	0.751 764	0.000 495	7×10^{-8}	3.85×10^{-9}	0.752 984	2.41×10^{-5}
X_{H_2}	21.816 87	1.33×10^{-6}	4.4×10^{-9}	4.79×10^{-9}	21.818 09	8.73×10^{-8}
X_I	1.481 467	3.42×10^{-5}	6.1×10^{-7}	5.99×10^{-7}	1.481 467	2.39×10^{-6}
S_{cation}	0	0	0	0	0	0
S_{anion}	0	0	0	0	0	0
$S_{H_{ion}}$	3.1072×10^{-11}	1.6911×10^{-9}	3.5806×10^{-11}	3.4364×10^{-11}	3.42×10^{-8}	6.8256×10^{-10}
$S_{va_{ion}}$	4.561 566	1.38×10^{-6}	1.2×10^{-9}	9.05×10^{-12}	0.000 596	0.000 596
$S_{bu_{ion}}$	5.894 126	1.44×10^{-6}	1.25×10^{-9}	1.09×10^{-11}	0.000 221	0.000 221
$S_{pro_{ion}}$	2.508 624	1.96×10^{-6}	2.17×10^{-9}	4.57×10^{-10}	0.000 257	0.000 257
$S_{ac_{ion}}$	10.033 27	0.013 589	2.57×10^{-6}	5.49×10^{-8}	0.002 759	0.002 759
$S_{HCO_3_{ion}}$	7.944 936	0.004 708	1.16×10^{-7}	1.07×10^{-8}	0.002 777	0.002 777
S_{CO_2}	0.550 861	0.000 137	4.26×10^{-7}	2.58×10^{-12}	8.493 704	7.56×10^{-5}
S_{NH_3}	0.004 091	0.000 183	1.68×10^{-7}	6.81×10^{-10}	9.07×10^{-6}	9.07×10^{-6}
$S_{NH_4_{ion}}$	0.126 136	0.000 18	1.56×10^{-7}	1.16×10^{-8}	0.130 235	8.93×10^{-6}
S_{gasH_2}	23 067.93	1.39×10^{-8}	2.88×10^{-10}	1.62×10^{-13}	23 072.65	7.14×10^{-9}
S_{gasCH_4}	15 218.74	0.011 416	3.74×10^{-5}	5.38×10^{-11}	15 218.23	0.006 348
S_{gasCO_2}	0.791 919	0.000 195	9.61×10^{-6}	4.35×10^{-12}	12.211 99	0.000 108

4.1.2. Absolute temperature inhibition

A non-linear least squares error analysis is done to find all parameters for the Arrhenius equation as shown in (2.14) and the acidogenic and acetogenic parameters for the cardinal temperature equation as shown in (2.15). This was done using the data of Table 3.3 and the estimated points (5, 0.01) and (45, 0.01). Normalization had to be applied to the Arrhenius equation as, due to the low amount of measurements available, the Arrhenius equation fitted over the value of 1.0. This means that in the original fit, some temperature values higher than the optimal temperature resulted in inhibition factor above value 1. This is in contrast with the definition of the inhibition function, which should not be able to increase the rates. Therefore, normalization was applied to vectors produced with the found relation, and the normalized vectors were used in a second least-squares analysis to find the Arrhenius constants for this normalized relation. This resulted in the parameters as shown in Table 4.2 and 4.3.

Using these parameters, relations between temperature and growth parameters shown in Figure 4.1 are produced. These appear similar to the once found in Donoso-Bravo et al. [28] and Rebac et al. [84], which supplied the original data. It can be seen that the Arrhenius relation has an mostly upward concavity, giving a 'steeper' relation. The concavity of the cardinal temperature equation is downward for most of the temperature region of interest, making these microbes more suitable for a broader range of temperatures. It could be hypothesised that digesters kept at steady temperatures will produce microbial consortia specialized at that specific temperature region, while in digesters with temperature fluctuations the microbes will be adapted to a broader range of temperatures. It is therefore expected that the microbial consortia of a digester with seasonal temperature fluctuations is better represented with the relation between temperature and microbial activity as described by the found constants for the cardinal temperature equation, compared to the Arrhenius.

Comparing the results of the Arrhenius equation and the cardinal temperature equation, it is found that the optimal temperature values for the Arrhenius relation are higher than the expected 35 °C. The overshoot is most strongly present in Figure 4.1c. This is likely the case because this reaction is most dependent on temperature, as can be found in the data found by Rebac et al. [84]. The optimal temperature as depicted with the cardinal temperature equation stays closer to the expected point of 35 °C. The course of this equation does however have an unexpected increase at temperature below 15 °C. This increase is an artifact of the equation used, but as temperatures of the simulations do not reach the values where this artifact is present, it is ignored. The cardinal equation does generally follow the expected curves, with one parameter less than the Arrhenius equation, and should therefore be favoured according to Occam's razor [86]. Based on these results the cardinal equation was chosen to be used in all other simulations, unless stated otherwise.

Table 4.2: Constants for the Arrhenius temperature inhibition equation as shown in (2.14) for each degradation step, found by non-linear least squares analysis and normalisation of the microbial activity with temperature coefficients as shown in Table 3.3

	k_1	a_1	k_2	a_2
K_{hyd}	0.620	7.82×10^{-2}	7.79×10^{-5}	0.976
$\mu_{m,acido}$	0.183	0.243	9.46×10^{-5}	0.998
$\mu_{m,c4}$	0.717	5.73×10^{-2}	7.86×10^{-5}	0.969
$\mu_{m,pro}$	0.732	5.41×10^{-2}	7.75×10^{-5}	0.969
$\mu_{m,H_2}, \mu_{m,ac}$	0.608	8.12×10^{-2}	8.17×10^{-5}	0.972

Table 4.3: Constants for the cardinal temperature inhibition equation as shown in (2.15) for each degradation step. The values with (*) are taken from Donoso-Bravo et al. [28]. The other values are found by non-linear least squares analysis of the microbial activity with temperature coefficients as shown in Table 3.3.

	T_{min}	T_{opt}	T_{max}
K_{hyd}^*	4.2	40.3	45.5
$\mu_{m,acido}$	12.6	40.9	45.0
$\mu_{m,c4}$	1.7	35.8	45.0
$\mu_{m,pro}$	2.4	34.9	45.0
$\mu_{m,H_2}, k_{m,ac}^*$	11.1	34.1	46.3

It is important to attain more data on growth coefficients over temperature data points of these microorganisms, especially at higher than optimal temperatures, so the inhibition functions can be compared for accuracy and better constants can be found for the used equations of these organisms. Similar research as the ones referenced in Bergland, Dinamarca, and Bakke [15] article should be undertaken to find the relation between the first-order and Monod maximum specific uptake rate coefficients and temperature.

In that case, also the difference between different metabolic pathways within the same digestion step could be investigated. In the model presented in this thesis, the relation between temperature and the Monod growth coefficient of hydrogenotrophic methanogens is assumed equal to the relation of acetogenic methanogens. However, it is known that the decrease in growth rates with temperature decrease of acetogenic methanogens is larger than in hydrogenotrophic methanogens [81]. Because this relation is set equal for both these species, the absolute inhibition factors for hydrogenotrophic methanogens will have more influence than expected in reality. Therefore, biogas produced at lower temperatures might be underestimated.

Similarly, the current model does not account for differences in the effect of temperature on the hydrolysis and acidogenic rates of different substrates. It is for example plausible that LCFA metabolizing acidogens react differently to temperature than amino acid metabolizing acidogens, but these microbes now have the same temperature inhibition constants. The exact effect of temperature on these rates will however vary between different substrate sources and might therefore be harder to define definitely. This could still be done for a given substrate with the used BMP curve fit procedure [7], combined with running the BMP at different temperatures, as proposed in Donoso-Bravo et al. [28].

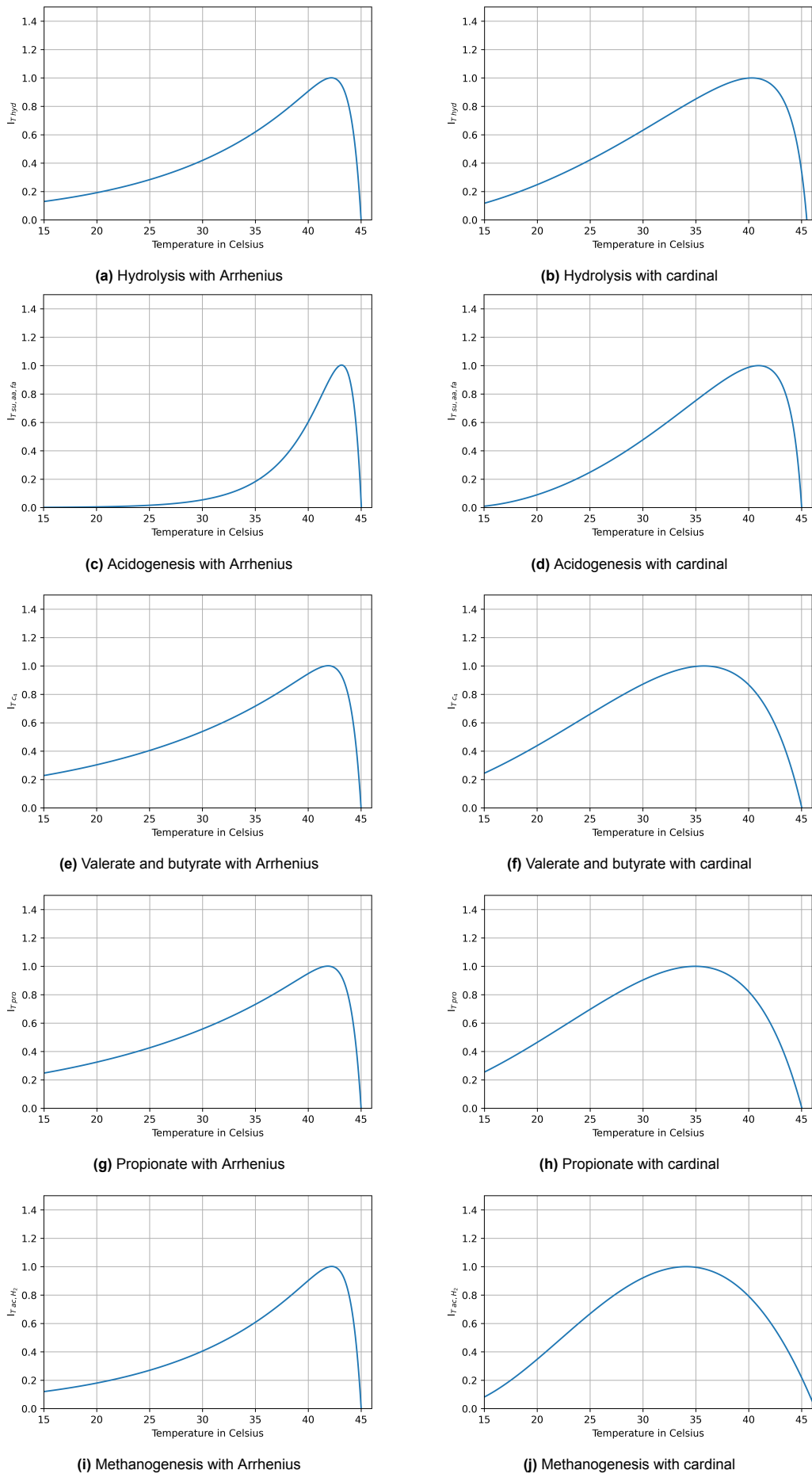
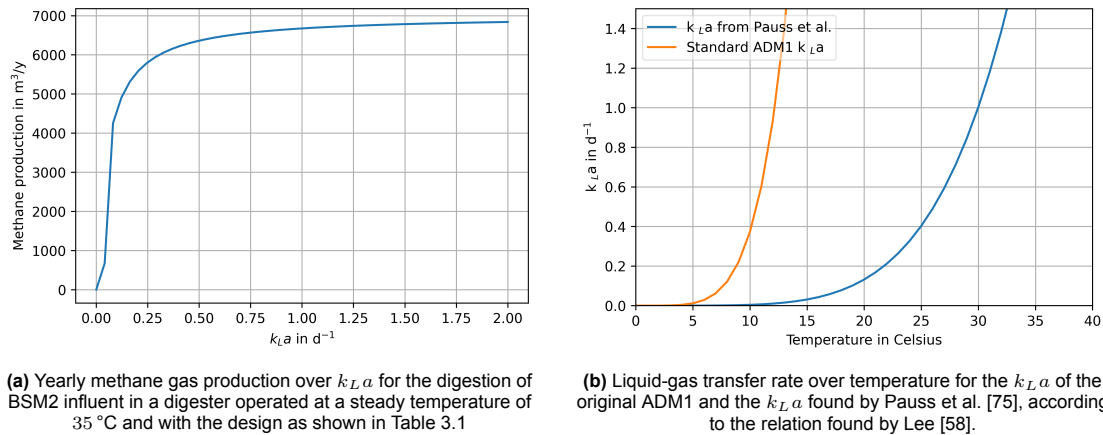


Figure 4.1: Temperature inhibition as a function of temperature with the found Arrhenius and cardinal equation constants shown in Tables 4.2 and 4.3 for different anaerobic degradation steps.

4.1.3. Liquid - gas transfer coefficient

The 5th order relation between k_{La} and temperature is used to predict the k_{La} of Paus et al. [75] and the standard ADM1 k_{La} at specific temperatures. Furthermore, the relation between k_{La} and yearly methane production from the digestion of BSM2 influent in a digester operated at 35 °C and with the design as shown in Table 3.1 is simulated. These relations are shown in Figure 4.2.



(a) Yearly methane gas production over k_{La} for the digestion of BSM2 influent in a digester operated at a steady temperature of 35 °C and with the design as shown in Table 3.1

(b) Liquid-gas transfer rate over temperature for the k_{La} of the original ADM1 and the k_{La} found by Paus et al. [75], according to the relation found by Lee [58].

Figure 4.2: Dependence of methane gas production on k_{La} and the influence of temperature on k_{La} . (a) The liquid gas transfer becomes rate limiting for biogas production at values for k_{La} lower than 1.0. (b) the dependence of k_{La} on temperature.

It can be seen in Figure 4.2a that for values of k_{La} above 1.0, methane gas production only increases slightly. Values lower than this point do impact the methane production rate negatively, as the liquid-gas transfer step becomes the rate limiting step in methane production. In these simulation, equal amounts of methane are produced, but only the difference between the concentrations in the soluble phase and in the gas phase are changed by the k_{La} . A similar result was found in a sensitivity analysis done by Feng et al. [33], who concluded that the biogas production in the ADM1 is not influenced significantly by the value of k_{La} unless it is lower than 1.0 d⁻¹. This is expected, as it can be noted in (2.5) that if the value of k_{La} becomes lower than 1.0, it effectively acts in the same manner as an inhibition function.

The k_{La} of the original ADM1 was set to a constant value of 200, under the assumption that all gas would desorb at 35 °C. Figure 4.2b shows that, using (3.8), this k_{La} would only be reduced to below 1.0 d⁻¹ if temperature would reach a value below 13 °C, which is unlikely to occur in a mesophilic reactor. However, using the k_{La} of 2.16 at 35 °C for methane found in the lab experiments of Paus et al. [75], the temperature at which an k_{La} of 1.0 is reached is 30 °C.

If this k_{La} is representative for unstirred, fixed-dome digesters, an undesirable phenomenon could occur. Methane gas would stay dissolved in the bulk liquid due to the low k_{La} and will therefore be present in the effluent digestate leaving the digester. If this digestate is exposed to the atmosphere, the gas will desorb immediately, as the partial pressure of methane in the atmosphere is negligible, increasing the degree of supersaturation of methane dissolved in the digestate. This would mean that the operation of a digester at that temperature would actively waste its product as a greenhouse gas. This could also be one of the reasons why the biogas production in unheated household anaerobic digesters is lower than expected in regions further from the equator, which causes these digesters to be abandoned [63, 61, 101]. Furthermore, due to the large amount of unheated household anaerobic digesters implemented around the world in the last two decades, this effect could potentially be a partial explanation of the unknown cause of the acceleration in methane emissions observed since 2007 [30].

However, as the k_{La} of a laboratory set-up is taken as a base for this argumentation, it must be stated that, to the authors' knowledge, the k_{La} of unstirred, unheated, fixed-dome digesters for different substrates is as of yet not available in literature. Furthermore, the formula of Lee [58] used for linking k_{La} to temperature was made for the absorption of oxygen in aeration systems. Even though both

methane and oxygen have similar values for solubility and the transfer of both gases are liquid-film dependent, it must first be determined if the found relation can be applied directly to the desorption of methane as well. Because these concerns have first to be researched for validity, the original ADM1 value for $k_L a$ was used in the following simulations, unless stated otherwise.

4.2. Heat transfer model and dynamic temperature inhibition

The La Trappe case

The heat transfer model was used to predict the temperature of an unheated digester with the design parameters as shown in Table 3.1 and the weather data of the Netherlands. The simulation for the year 2021 resulted in the operational temperature (T_{op}) and the attuned temperature of acetoclastic methanogens (T_a) as shown in Figure 4.3a. Furthermore, the value for the dynamic inhibition function is found for the duration of this year, and shown in Figure 4.3b. The heat flows in Joules per heat transfer process contributing to temperature change over this simulation are shown in Figure 4.3c. Lastly, the same figures are produced for simulation of a reactor with 2 cm of fiberglass insulation, and these are shown in Figures 4.3d till f.

The yearly heat fluctuation follows similar values as could be expected from literature, as Merlin et al. [66] reported similar temperature fluctuation of an unheated but insulated digester of similar dimensions, fed with heated influent and exposed to the weather conditions of the French Alps. The large increase in temperature occurring at day 150 coincides with the largest decrease in the dynamic temperature inhibition factor I_{shock} , as expected. It will therefore become beneficial for acetogenic methanogenesis to limit the speed of temperature change, with the implementation of this function.

Comparing figure 4.3a and d, it can be observed that adding a 2 cm fiberglass insulation layer increases the minimum, mean and maximum temperature attained. The insulation increases the resistance for convection, which therefore lowers the amount of heat lost especially in summer, as is shown in Figures 4.3c and f. The convective heat loss is already lower than conventional reactors due the fact that the digester is buried. Due to the lower amount of heat loss in summer, the maximum temperature increases. However, the addition of insulation increases the minimal temperature in winter less then the maximum of summer, due to the fact that in winter radiance is an equally important sink of heat as convection. The yearly temperature fluctuation is therefore increased with insulation. To increase heat retention in winter efficiently, a combination of convective and radiative insulation is needed.

Figure 4.3d shows that in summer, for a short period, the temperature in the digester rose to above 35 °C, making influent advection a heat sink instead of a source. This can be seen in Figure 4.3f by the fact that during this event, advection attained negative values. This occurrence is caused by the high amount of solar irradiance during these days. The heat captured from irradiance is not dependent on digester temperature and will therefore always be a source. However, this interpretation of the effect of solar irradiance might be an oversimplification.

In reality solar irradiance heats up the cover of the digester, and convective and conductive heat transfer process then transport this heat from the cover to the bulk liquid. This kind of approach is taken in the heat transfer model developed by Terradas-III et al. [94], where the temperature in the cover and in the biogas are taken as states as well as the operational bulk liquid temperature. This model will result in more realistic effect of solar irradiance on operational temperature then using the factor η , which is used in the model of this thesis and in the model of Vilms Pedersen et al. [98]. However, the high dependence of bulk liquid temperature on solar irradiance was also found in the validated heat transfer model of a buried household anaerobic digester of Bandgar et al. [10].

The found yearly mean dynamic temperature inhibition function and the absolute inhibition function of acetoclastic methanogens for both simulations are given in Table 4.4. It shows that the shock inhibition function decreases with insulation. This is due to the increased temperature fluctuations. This effect is however overshadowed by the increase of the absolute inhibition function. It was therefore deemed beneficial to include insulation for biogas production under Dutch climatic conditions, and insulation is therefore included in subsequent simulations.

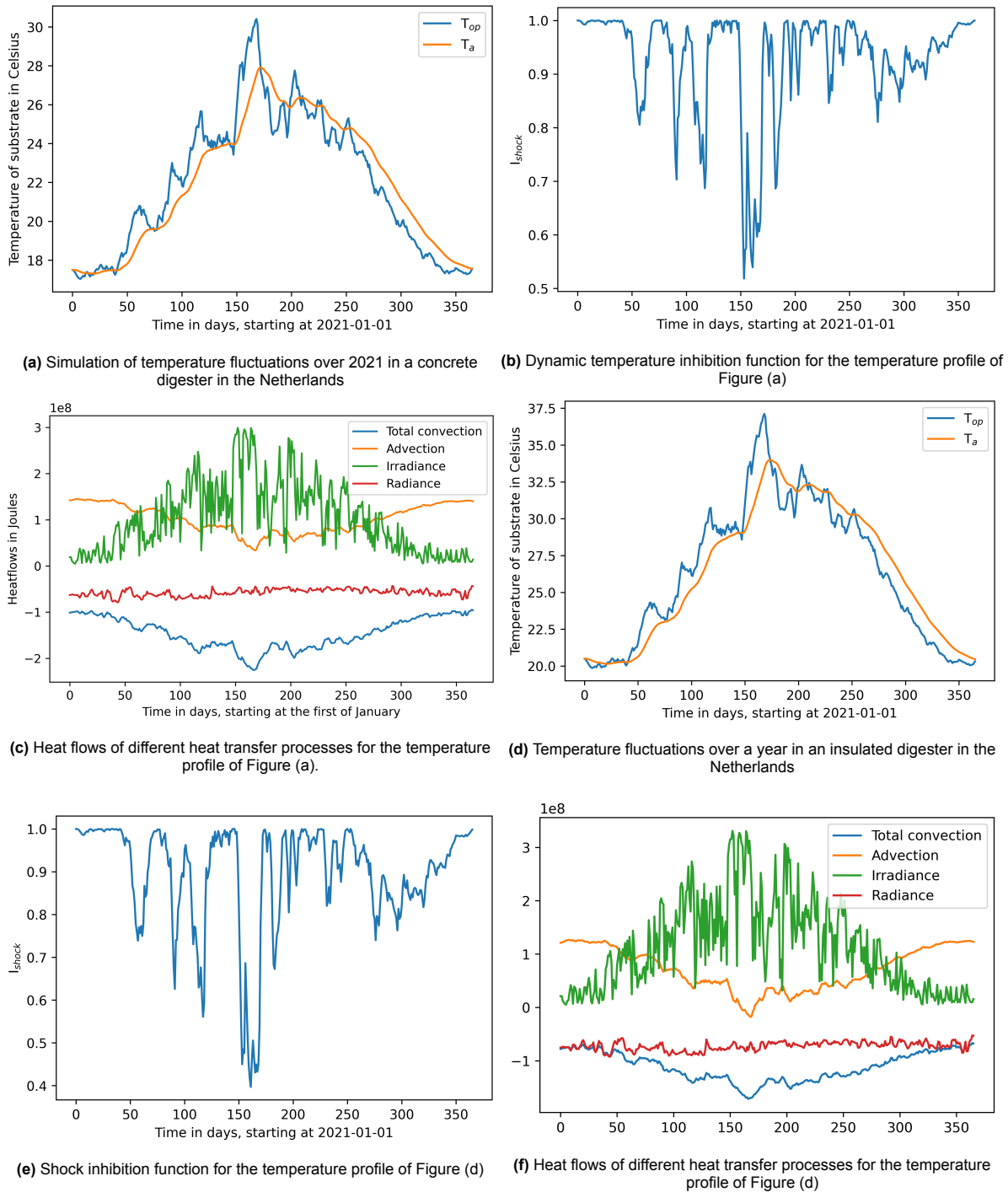


Figure 4.3: Simulations of the influence of the weather conditions of the Netherlands of 2021 on operational temperature and the attuned temperature of the acetoclastic methanogens for concrete and insulated digesters. The shock inhibition function and different heat flows over time for the simulations are shown as well. In Figures (a) till (c) simulation was done without the insulation layer, while in the simulation of Figures (d) till (f) the insulation layer as given in Table 3.1 was present.

Climate

Different climatic cases for concrete digesters in Norway and Uganda were compared for their influence on operational temperature. The simulated digester has the design and operational parameters as shown in Table 3.1 without insulation. Resulting yearly temperature fluctuations and heat transfer processes are shown in Figure 4.4.

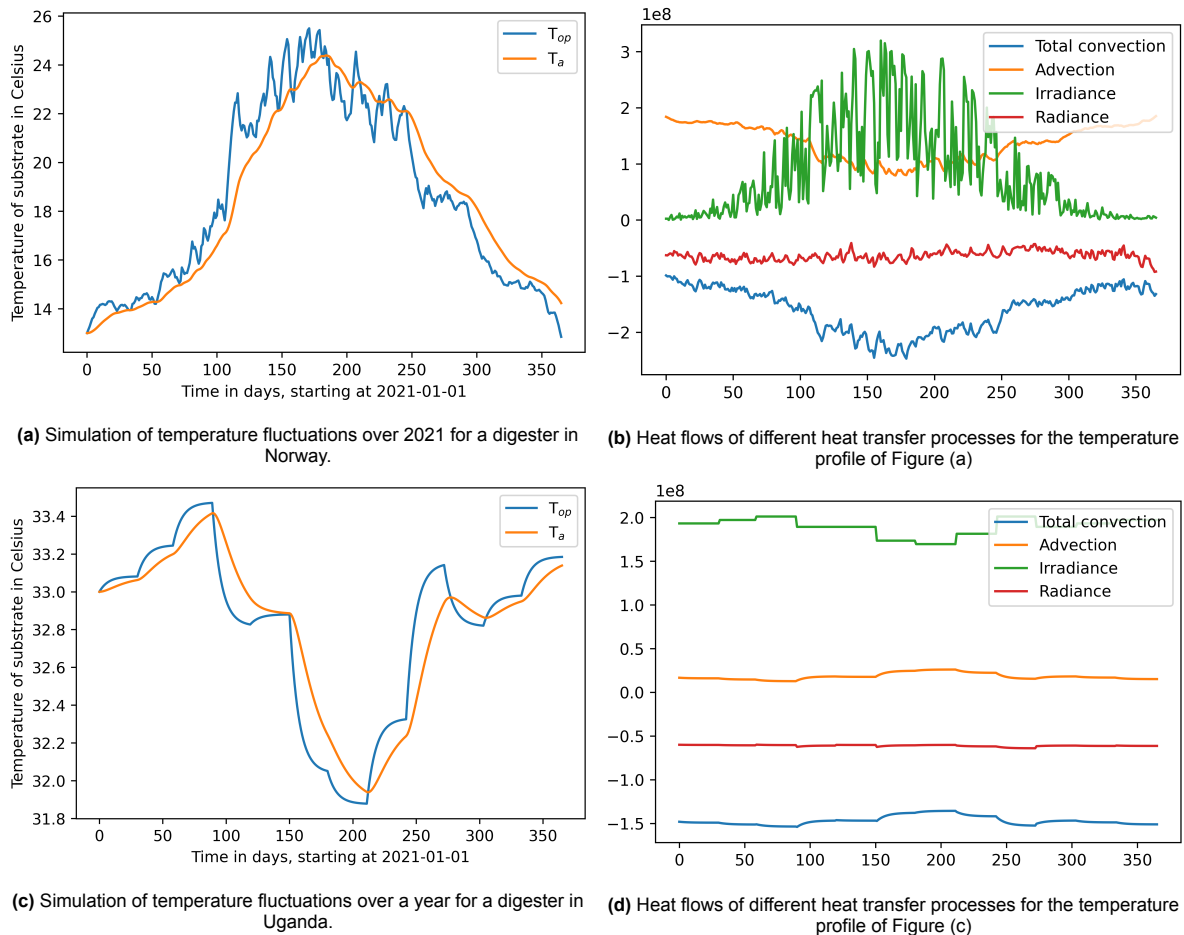


Figure 4.4: Simulation of the yearly temperature profile of digesters subjected to the climatic conditions of Norway and Uganda.

The heat flows per simulation show that in winter, advection is the key contributor to temperature for the Norwegian case. In winters in Norway, the amount of sunlight is limited, causing the solar irradiance to approach zero. In summer however, solar irradiance becomes a larger source of heat than advection.

For Uganda, which is located on the equator, seasonality causes less changes to the reactor over the year, and irradiance throughout the year is the largest source of heat. As irradiance is quite constant, the addition of insulation could potentially result in temperatures within the reactor higher than influent temperatures as well. It must be noted that the influent temperature of $35\text{ }^{\circ}\text{C}$ for comparison with the other weather cases. The high bulk liquid temperature and low temperature fluctuation of this simulation will allow for low values of temperature inhibition functions.

The yearly mean of the absolute temperature inhibition function for acetoclastic methanogens and the dynamic temperature inhibition function for the four studied scenarios are shown in Table 4.4. The values of these inhibition functions highlight why unheated digesters are feasible around the equator and why heating is applied in anaerobic digesters in colder climates.

Design and operational parameters

In order to investigate the influence of the design and operation of the digester on yearly temperature fluctuations, the effects of volume, flow rate and the influent temperature have been simulated in an OAT sensitivity analysis. The operational temperature over the year has been simulated over a certain range for each parameter. The resulting relation between these factors and operational temperature is shown in figure 4.5. Here the minimal, maximal, mean, 25th percentile and 75th percentile of the temperature in each simulation are presented over the parameter range.

As can be expected, a larger volume will result in a more stable temperature, as shown in Figure 4.5a. This is due to two factors. By having a larger volume, the amount of surface area per unit of volume decreases, which lowers the relative amount of conductive heat loss. Therefore, the heat in the digester is stored more efficiently. The second factor encompasses that, by having a larger volume, the overall heat capacity of the reactor increases, simply by having more volume to store heat in. This effect is also known as thermal inertia, and could be achieved in smaller digesters by including a layer of material with a high heat capacity between the concrete and insulation, like basalt [89].

The operational bulk liquid temperatures dependency on flow rate is shown in Figure 4.5b. Operational temperature will approach influent temperature at high flows. This supports the building of high-volume and high-rate digesters. For HRT, it is shown in Figure 4.5c that a larger volume gives less temperature fluctuations. A smaller HRT, given that influent temperature is constant, will therefore also increase operational temperature and decrease temperature fluctuations.

In the model, volume determines the dimensions of the digester, which is assumed to be a cube. When volume increases, the area of each side of the cube increases, which in turn influences the surface area for conduction between the soil and the digester wall. It is therefore beneficial to build the buried digesters in spheres, as this would maximize the volume to surface area ratio. Furthermore, less dead zones would emerge in such a reactor, optimizing volume utility and mixing.

The found influence of climatic conditions, reactor design and operational strategies can be used to predict what type of digester would be able to operate where, under which conditions. This kind of research is recently been published for other climates. Rashidian, Mahmoudimehr, and Atashkari [83] used similar relations to determine minimal volume, burial depth and influent temperature to operate fixed-dome digesters in Iran. Yan et al. [107] recommended sustainable types of heating for buried fixed-dome digesters for each region in China, based on available renewable energy sources and potential increase in biogas production. Similar research could be done with the proposed model, but this was deemed out of the scope of this thesis.

Solar irradiance

The absorptivity parameter η , which determines the amount of solar irradiation heat reaching the bulk liquid, has been investigated for its influence on the temperature and on the temperature variability. Figure 4.5f shows this relation.

The solar irradiance has especially influence on the maximum operational temperature. This is inline with the thermal model and validation experiments of Bandgar et al. [10], which found a strong relation between solar irradiance and biogas production. In the model used in this thesis, the amount of energy in J transferred from the solar rays to the bulk liquid is determined by the absorptivity constant η , as in (2.17). This constant was set to 75 % in the model used by Vilms Pedersen et al. [98], and this value was adopted in this study. This means that 75 % of all direct solar energy ends up in the bulk liquid.

However, considering the pathway of heat flow, this might be an overestimation. As the absorptivity determines the amount of heat transferred from the solar rays to the cover concrete, the heat will still have to flow either through the concrete to the bulk liquid, or be passed via the biogas to the bulk liquid. The heat loss to the air and soil can be expected to be higher than 25 %, or at least be dependent on more factors than the absorptivity of concrete. However, as the solar irradiance heats up the concrete,

Table 4.4: The yearly mean of the absolute temperature inhibition functions for acetoclastic methanogens and the dynamic inhibition function for the simulations shown in Figures 4.3a & d, and 4.4a & c. For the simulations of Norway and Uganda, no insulation was present around the digester. A value of 1 gives uninhibited reactions and a value of 0 completely inhibits a reaction.

	Dutch concrete	Dutch insulation	Norway	Ugandan
$I_{\text{Arrhenius}}$	0.227	0.336	0.167	0.510
I_{cardinal}	0.494	0.714	0.282	0.991
I_{shock}	0.925	0.889	0.933	0.998

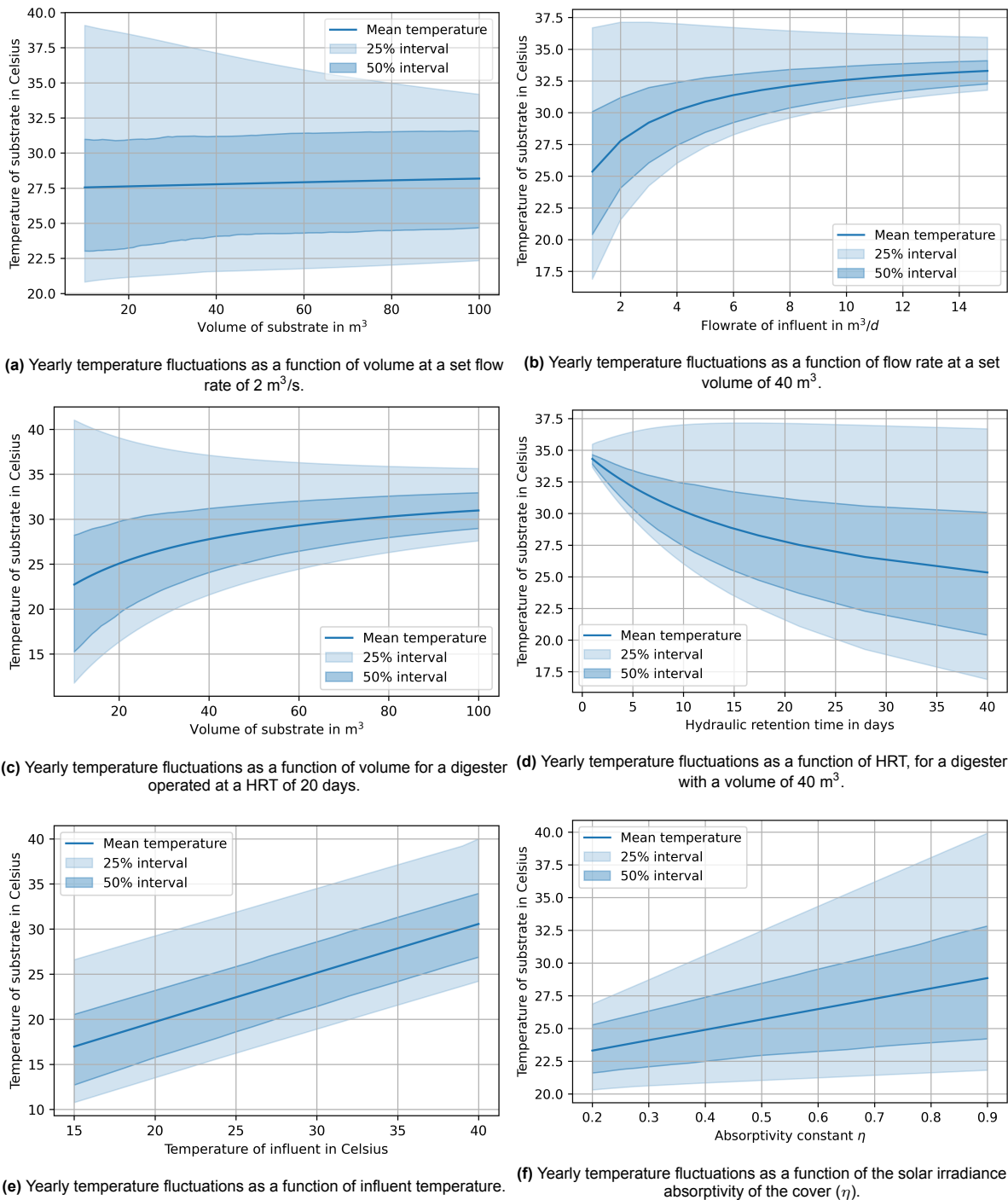


Figure 4.5: Simulations of the effect of design and operational parameters and the absorptivity constant η on the yearly mean temperature and the yearly temperature fluctuations for a digester subjected to the Dutch climatic conditions of 2021. For each simulation, the values of the unvaried parameters are as shown in Tables 3.1 and 3.2.

the temperature gradient between the bulk liquid and the concrete lowers. This will result in less heat loss due to conduction and convection. The decrease in solar irradiance heat gain, and the decrease in convective and conductive heat loss might cancel each other out and result in net operational temperature as presented here. This could possibly be the reason why Vilms Pedersen's model was able to predict operational temperatures without calibration [98]. This is supported by the fact that Bandgar et al. [10] found a high relation between solar irradiance and bulk liquid temperature. However, the

current implementation gives distorted results when comparing heat flow pathways, as both the solar irradiance and the conduction/convection processes should have lower values. To accurately simulate the relative effect of different heat flow pathways, a model as proposed by Terradas-III et al. [94] should be used. This model calculates the temperature of the cover and the temperature of the biogas as model states as well as temperature. Such a more complex model structure would allow the inclusion of an advection factor for gas outflow as well.

In warmer climates, and especially when heating is applied to attain optimal operational temperatures for biogas production, solar irradiance can cause overheating [13, 64]. These papers also mention the effect of passive cooling by painting the digesters white to increase the albedo. The opposite is done in unheated digesters, where the digester is painted black to increase the absorptivity of the digester and therefore the heat gain from solar irradiance [51]. The increase or decrease in operational temperature found in these papers substantiates the large effect that modifying the solar irradiance absorptivity of the digester can have on the whole heat balance equation. Furthermore, it could potentially be beneficial for La Trappe to consider painting the digester black as well. Additionally, the exposure of the digester to solar irradiance should be maximized for heat gain, and the location of the digester should therefore be chosen so no trees or buildings block the solar rays from hitting the digester.

Temperature shock inhibition effect

The parameters determining the temperature shock effect, τ_a and s_{hg} , are varied over a range to determine their effect on gas production in the insulated Dutch case with the design and operational values as shown in Table 4.5. The adaptation time constant τ_a , that represents the time needed for the microbial group to adapt to a set temperature, is tested over a range from 10 to 30 d. The constant s_{hg} represents the temperature change needed to half microbial activity and is varied from 1 to 5 °C. These values are taken for consideration as these were found representative for a similar case in the research of Kovalovszki et al. [56]. Their combined resulting relations with methane production is shown in Figure 4.6.

Figure 4.6 shows that for high values of s_{hg} , the mean I_{shock} will be closer to 1, which represents no inhibition. The reverse relation is found for τ_a . If this parameter is lower, the mean I_{shock} will be higher for the set year. The mean I_{shock} can vary from close to 1 to around 0.4 for the investigated range and temperature profile, depending on the chosen value of s_{hg} and τ_a . This shows how important it is to validate the chosen values for modelling and control of reactors with highly fluctuating temperatures. However, these values can be dependent on many factors. Figure 4.6 also shows that the value of s_{hg} has a larger influence on the dynamic inhibition function than the value of τ_a in the investigated range.

Boušková et al. [17] and Sudiarta, Imai, and Hung [90] found different responses to shocks in temperature within the mesophilic range than from the mesophilic to the thermophilic range. The combined effect of the absolute and dynamic temperature inhibition function as presented in this thesis do how-

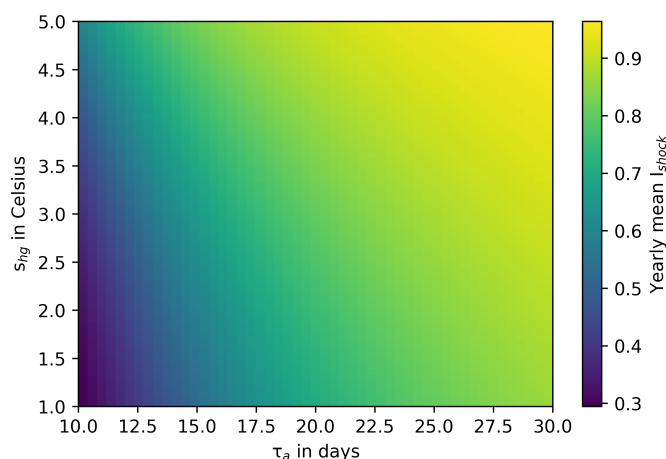


Figure 4.6: The effect of s_{hg} and τ_a on the yearly mean of the dynamic temperature inhibition function I_{shock} for simulation of a reactor with the design and operation as shown in Table 4.5 and subjected to the Dutch weather conditions of 2021.

ever give similar results for the initial temperature response as found in these studies. However, the temperature inhibition functions are not capable of simulation of thermophilic digestion. Furthermore, Boušková et al. [17] found that it is better to have an abrupt switch in temperature than a gradual when switching from mesophilic to thermophilic or the other way around, as the microbes will be able to adapt faster to a new temperature if the gap between the old and new temperature is larger than when the temperature changes gradually over time. This faster adaptation time for larger temperature shocks, and slower adaptation for smaller shocks is included in this dynamic temperature inhibition function as well. It is therefore deemed as an accurate model, but calibration of τ_a and especially s_{hg} is needed for different cases, as these can be dependent on many factors.

4.3. Sludge Characterisation

4.3.1. Chemical analysis

Five different samples were analyzed for chemical composition. These include the belt-thickened sludge, the wort from the blond beer and the quadruple beer, and the influent and effluent of the MNR. Detected ethanol found in the VFA analysis has been left out of the total VFA calculation, as the found concentrations were low and no state for ethanol is present in the ADM1. Chemical composition and relative standard deviation of these samples are shown in in Table 4.5.

The results of the chemical analysis on the different streams at La Trappe are shown in table 4.5. The belt-thickened WAS has a high amount of TS and tCOD and will need to be diluted for liquefaction before it can be digested, as it is quite solid. Lower concentrations were found than expected for the proteins and carbohydrates, and VFAs. For the blond spent wort, it was found that around two thirds of it is comprised of carbohydrates. This finding is lower than expected, as literature states that wort consists of around 90 % carbohydrates [40]. The ratio between tCOD and sCOD of the spent wort is as expected, as it is an amber transparent liquid with few grainy flakes floating in it. The quadruple spent wort has a three times higher concentration of tCOD than the blond spent wort, and the carbohydrates to tCOD ratio is in-line with literature. Proteins were expected to be the main component of the WAS [88], but only low concentrations were found with the used method.

Analyzing the results critically, it must be stated that, to make definite statements on the chemical compositions of the different streams at La Trappe, some tests should be iterated. For the blonde spent wort, the influent and the effluent samples, the concentration of proteins in mg N/L was found higher than the total amount of nitrogen. This result could be caused by errors in the measurement methods, with the HACH kits or the TKN determination. Another reason can be the formula used for protein determination (3.9), which has not been calibrated for this substrate. This formula is used for estimation of the amount of proteins inside of microbial cells. However, if large amounts of EPS are present, the ratio between nitrogen and amount of proteins can change. It is plausible that the MNR technology in the activated sludge step of the La Trappe WWTP influences the concentration of EPS, as the plant roots promote biomass retention via bio film production. This will change the protein ratio's, and calibration of (3.9) is therefore needed.

Table 4.5: Results of the chemical analysis of the different streams of La Trappe

	Unit	Belt-sludge	Blonde	Quadruple	Influent	Effluent
TS	g L ⁻¹	160.58 ± 1.79	12.93 ± 0.10	36.82 ± 0.08	3.13 ± 0.07	3.30 ± 0.05
VS	g L ⁻¹	142.11 ± 1.47	12.60 ± 0.09	35.90 ± 0.07	1.57 ± 0.03	1.20 ± 0.12
tCOD	mg L ⁻¹	137 573 ± 31 567	15 400 ± 25	47 260 ± 1401	3181 ± 93	1244 ± 133
sCOD	mg L ⁻¹	37 660 ± 573	14 973 ± 62	41 215 ± 306	2504 ± 26	610 ± 3
tN	mg tN/L ⁻¹	11 327 ± 435	22.0 ± 3.3	463.0 ± 4.1	37.5 ± 0.4	29.2 ± 0.3
NH ₄	mg NH ₄ -NL ⁻¹	1015 ± 44	9.8 ± 0.4	17.2 ± 0.3	1.05 ± 0.02	2.11 ± 0.10
tP	mg PO ₄ ³⁻ -PL ⁻¹	1603 ± 84	17.4 ± 1.9	44.4 ± 13.5	11.7	9.1 ± 0.5
pH				5.9	5.78	8.08
tVFAs	mg COD L ⁻¹	1076.5 ± 152.7	276.4 ± 131.4	801.1 ± 460.7	1500.4 ± 11.9	375.9 ± 2.3
Carbs	mg COD L ⁻¹	17 683 ± 3297	9035 ± 808	41 602 ± 5872	155 ± 23	116 ± 17
Proteins	mg NL ⁻¹	2089 ± 353	577 ± 186		71.10 ± 4.68	62.20 ± 2.63

Furthermore, the low amount of carbohydrates found in the blond spent wort sample was against expectation. This could be due to the high dilution factors needed for VFA and carbohydrates determination [29]. As the samples were stored for two months for analysis, some degradation processes could have taken place, converting carbohydrates to VFAs. VFA analysis was done before carbohydrate determination, which could possibly explain the low amounts of carbohydrates and high amount of lipids found. COD in carbohydrate form was not observed during VFA analysis, while it was also missed at carbohydrate determination as it, at that time, was converted to VFAs. The COD which was not observed during these test was allocated to the concentration of lipids with the used biochemical fractionation method. The same process could have taken place for the proteins in the WAS.

For possible diluents of the WAS and wort in the digester, the influent and effluent of the MNR were analysed as well. The influent comprises of a large amount of VFAs, which could possibly be digested as well. These VFAs do contribute to the low pH in the influent, which could cause methanogenic inhibition to occur in the reactor. However, it is possible that these VFAs come from the wort now treated in the MNR. These would therefore not be present after the commissioning of the digester, changing the composition of the influent. On the other hand, the effluent of the MNR has a high pH, which could help digester stability. As the MNR is situated in a greenhouse, the effluent of the MNR will also have a higher and more stable temperature throughout the year, which would benefit digester operation. This flow is therefore deemed a better option for dilution.

The spent worts of blonde and quadruple beer are characterized for their concentrations, but in reality the spent wort of eleven different types of La Trappe beer in the quantities produced in the brewery will be introduced to the reactor. In the following simulations, it is assumed that the concentrations of the mixture of all spent wort deviates inconsequentially from the concentrations of a mixture of the blond and quadruple spent wort in a 1:1 ratio. Furthermore, in the current situation, the wort is treated in the WWTP, and therefore has influence on the concentrations of the influent and effluent of the MNR, as well as the belt-thickened sludge. As with the implementation of the anaerobic digester the wort will not be directly treated in the WWTP, the characteristics of these flows will change. However, this change was assumed to be not substantial, and the characterisation as done here is therefore still deemed representative.

4.3.2. Biochemical methane potential test

The methane flow of the BMP test is shown in Figure 4.7a and 4.7b. BMP tests were done on three different mixtures as shown in Table 3.4, resulting in the methane production rates as shown in Figure 4.7. The BMP test experienced some errors in data collection, which resulted in the fact that after approximately 18 days, no new data was collected. However, all graphs attained an almost horizontal trajectory after day 10, which insinuates that all readily-biodegradable COD had been digested. Furthermore, for the cellulose control bottles, it can be observed that 270 N mL of methane was produced per gram of COD, instead of the expected 350 N mL. This could be due to the failure of recording biogas produced after day 18, or by errors in the dosing of the bottles. Figure 4.7b shows that all three bottle compositions attained similar biogas production levels. The bottle containing the effluent of the MNR had slightly less biogas, which could indicate that the COD in this effluent is slightly less biodegradable than the influent.

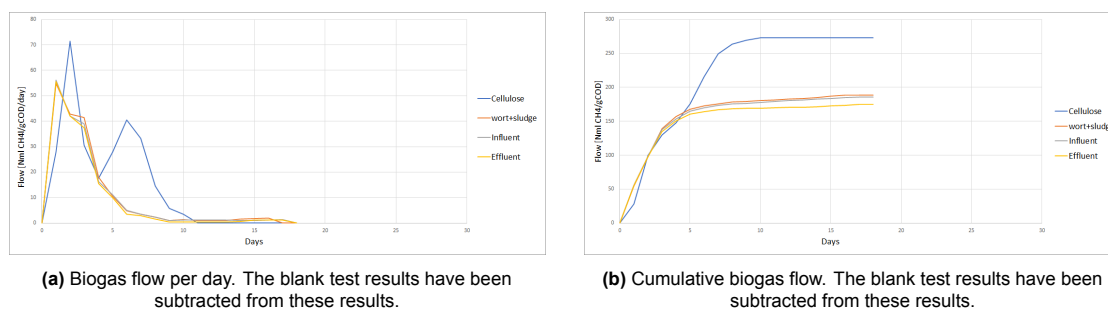


Figure 4.7: Methane production curves resulting from the BMP tests with compositions as shown in Table 3.4.

4.3.3. Biochemical fractionation

The method of Arnell et al. [7] was used to determine the input values of the ADM1. The resulting values are shown in Table 4.6, where the unit of each value is kg COD m^{-3} . The same ratios for sludge, wort, influent and effluent have been used as in the BMP bottles as shown in Table 3.4. The missing value for proteins of the quadruple wort has been estimated using the same COD to protein ratio as the blonde wort.

The biochemical fractionation method was used to calculate the input states for the ADM1 as presented in table 4.6. The results deviated from expected values in the same manner as the results from the chemical analysis. As generally wort contains around 90 % carbohydrates [40] and the activated sludge contains mainly microorganism, it was expected that the lipid concentration would be rather low. As the amount of carbohydrates and proteins found in experiments were lower then expected, the calculated lipid concentration became the main component of the influent. As the concentration of lipids is calculated as the remainder of the total COD, after the concentration of proteins and lipids had been subtracted, the amount is probably overestimated.

This results raises a concern for this method, as measurement errors propagate over the used balance equations. Therefore, extra care should be taken in the chemical analysis, especially in macro nutrient determination. For carbohydrate determination for example, dilutions should be done in triplicate as well, as small errors give large deviations in results due to the high dilution factors needed for the used sample and method. Furthermore, due to dilutions to concentrations under measurement ranges, the concentration of VFAs might have been underestimated. This means that the actual composition would have higher concentrations of VFAs, results in lower pH in ADM1 simulations. Therefore, more base could be needed to prevent acidification than in the simulations done with the found results.

Lastly, as the amount of sCOD is dominant for the wort, the used method and equations might not be ideal for this kind of substrate. A proposal for equations for this procedure for substrates which consist for a major parts of soluble COD is done in Appendix D. These will result in more representative characterisations for substrates such as the wort. Another way to fractionate substrates with the more equal distribution between sCOD and pCOD concentrations is by determining macro nutrient concentrations separately for soluble and particulate COD by filtration.

Table 4.6: ADM1 input values calculated with the biochemical fractionation procedure from the chemical analysis and the BMP test in kg COD m^{-3} . These inputs represent the BMP tests with ratios as shown in Table 3.4.

parameter	Wort and sludge	Influent	Effluent
sCOD	32 877	16 003	14 961
pCOD	51 563	23 293	23 138
Proteins	4340	2274	2225
Carbs	22 104	9915	9900
Lipids	57 997	27 413	26 095
f_d	0.66	0.66	0.63
S_I	11 178	5441	5536
X_I	17 532	7920	8561
X_{pr}	2864	1501	1468
X_{ch}	14 588	6544	6534
X_{ji}	16 579	7328	6575
S_{ac}	545	574	400
S_{pro}	0	281	20
S_{bu}	0	191	19
S_{va}	262	147	129
S_{su}	8955	3988	3970
S_{aa}	1758	915	892
S_{fa}	10 177	4467	3995
S_{IN}	37	3	2

4.4. Calibration and simulation

4.4.1. BMP calibration

Simulation of the BMP test was done in order to calibrate the hydrolysis constants. In order to simulate the inoculum, the steady state output values of the BSM2 was used. It was found that the summed COD concentration of these output values were very similar to the tCOD of the inoculum (32.81 and 33.03 kg COD m⁻³, respectively). One change was made to the BSM2 output values, as 1.35 kg COD m⁻³ of particulate inert concentration (X_I) was transferred to particulate composite concentration (X_{xc}). This was done to attain similar levels of biodegradability. The inoculum simulation and the experimental results of the blank BMP test are shown in Figure 4.8a. The wort and sludge mixture simulation and the experimental BMP results are shown in Figure 4.8b.

The BMP test of the wort and sludge mixture was simulated with the ADM1 model. The blank simulation was subtracted from the results of the wort and sludge mixture simulation in order to find the methane originating from the wort and sludge, without the digestate. The found BMP curve simulation followed the experimentally found results well, which was against expectations. The article from the biochemical fractionation procedure describes how the first-order hydrolysis rate coefficients can be found by fitting the simulated BMP curves through the experimental curves [7]. By adjusting these parameters, a fit should be found, giving the correct first-order hydrolysis rate coefficients for a given substrate.

As the curves already fit each other reasonably well, it can be either concluded that the standard ADM1 first-order hydrolysis rate coefficients are representative for the wort and sludge substrate, or that hydrolysis is not the rate-limiting factor in the digestion of this substrate. However, as VFA concentrations were not measured in these test, it is unknown if VFA accumulation has occurred. This would have been an indicator that methanogenesis was actually the rate limiting step. Nevertheless, high biodegradability is observed in Figure 4.8b, and it is therefore still expected that methanogenesis is the rate limiting step, but BMP tests with VFA concentration measurements are needed to determine this with more certainty.

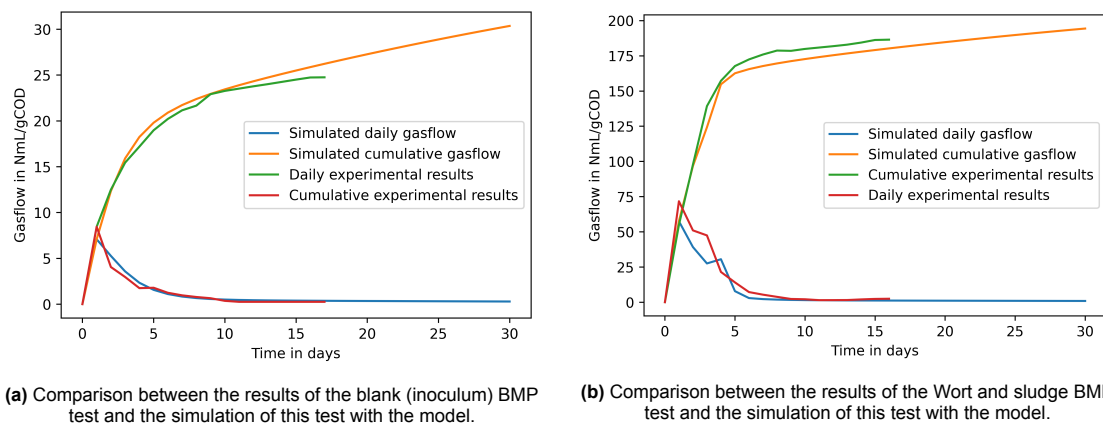
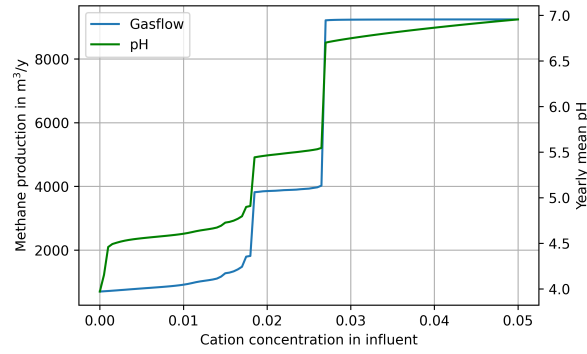


Figure 4.8: Daily and cumulative results of the experimental and simulated BMP results of inoculum and the wort and sludge. The results of the blank BMP simulation are subtracted from the wort and sludge simulation results to find the exclusive effect of the wort and sludge substrate, as is done in the experimental results.

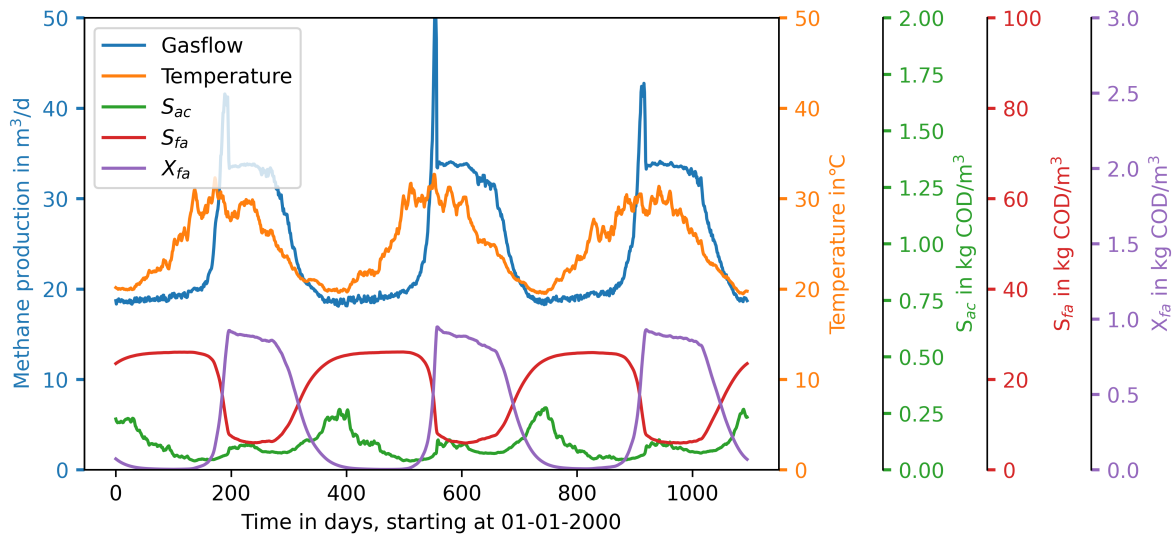
4.4.2. Simulations

La Trappe

For simulation of the digestion of the wort and sludge in a digester with the design and operation as shown in Table 3.1 and subjected to the Dutch weather, further configuration of the influent states is needed. Because the unknown states are set to a concentration of 0, no buffering capacity is present in the influent and it was found that acidification occurs in simulation of the digestion of the wort and sludge mixture. Therefore, the effect of dosing base to the influent is simulated by finding the effect increased cation concentration on yearly biogas production and mean pH for the year 2021. This influence is shown in Figure 4.9a.



(a) Methane production and pH as a function of cation concentration for the influent as presented in Table 4.6.



(b) Digestion of the wort and sludge mixture as presented in Table 4.6 in a digester with the design and operation as shown in Table 3.1 and exposed to the Dutch weather conditions from 2000 till 2003.

Figure 4.9: Simulation of the La Trappe case with influent based on the biochemical fractionation. The concentration of cations represents the addition of base to the influent substrate to prevent acidification. The found result is then added to the influent and sludge mixture, which is used to simulate methane production for three years in Figure (b).

A step function corresponding with the three pH inhibition functions as depicted in Figure 2.1 can be observed. A pH of 7, coinciding with no pH inhibition and the peak in methane production, is reached if the influent has a concentration of $0.03 \text{ kmole m}^{-3}$ of cation. Simulation of the digestion of the wort and sludge mixture with the addition of $0.04 \text{ kmole m}^{-3}$ of cation is done for the the Dutch weather conditions from 2000 till 2003. The cation concentration is increased from 0.03 to $0.04 \text{ kmole m}^{-3}$ because the winter of 2001 reached lower temperatures than the winter of 2021, and acidification did occur.

The resulting methane production and digester temperature are shown in Figure 4.9b. Furthermore, the bulk liquid and effluent concentrations of acetate (S_{ac}), LCFA (S_{fa}) and the long-chain fatty acid metabolizing acidogens (X_{fa}) is shown. A clear seasonal dependence of methane production on temperature can be observed. This is inline with expectations, as methane production is known to correspond with bulk liquid temperatures in unheated digesters [45]. However, to the author's knowledge, this is the first model which combined heat transfer with continuous temperature inhibition functions to the ADM1 for simulation of this effect.

In this simulation, the combined concentration of lipids and LCFA contributes for almost half of the biodegradable COD. It can therefore be observed that the daily biogas production is largely dependent on X_{fa} concentration. Each year in winter, the amount of X_{fa} is low, as the temperature inhibition function lowers the metabolism of the acidogens causing washout due to low reproduction. Due to

the low metabolism and concentration of X_{fa} , accumulation of S_{fa} occurs till steady-state with influent concentrations is reached. This coincides with the low methane production in winter, which is lower than $20 \text{ m}^3 \text{ d}^{-1}$.

However, as temperatures start to increase towards summer, the growth rates of the acidogens becomes larger than the effluent concentrations, and X_{fa} concentration starts to increase exponentially due to the high concentrations of their substrate S_{fa} after accumulation. This exponential growth results in a clear short peak in biogas production in mid summer, where in a short time interval a large portion of the S_{fa} is consumed. As the S_{fa} concentration becomes rate limiting after this event, the growth in X_{fa} abruptly starts to decline. Subsequently, temperatures start to decline again at the end of summer. Due to this decline, accumulation of S_{fa} starts again, restarting the cycle.

Temperature has therefore major influence on biogas production in the anaerobic digestion process of this substrate. This high temperature dependence is caused by the low value for the Monod maximum specific uptake rate of LCFA $\mu_{m,fa}$. The metabolism on this substrate has the lowest values of all μ_m coefficients in the ADM1 [85] at 6 d^{-1} . Furthermore, absolute temperature inhibition has the most drastic effect on acidogenesis [15, 28], causing a small temperature range at high temperature values for low inhibition, as can be seen as well in Figures 4.1c and 4.1d.

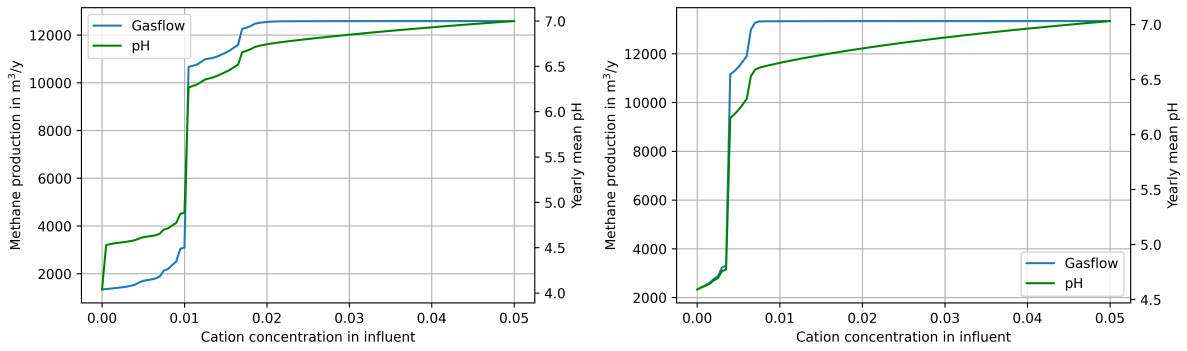
This dependence was found as well by Erdirencelebi and Ebrahimi [32], who concluded enhanced oil and grease removal at the upper mesophilic range ($40 \text{ }^\circ\text{C}$), compared to digestion at $35 \text{ }^\circ\text{C}$ of waste activated sludge. This finding is inline with the found absolute temperature inhibition function. Furthermore, Merlin et al. [66] found that for the digestion of dairy wastewater, temperatures should be kept above $23 \text{ }^\circ\text{C}$ to prevent fatty acid accumulation-induced acidification. These findings are inline with the simulation produced here with absolute temperature inhibition function for LCFA acidogenesis.

However, the effect of temperature on acidogenesis has been determined on the digestion of glucose [28], whose acidogenic species might react differently to temperature change than LCFA metabolising acidogens. It is therefore important to study the temperature inhibition effect for different acidogenic species, by using their representative substrates.

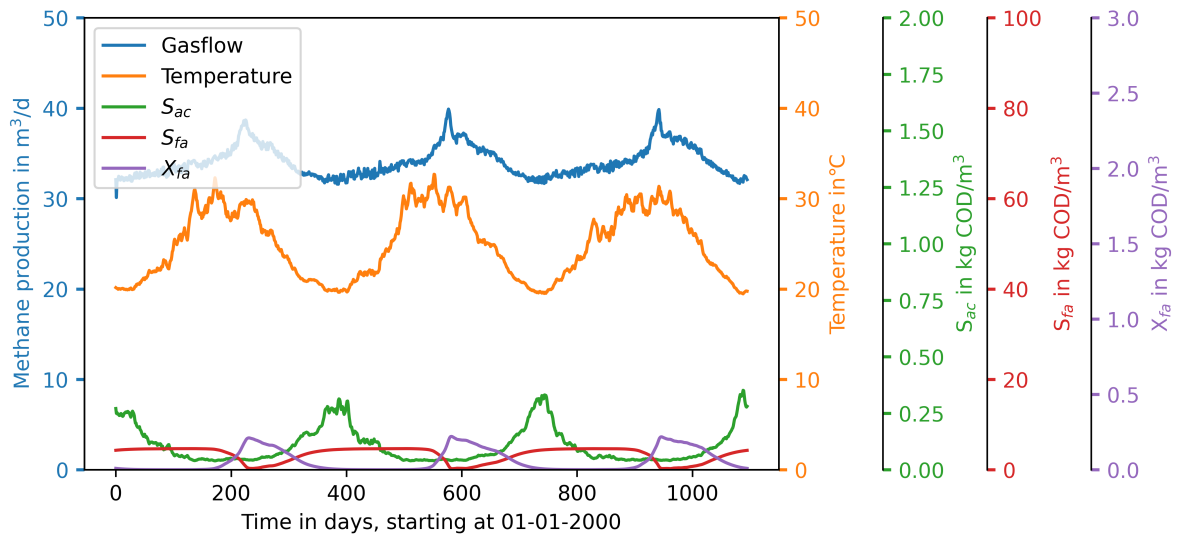
To conclude what the rate limiting step is in the simulation, the concentration of acetate (S_{ac}) is included in Figure 4.9 as well. It can be seen that during the summer peaks in biogas production, acetate concentrations increase as well. This is expected, as this is an intermediate in the conversion of S_{fa} to S_{CH_4} . However, a peak in acetate is observed as well at the coldest points of each year. This indicates that methanogenesis is rate limiting in winter, while hydrolysis is rate limiting in other periods. Even though methanogenesis is rate limiting, and acetate accumulation is occurring in winter, the addition of the cation prevents acidification and methanogenic inhibition from taken place. The fact that methanogenesis is only rate limiting in winter suggests that the concentration of base needed in summer can be lower than in winter.

As was stated before, the amount of carbohydrates and proteins in the wort and sludge is probably underestimated and the used biochemical fractionation method therefore caused an overestimation of the amount of lipids in the influent. It is known that spent wort consist for 90 % of carbohydrates [40], and WAS consists for its majority out of proteins [88]. Based on these, it is expected that the values from carbohydrates and proteins as presented in Table 4.6 should be multiplied with a factor of 1.8 to gain representative substrate for the wort and sludge mixture of La Trappe.

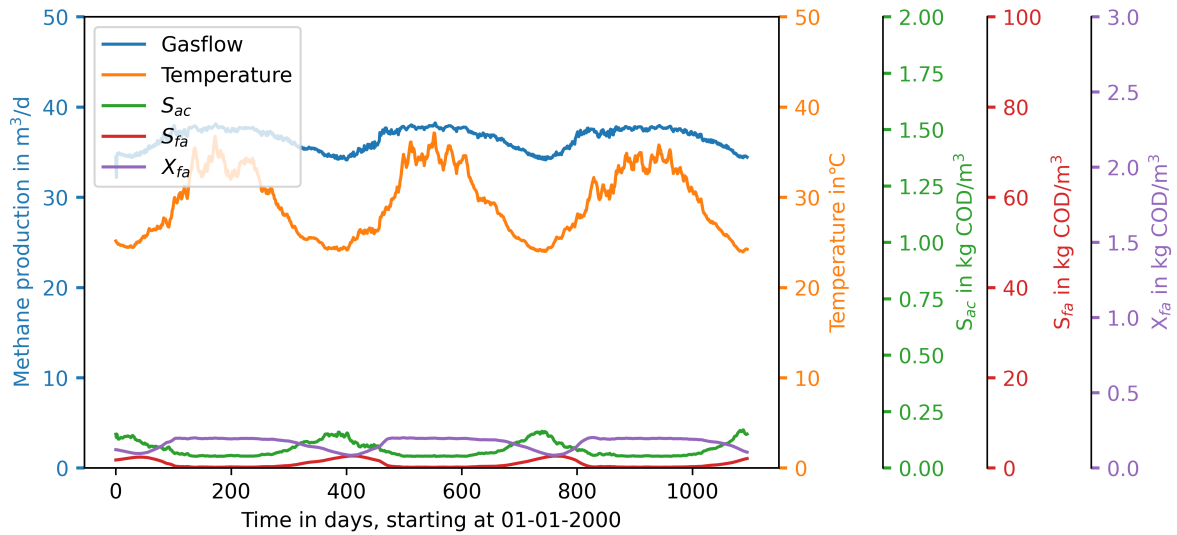
Recalculation of the other input values according to the biochemical fractionation method resulted in a new influent substrate which was used to simulate the influence of temperature on biogas production for a more representative substrate for the La Trappe case. In this simulation, again acidification occurs if no base is dosed. Figure 4.10a shows that a concentration of $0.02 \text{ kmole m}^{-3}$ of cations as base in the influent is needed to prevent acidification from occurring for the temperature profile of 2021. Again however, higher dosage was needed for simulation from 2000 till 2003, as these winters were colder. Simulation of the digestion of the new wort and sludge states with a cation concentration of $0.03 \text{ kmole m}^{-3}$ resulted in biogas production as shown in Figure 4.10c.



(a) Methane production and pH as a function of cation concentration in the influent substrate for the influent based on literature and with a constant temperature of 35 °C. (b) Methane production and pH as a function of cation concentration in influent for the influent based on literature and with a constant temperature of 45 °C.



(c) Digestion of the wort and sludge mixture based on literature in an digester with the design and operation as shown in Table 3.1, an influent temperature of 35 °C and exposed to the Dutch weather conditions from 2000 till 2003.



(d) Digestion of the wort and sludge mixture based on literature in an digester with the design and operation as shown in Table 3.1, an influent temperature of 45 °C and exposed to the Dutch weather conditions from 2000 till 2003.

Figure 4.10: Simulation of the La Trappe case with influent concentrations based on literature. The concentration of cations represents the addition of base to the influent substrate to achieve pH neutrality. The found result is then added to the influent and sludge mixture, which is used to simulate methane production.

Mean biogas production for this substrate is higher than for the substrate with high lipid concentration, and daily biogas production variability between summer and winter is lower. The digestion of this substrate is therefore less dependent on temperature than a substrate with high lipids content. This suggests that substrates with high lipid content are less suitable for digestion in unheated digesters with temperature fluctuations below a certain threshold temperature than substrates with high concentrations of carbohydrate and proteins. The μ_m of monosaccharides and amino acids is 30 and 50 d⁻¹, which allows for more inhibition before the rate of the acidogenic process becomes rate limiting, compared to lipids with an μ_m of 6 d⁻¹.

Even though lipid concentrations are lower in this simulation, the peaks in biogas production in summer in Figure 4.10c still coincide with the lipid digestion, just like in Figure 4.9b. In addition, the change in rate-limiting step between hydrolysis in summer and methanogenesis in winter still occurs in this simulation, as acetate concentration increases in winter. It is therefore important to either maintain pH especially well in winter, or to increase temperatures so methanogenesis will not become the rate limiting step. A simulation with an influent temperature of 45 °C instead of 35 °C is shown in Figures 4.10b and d.

It is shown that by increasing influent temperature, acetate concentrations in winter will remain lower, and less base is therefore needed to be dosed. Base dosage, represented by cation concentration in influent, can be halved from 0.02 to 0.01 kmole m⁻³, as shown in Figure 4.10b. Most importantly, biogas production is higher and more stable throughout the year, even though there is still a temperature fluctuation of 10 °C between summer and winter. As the wort leaves the brewery at 72 °C and the WAS comes from the greenhouse at 27 °C, mixture of these two flows could reach 49.5 °C, assuming no heat loss occurs and volumes and heat capacity of these substrates are equal. An influent temperature of 45 °C should therefore be possible and advisable.

Furthermore, as the amount of base needed for stabilisation is low, local sources of base or buffer available to La Trappe can be explored for sufficiency. Wasajja et al. [101] found that in household anaerobic digesters in Uganda, cow urine was used as a diluent instead of water. This resulted in increased pH in the digester due to the ureolysis reaction [26]. This suggests that urine could possibly be used as a steady and sustainable source of base for La Trappe, especially in operation with an influent at 45 °C, as only low amounts of base are required to prevent acidification.

Washout

Simulations were done to investigate the relation of reactor volume and temperature on methane production for the BSM2 influent with a constant flow rate of 2 m s⁻¹. Figure 4.11a shows that volumes smaller or equal to 10 m³, giving HRTs of 5 days or smaller, result in washout of biomass and low amounts of biogas production. From a volume of 10 m³ and larger, it is dependent on temperature if washout occurs. This is due to the increased growth rates of the microbes at higher temperatures, which allows for a lower HRT. However, for more complete digestion, both temperature and volume need to be of a sufficient value.

These results suggest that for reactors operating at low HRTs, a drop in temperature could trigger washout. This is undesirable in the case of biogas production plants, but it also creates an opportunity. In anaerobic digestion research, instead of methane production for energy generation, increased focus is laid on fermentation product accumulation such as VFAs, which can be used as precursors for bio-based products [23, 79, 53]. Methanogenesis has to be prevented for this [53], and washout of methanogens is therefore an explored strategy [77].

The sum of all VFA concentrations in the bulk liquid and effluent of the reactor at steady-state after 365 days simulation is shown in Figure 4.11b. Both graphs show a clear region of temperature dependence for the occurrence of washout. Peces et al. [77] concluded that it is not HRT alone that promotes washout of methanogens and accumulation of VFA, but the combination of HRT with other operational parameters. It is shown here that temperature is one of these parameters, and that the occurrence of washout follows a similar relation with temperature as the absolute temperature inhibition function of methanogens as shown in Figure 4.1j.

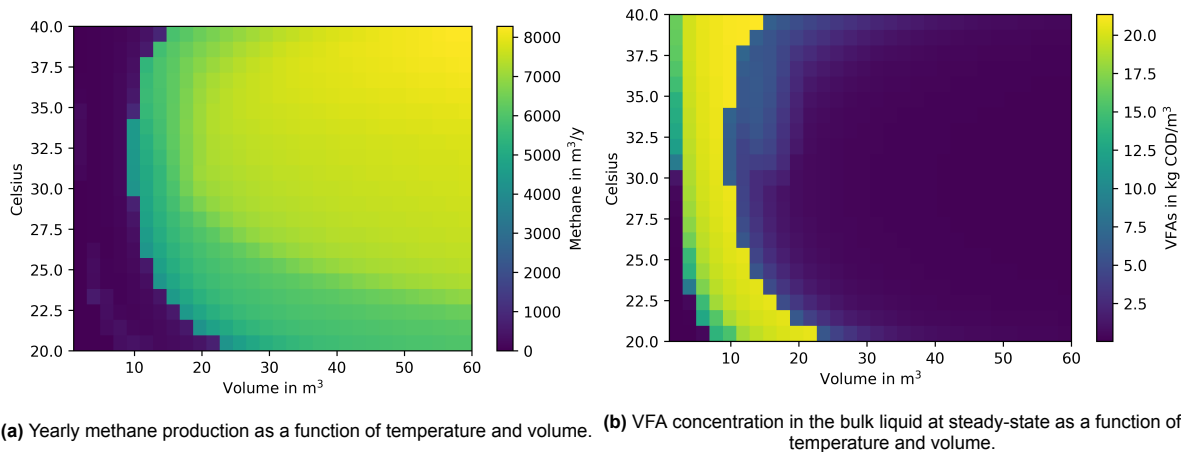


Figure 4.11: Steady-state simulations were done for the investigation of washout as a function of operational temperature and volume for the digestion of BSM2 influent and a flowrate of $2 \text{ m}^3 \text{ s}^{-1}$. At low volumes, methanogens are washed out and high concentrations of VFAs are attained in the simulation.

Furthermore, it suggests that for VFA accumulation, digestion at lower temperatures might be feasible. The amount of VFAs is highest at high temperatures, but VFAs can be accumulated at temperatures of $20 \text{ }^\circ\text{C}$ as well. Especially in substrates with low lipid concentrations or if the $\mu_{m,fa}$ can be enhanced [1, 91], digestion of already hydrolysed substrate at lower temperatures with specific retention times can ensure washout of acetogenic methanogens, while the other microbial species for anaerobic digestion are maintained. However, as these are steady-state simulations, the kinetics are not shown, and achieving these equilibrium concentrations takes longer for digesters at lower temperatures.

Acidification

To simulate acidification due to overloading, the relation between temperature, OLR and methane production has been simulated for BSM2 influent. The results are shown in Figure 4.12a. The values OLR only account for the biodegradable fraction of the BSM2. Furthermore, for the La Trappe case with wort and sludge substrate concentrations based on literature and an influent temperature of $45 \text{ }^\circ\text{C}$, the relation between volume and cation dosage is investigated in Figure 4.12b. Lastly, simulation of reactor failure due to low base dosage in cold winters is shown in Figure 4.12c.

It is shown that at low temperatures and increasing OLR, a clear cutoff point exists. If influent concentrations are higher than this point, VFA accumulation lowers pH to trigger the positive feedback cycle of acidification, rapidly lowering methane production. Reactors operated at higher temperatures can handle higher OLR because of the higher methanogenic metabolism. This effect is seen with the increase in OLR before acidification with increasing temperature from $20 \text{ }^\circ\text{C}$ to $30 \text{ }^\circ\text{C}$.

However, above $30 \text{ }^\circ\text{C}$, an inverted relation is found. Because the BSM2 anaerobic digester influent mainly consists of proteins, the amount of inorganic nitrogen in the bulk liquid increases with increasing OLR and temperature. Free ammonia (NH_3) is one of the inhibitors of methanogenesis included in the ADM1, as shown in Figure 2.1. Due to this inhibition, the optimum OLR for biogas production is not found at the expected $35 \text{ }^\circ\text{C}$, but at a lower temperature of $30 \text{ }^\circ\text{C}$. This is due to the fact that at temperatures higher than $30 \text{ }^\circ\text{C}$ and OLR higher than $14 \text{ kg COD m}^{-3} \text{ d}^{-1}$, free ammonia is present in inhibiting concentrations, as all proteins are degraded, and their nitrogen is converted to inorganic forms.

This phenomenon is well known in the digestion of WAS at high OLR [109]. Free ammonia equilibrium concentrations are influenced by temperature, through Van 't Hoff's law, and pH [49], and these relations are included in the simulation [38]. These relations would shift the acid-base equilibrium from free ammonia towards ammonium at increasing temperatures. However, due to the increased process rates at higher temperatures, the total concentration of free ammonia increases more than this shift in acid-base equilibrium lowers it, and acetoclastic methanogenesis is still inhibited. Because of the inhibition of methanogens, acetate starts to accumulate, causing acidification and further inhibition.

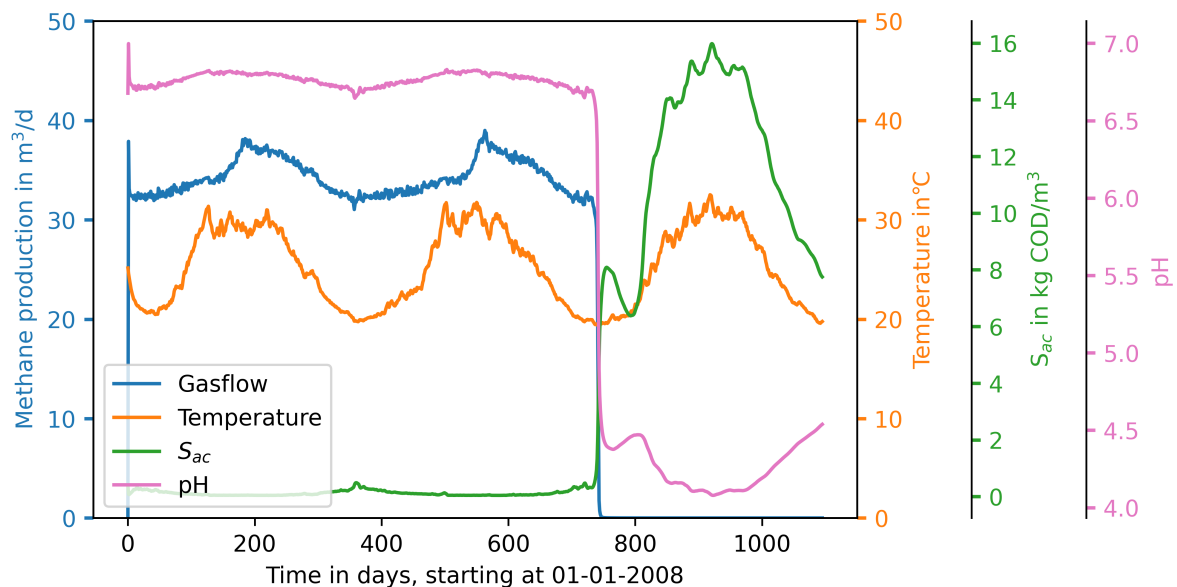
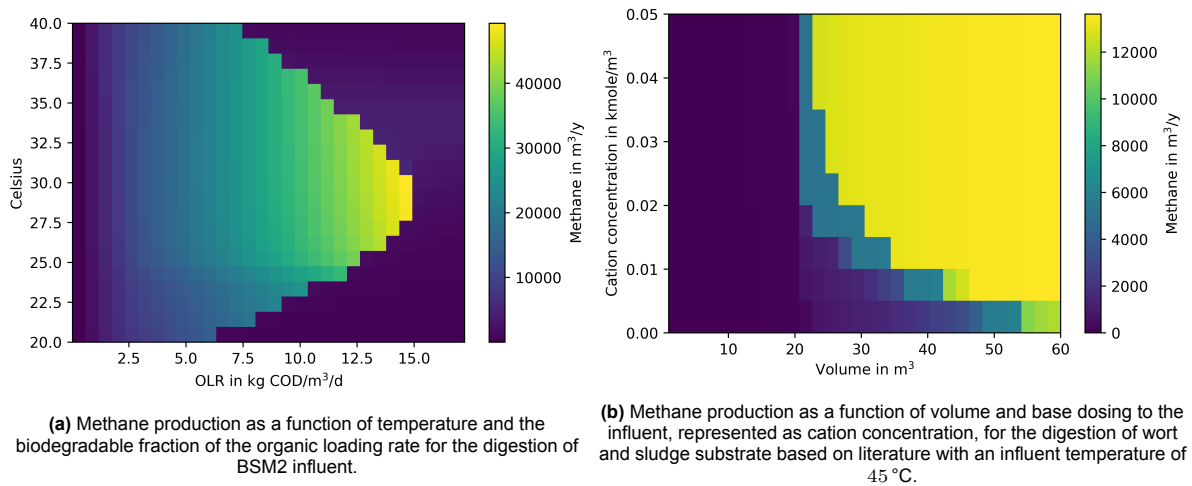


Figure 4.12: Investigation on the effect of temperature on maximum OLR.

This results in higher concentrations of biodegradable COD in the effluent and should therefore be prevented in the digestion of WAS. Ahlberg-Eliasson et al. [3] found similar results for increasing the OLR for cow manure digestion, where free ammonia concentrations became inhibiting, increasing the residual methane potential in the digestate. However, it was also found that when organic loading rate is gradually increased, the methanogens are able to adapt to higher ammonia levels, making them able to handle OLR of up to $50 \text{ kg COD m}^{-3} \text{ d}^{-1}$ for WAS [65, 106]. These kind of effects are however excluded in the model.

Digestion of the wort and sludge mixture based on literature and with an influent temperature of 45 °C is simulated over the temperature profile of 2021 for different reactor volumes and base dosages. It can be seen in Figure 4.12b that acidification is both dependent on the amount of base dosed to the influent and the reactor volume. Having a larger volume decreases the OLR, and therefore relatively lowers the amount of acetate accumulation in the reactor. For the La Trappe case, which has an influent flow rate of $2 \text{ m}^3 \text{ s}^{-1}$, full digestion with reasonable safety margins is attained at a reactor volume of 40 m^3 and a base dosage representative of a cation concentration of $0.02 \text{ kmole m}^{-3}$.

This optimization of OLR has been studied before, and the existence of this cutoff point before

acidification is well known [37], but the inclusion of temperature fluctuations is often not regarded [5]. These results suggest that for reactors operating at a certain OLR, a drop in temperature could trigger an acidification event.

This is simulated for the La Trappe case. The month of January in 2010 was especially cold for the Netherlands, with an average temperature of $-0.5\text{ }^{\circ}\text{C}$, instead of the normal average of $2.8\text{ }^{\circ}\text{C}$ [55]. Simulation of digestion of the La Trappe case over the period 2008–2010, with an influent temperature of $35\text{ }^{\circ}\text{C}$ and a cation concentration of $0.025\text{ kmole m}^{-3}$ is shown in Figure 4.12c.

This cation dose was found by iteration to be as low as possible to prevent acidification in the winters of 2008 and 2009. The pH does fluctuate with the seasons, lowering as acetate concentrations increase in winter. Due to the minimized base dosage, pH lowers in winter so the acidification reaction is just narrowly prevented. However, due to the prolonged cold in the winter of 2010, methanogenic activity is lowered to such an extent that enough acetate accumulation took place to trigger the positive feedback cycle of acidification as shown in Figure 1.1b.

This could be prevented in two ways, by lowering the OLR in especially cold times to prevent acetate accumulation, or by increasing the addition of base to prevent acidification due to acetate accumulation. This example illustrates the need for taking temperature fluctuations in consideration when determining the safety factors in competitive reactor design, as temperature influences many factors. The importance of keeping the pH in the neutral range should not be underestimated, as acidification can happen fast and unexpectedly, due to factors out of the control of operators. However, with knowledge about the effects of factors that are controlled such as the loading rate or base addition, actions can be taken to prevent reactor failure.

Heating

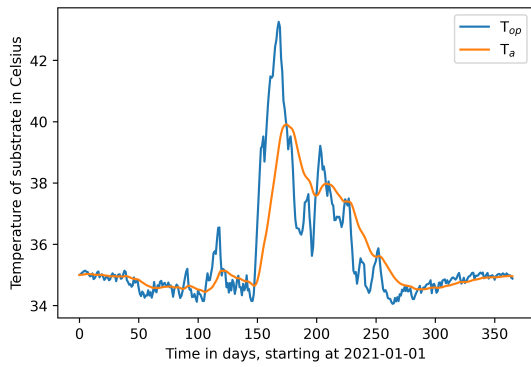
The effect of heating the digester with biogas on net biogas production was investigated. To exemplify how the addition of the biogas heating system affects the temperature model, the temperature fluctuations over the year for setting the heating system (T_{Heater}) to $35\text{ }^{\circ}\text{C}$ is shown in Figure 4.13a.

It shows that the attuned temperature of the acetoclastic methanogens (T_a) will approach the operational temperature when heating is applied in winter, which suppresses the dynamic temperature inhibition function. In summer however, higher than optimal temperatures are reached even though no active heating is applied. This happens due to the high solar irradiance in summer, which actively heats the digester above optimal values, and therefore lowers microbial activity and biogas production.

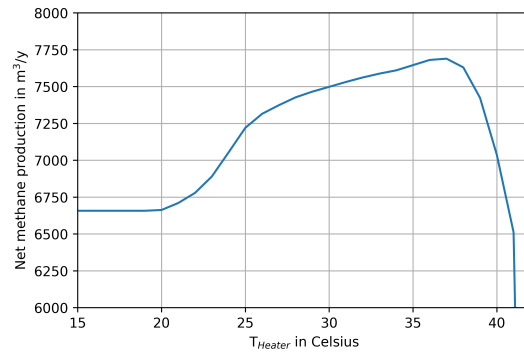
The need for active cooling in heated digesters exposed to solar irradiance has been observed in other studies [13, 64]. The used temperature inhibition functions do considerate the adverse effect of these overheating event, which are included in the produced results. Nevertheless, looking at the whole year, the increase in mean temperature and decrease in temperature fluctuations will allow for higher absolute biogas production with higher T_{Heater} .

However, the difference between absolute and net biogas production will also become larger, as more biogas will be used for heating. The model was used to find the optimum value for T_{Heater} for net biogas production for the BSM2 influent, the biochemical fractionation based wort and sludge mixture and the literature based wort and sludge mixture. For this simulation, an influent temperature of $35\text{ }^{\circ}\text{C}$ was assumed and 0.20 kmole m^{-3} of cations was added to both the biochemical fractionation based and literature based wort and sludge substrates to prevent acidification in overheating events.

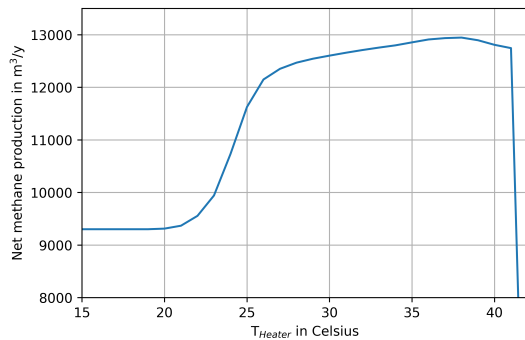
It was found in Figure 4.13b that for optimal digestion for methane production of the BSM2 influent, the heating system should keep the bulk liquid in the digester at $36\text{ }^{\circ}\text{C}$. Figure 4.13c shows that for lab results based wort and sludge influent this optimum was found at $38\text{ }^{\circ}\text{C}$, while Figure 4.13d shows that the optimum for the literature based wort and sludge mixture can be found at $39\text{ }^{\circ}\text{C}$. The lower optimum for BSM2 influent was due to free ammonia inhibition at simulations with a T_{Heater} higher than $36\text{ }^{\circ}\text{C}$, as was found in Figure 4.12a as well.



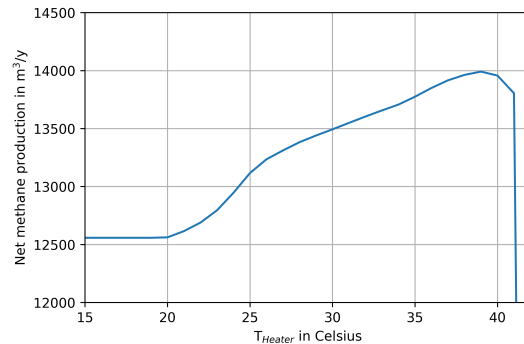
(a) Temperature fluctuations over the year of a digester with the design and operation as in Table 4.5, subjected to Dutch weather conditions of 2021 and with a heating system with a T_{Heater} of 35 °C.



(b) Net yearly biogas production as a function of operational heating temperature for the digestion of BSM2 influent.



(c) Net yearly biogas production as a function operational heating temperature for the digestion of the wort and sludge mixture based on the biochemical fractionation procedure.



(d) Net yearly biogas production as a function of operational heating temperature for the digestion of the wort and sludge mixture based on literature.

Figure 4.13: Simulations of the effect the operational heating temperature set in an internal biogas burner for heating on the net biogas production.

Furthermore, the increase in gas production between having no heating, shown in the gas production level at T_{Heater} values between 15 °C and 20 °C, and having optimum heating is different for between the substrates. The wort and sludge mixture based on the lab results contained the most lipids, which showed the most dependence on operational temperature as seen in Figure 4.9b. This gave this substrate also the largest increase in methane production with heating at optimal temperature compared to no heating, with an increase of 39 %. The highest increase in yearly methane production for this substrate happens with the increase of heating temperature from 22 °C to 26 °C. By increasing the bulk liquid temperature within this range prevents the washout of LCFA metabolising acidogens in winter.

The wort and sludge mixture based on literature data and the BSM2 influent had lower increases in methane production with heating temperature, with an increase of 12 % each between having no heating and having optimal heating. The increase of methane production with heating temperature for the BSM2 substrate and the literature-based wort and sludge mixture substrate followed a more linear relation than the wort and sludge mixture with high lipid content. This shows that the relative increase in methane production with installing a heater in an digester is dependent on substrate composition.

These results shows that different substrates have different optimum digestion temperatures. Similar results have been found for the digestion of thin stillage, with better overall digestion at 40 °C than at 35 °C [69]. Moestedt, Rönneberg, and Nordell [68] found that the temperature for optimal biogas production and sludge mass reduction for the digestion of WAS at a Swedish WWTP was found at 38 °C, instead of at 34 °C or at 42 °C. Free ammonia concentrations increase with operational temperature and inhibits methanogenesis at higher temperatures in this study as well. Furthermore, the results of the simulations of this thesis are also inline with practical knowledge, as most digesters with internal biogas use for heating are operated at temperatures around the values found here [67].

5

Conclusion and recommendations

5.1. Conclusion

This thesis aimed to answer the question how seasonal temperature fluctuations influence the biogas production of an unheated digester in cold climates. It was found that this is dependent on a multitude of factors, such as reactor design, the substrate composition and the HRT. However, in general it was found that biogas production decreases with operational temperature in winter, and increases again in summer.

A Python version of the ADM1 was used to find these results. To deal with the stiffness of the ADM1, three methods for pH calculations and two numerical solvers have been compared. The usage of the Python version, the pH calculation methods and the numerical solver was validated by steady-state simulation of BSM2 influent. It was found that the DAE method with the Radau solver gave the lowest absolute errors and computational burden. Furthermore, the effect of temperature on the liquid-gas transfer coefficient in the ADM1 was investigated. It was found that the liquid gas transfer process could potentially be rate limiting in digesters operated at temperatures below 30 °C, but this result has not been validated.

The heat transfer model was used to simulate yearly temperature fluctuations in the operational bulk liquid temperature of a digester in the Netherlands. The main heat pathway which increases temperature in summer is solar irradiance, while advection from the influent substrate largely determines the temperature in winter. Mean temperature and yearly temperature fluctuations were found to be dependent on several design and operational parameters. Larger volumes and flow rates lowered temperature fluctuations throughout the year, favouring large and high-rate reactors for temperature stability.

Bulk liquid temperature was used to calculate absolute temperature inhibition functions for each digestion step. The constants for both the Arrhenius and the cardinal temperature equation were found for each digestion step, but no comparison or validation study is as of yet done. Furthermore, a dynamic heat shock inhibition function is added for acetogenic methanogenesis, simulating the inhibitory effect of fast temperature change to biogas production. It was found that the climate around the equator suppresses the inhibition for both the absolute and dynamic inhibition function, allowing for high biogas production without active heating, while at colder climates inhibition will take place.

The temperature inhibition functions are used in the ADM1 to simulate the effect on biogas production. The coupled heat transfer and ADM1 model was used to investigate the co-digestion of wort and WAS of the La Trappe brewery in the Netherlands. The substrate composition found using the biochemical fractionation procedure contained a higher fraction of lipids than was expected in literature. Therefore, simulation of the digestion of the found substrate composition and the expected substrate composition based on literature was done.

For the found substrate composition, metabolism of LCFA consuming acidogens lowered in winter, causing washout, LCFA accumulation and low biogas production. This effect was less considerable in the substrate composition based on literature, and it is therefore concluded that substrate composition determines the magnitude of the effect of temperature inhibition on biogas production. LCFA accumulation can however be largely prevented for this case if bulk liquid temperature is kept above 25 °C.

Furthermore, the rate of methanogenesis is limited in winter by the temperature inhibition functions, increasing acetate concentrations and lowering pH. Base has to be dosed to the influent substrate to prevent acidification, but the amount needed is dependent on substrate composition, bulk liquid temperature and reactor volume. Less base is required at lower concentrations of lipids, at higher operational temperatures and at larger volumes. It was found that an exceptionally cold winter could trigger an acidification event if base dosage or OLR is not adjusted. The amount of base needed can therefore be made dependent on operational temperature. Decreased base dosage can be achieved by feeding the digester with higher influent temperature. It was found that increases the influent to 45 °C increased biogas production stability and lowered acetate accumulation in winter.

The relation between HRT and temperature was investigated, and it was observed that washout of methanogens and the consequential increase in VFA concentration follows the same relation with temperature as the temperature inhibition function. A relation between OLR and temperature was found for the digestion of BSM2 WAS, where it was found that acidification and free ammonia inhibition are both affected by temperature. These combined effects determine the maximum OLR.

Lastly, the internal usage of biogas for heating was investigated, and optimal operational temperatures for maximizing net biogas production were found between 36 °C and 39 °C, depending on substrate composition. Furthermore, the largest increase in biogas production was observed by increasing the heating temperature from 22 °C to 25 °C.

Overall, the model was found capable of simulating the effect of temperature on the anaerobic digestion as expected. Validation is however still required. For now, it can therefore only be used as a tool for theoretical calculation of the effect of different design and operational scenarios. However, these calculations can help to recommend on the design of new reactors as a 'best guess'.

5.2. Recommendations

5.2.1. La Trappe design

At the brewery of La Trappe, a fixed-dome anaerobic digester will be build for the digestion of the wort and sludge mixture. However, due to the uncertainty of the influence of temperature fluctuations on the anaerobic digestion process of such a reactor in the Dutch climate, recommendations based on this model will be used for design. This digester will be used to validate the model from this thesis, which then can be used more reliably. For now however, as a 'best guess', the results from this thesis will be used. These recommendations are summarised in the cost-benefit analysis of Table 5.1.

As the situation of La Trappe is quite complex, the model is not able to fully simulate all effects which will influence biogas production at La Trappe. Some general recommendations about other effects considered but not researched in this thesis are therefore given in Appendix E.

First of all, it was found that biogas production increases with temperature and that including insulation increased mean temperature and biogas production. Insulation is therefore recommended in the digester. As found with the heat transfer model, solar irradiance is an important source of heat, especially in summer. It is therefore important that the amount of sunlight to which the digester is exposed is maximized. The digester should therefore be positioned at a location without any buildings or trees blocking solar rays. A consideration for further optimal usage of solar irradiance is explored below in the recommendations on future research.

Table 5.1: Design considerations for the La Trappe case. C stands for costs and B for benefits. The pluses and minuses then determine of the cost or benefit increases or decreases with the implementation of the proposed influent or technology to the digester

	C/B	Pre-treatment	Urine	MNR	Base	Insulation	Heating
Mean temperature	B	+	+/-	-	+/-	++	++
Biogas production	B	+	++	+	++	+	+
Reactor volume	C	-	+	++	+/-	-	-
Temperature variability	C	-	-	-	+/-	+	++

It was found in the model that a volume of 40 m^3 should be sufficient for the digestion of $2 \text{ m}^3 \text{ d}^{-1}$ of influent wort and sludge mixture with a temperature of $45 \text{ }^\circ\text{C}$ and a cation concentration of $0.02 \text{ kmole m}^{-3}$. However, one important factor has not been taken into account in the model, as day and night bulk liquid temperature fluctuations and their effect on biogas production are excluded in this thesis. It was however shown that smaller digesters are prone to larger temperature fluctuations, and that these fluctuations can have a considerable effects on biogas production stability. If these daily temperature fluctuations are larger than $0.5 \text{ }^\circ\text{C}$, it is likely that they will have negative impact on the biogas production. These effects can cause acetate accumulation, and therefore relative higher amounts of base are needed for dosing in these smaller reactors. Furthermore, lower temperatures at night will lower daily methane production, meaning that yearly methane production might be overestimated in the used model, and this effect becomes larger when decreasing reactor volume. These effects can however possibly be mitigated by increasing the total heat capacity of the reactor, as is explored below in the recommendations on future research.

In the model, it is assumed that the influent is continuous, completely mixed and homogeneous over time. In practicality, a mixer and buffer tank will be needed to achieve this, as the belt-thickened sludge is dense, and the variability of spent wort is high. Furthermore, to limit influent temperature variability, a heat exchanger will need to be installed in this tank as well. This tank will therefore prepare the substrate for digestion and can be seen as a pre-treatment tank. This pre-treatment tank will ensure an influent temperature of at least $45 \text{ }^\circ\text{C}$, so bulk liquid temperatures will vary between $25 \text{ }^\circ\text{C}$ and $35 \text{ }^\circ\text{C}$ between winter and summer. This will prevent LCFA accumulation in the reactor. The energy needed to attain this influent temperature is expected to be low, as the heat already present in both substrates at their current end-of-life is already high enough to reach $45 \text{ }^\circ\text{C}$. However, some heat loss is expected over transportation and buffer time, and it is expected that heating is necessary, especially in winter. The increase in bulk liquid temperature and the fact that substrate can be introduced continuously and homogeneously with the pre-treatment tank will increase biogas production and lower needed volume, as the substrate will be better available for digestion by the microbes after the WAS has been liquefied with the wort.

Higher and more stable yearly bulk liquid temperatures could also be achieved with internal usage of the biogas in a heater. However, this was deemed unfavourable as sufficient heat is already available at the current end-of-life of the waste streams. The increase in biogas production with a biogas heater does not compensate for the large increase in the initial expenses, and it decreases the frugality of the designed reactor.

It was found that the model predicts that acidification will occur, and that therefore base needs to be dosed or the influent needs to be diluted. However, at an influent temperature of $45 \text{ }^\circ\text{C}$, the concentrations needed are relatively low. It can therefore be hypothesized that human urine can be used as a base for the digester as well, as this could potentially meet the demand with the use of the urinoirs or urine-separating toilets in the monastery, the brewery and the restaurant. It should however be checked that free ammonia concentrations are limited in the substrate, as otherwise urine could potentially inhibit methanogenesis. The urine could be introduced in the pre-treatment tank, as it would also help liquefy the WAS.

If diluent is needed for further liquefaction of the WAS, or to lower the OLR, the effluent of the MNR is recommended, as the pH and temperature are higher and more stable then the influent. However,

this would require an increase in reactor volume to stay at the HRT, and is therefore discouraged unless necessary. Base like lime could be dosed as well, but this would increase operational expenses, as well as lower the frugality of the whole design, and is therefore discouraged as well. However, this could be considered as a temporary option in the start up or in especially cold winters.

5.2.2. Further research

Experimental

The implementation of the temperature inhibition functions in this thesis heavily relied on the research papers on the effect of temperature on microbial activity within the mesophilic range done by Rebac et al. [84] and Donoso-Bravo et al. [28]. However, the substrates considered and the number of measurements done in these studies does not cover all processes within the ADM1 and the simulations considered in this thesis. To validate the temperature inhibition functions, similar studies should be done, as this would also help in considering the differences between the Arrhenius and cardinal temperature equation. Furthermore, the 5th order temperature relation to k_{La} found by Lee [58] should be validated for the desorption of methane from digestate as well, as validity could have large implications on methane leakage from digestate in unheated digesters.

Modelling

In its current version, the main shortcoming of the coupled heat transfer and ADM1 model is its inability for daily temperature fluctuations. It is expected in smaller reactors that these fluctuations can have large effects on biogas production, and the temperature inhibition functions already have the capabilities to showcase these effects. The implementation of the daily fluctuations should be feasible, as this already done in the original model of Vilms Pedersen et al. [98], and the heat transfer dynamics are well known. Furthermore, the effect of burial depth could be added to the model as well.

Other considerations for passive heat management

It was found that the total heat capacity has a large effect on temperature fluctuations, with higher fluctuations at lower heat capacities. In the current model, the only way to increase the heat capacity would be by increasing the volume. However, it would be interesting to see the effect of adding a layer of building material with high heat capacity such as basalt between the insulation and cement layer. This could help stabilize the temperature of digesters, especially those with smaller volumes.

In digesters with heating in warmer climates, solar irradiance can cause overheating [13, 64]. Passive cooling by painting the digesters white is done to increase the albedo. The opposite is done in unheated digesters, where the digester is painted black to increase passive heating from solar irradiance. Overheating events occur in summer, when solar irradiance is strongest and the sun is the highest in the sky. While reactor are actively heated in winter when the sun is generally low in the sky. It would be interesting to see the net effect of having a black ring around the base of a fixed-dome digester, or on the vertical walls of an industrial digester, to stimulate the uptake of solar irradiance in winter, and having a white top or roof to limit solar irradiance in summer.

A cross-sectional representation of a fixed-dome digester with this type of painting and a basalt layer to improve passive heat management is shown in Figure 5.1. To the authors knowledge, reactors with such modifications are as of yet unexplored, and therefore recommended for future research.

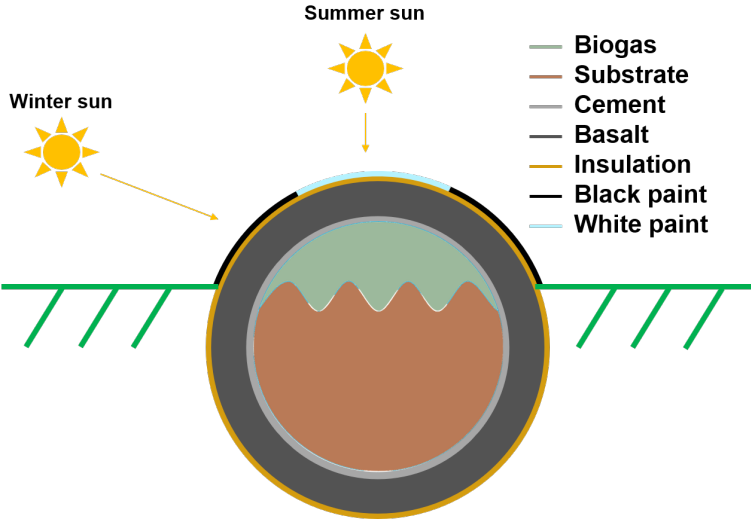


Figure 5.1: Cross-sectional representation of having black and white paint for passive heating and cooling in winter and summer, and having a basalt layer in the reactor walls for improved heat capacity. The effect of these measurements could be explored in future research.

References

- [1] Abdelfatah Abomohra et al. "Recent advances in anaerobic digestion of lipid-rich waste: Challenges and potential of seaweeds to mitigate the inhibitory effect". In: *Chemical Engineering Journal* 449 (Dec. 2022), p. 137829. ISSN: 1385-8947. DOI: 10.1016/J.CEJ.2022.137829.
- [2] Nouceiba Adouani et al. "Control of a farm anaerobic digester for agricultural wastes". In: *IFAC-PapersOnLine* 50.1 (July 2017), pp. 3923–3928. ISSN: 24058963. DOI: 10.1016/J.IFACOL.2017.08.366.
- [3] Karin Ahlberg-Eliasson et al. "Anaerobic Digestion of Animal Manure and Influence of Organic Loading Rate and Temperature on Process Performance, Microbiology, and Methane Emission From Digestates". In: *Frontiers in Energy Research* 9 (Dec. 2021). ISSN: 2296598X. DOI: 10.3389/FENRG.2021.740314.
- [4] René Alvarez and Gunnar Lidén. "The effect of temperature variation on biomethanation at high altitude". In: *Bioresource Technology* 99.15 (Oct. 2008), pp. 7278–7284. ISSN: 0960-8524. DOI: 10.1016/J.BIORTECH.2007.12.055.
- [5] Sepideh Ansari, Javad Alavi, and Zaher Mundher Yaseen. "Performance of full-scale coagulation-flocculation/DAF as a pre-treatment technology for biodegradability enhancement of high strength wastepaper-recycling wastewater". In: *Environmental Science and Pollution Research* 25.34 (2018). ISSN: 16147499. DOI: 10.1007/s11356-018-3340-0.
- [6] APHA. "Standard Methods for the Examination of Water and Wastewater". In: *Standard Methods* (2005). ISSN: 15585646. DOI: ISBN9780875532356.
- [7] Magnus Arnell et al. "Modelling anaerobic co-digestion in Benchmark Simulation Model No. 2: Parameter estimation, substrate characterisation and plant-wide integration". In: *Water Research* 98 (2016). ISSN: 18792448. DOI: 10.1016/j.watres.2016.03.070.
- [8] Greg Austin and Glynn Morris. "Biogas Production in Africa BT - Bioenergy for Sustainable Development in Africa". In: ed. by Rainer Janssen and Dominik Rutz. Dordrecht: Springer Netherlands, 2012, pp. 103–115. ISBN: 978-94-007-2181-4. DOI: 10.1007/978-94-007-2181-4_{_}10. URL: https://doi.org/10.1007/978-94-007-2181-4_10.
- [9] P. Axaopoulos et al. "Simulation and experimental performance of a solar-heated anaerobic digester". In: *Solar Energy* 70.2 (Jan. 2001), pp. 155–164. ISSN: 0038-092X. DOI: 10.1016/S0038-092X(00)00130-4.
- [10] P.S. Bandgar et al. "Thermal modelling and experimental validation for biogas production in anaerobic digestion". In: *Bioresource Technology Reports* (Oct. 2022), p. 101243. ISSN: 2589-014X. DOI: 10.1016/J.BITEB.2022.101243. URL: <https://linkinghub.elsevier.com/retrieve/pii/S2589014X22003000>.
- [11] D. J. Batstone et al. "The IWA Anaerobic Digestion Model No 1 (ADM1)." In: *Water science and technology : a journal of the International Association on Water Pollution Research* 45.10 (2002). ISSN: 02731223. DOI: 10.2166/wst.2002.0292.
- [12] Damien J. Batstone and J. Keller. "Industrial applications of the IWA anaerobic digestion model No. 1 (ADM1)". In: *Water Science and Technology* 47.12 (June 2003), pp. 199–206. ISSN: 0273-1223. DOI: 10.2166/WST.2003.0647. URL: <http://www.aquasim.eawag.ch>.
- [13] Matteo Bavutti et al. "Thermal Stabilization of Digesters of Biogas Plants by Means of Optimization of the Surface Radiative Properties of the Gasometer Domes". In: *Energy Procedia* 45 (Jan. 2014), pp. 1344–1353. ISSN: 1876-6102. DOI: 10.1016/J.EGYPRO.2014.01.141.
- [14] Edem Cudjoe Bensah, Edward Antwi, and Julius Cudjoe Ahiekpor. "Improving sanitation in ghana-role of sanitary biogas plants". In: *Journal of Engineering and Applied Sciences* 5.2 (2010), pp. 125–133. ISSN: 1816949X. DOI: 10.3923/JEASCI.2010.125.133.

- [15] Wenche Hennie Bergland, Carlos Dinamarca, and Rune Bakke. "Temperature Effects in Anaerobic Digestion Modeling". In: *Proceedings of the 56th Conference on Simulation and Modelling (SIMS 56), October, 7-9, 2015, Linköping University, Sweden*. Vol. 119. 2015. DOI: 10.3384/ecp15119261.
- [16] Júlia C.B.F. Bijos et al. "Methane liquid-gas phase distribution during anaerobic sludge digestion: A thermodynamic approach". In: *Chemosphere* 298 (2022). ISSN: 18791298. DOI: 10.1016/j.chemosphere.2022.134325.
- [17] A. Boušková et al. "Strategies for changing temperature from mesophilic to thermophilic conditions in anaerobic CSTR reactors treating sewage sludge". In: *Water Research* 39.8 (2005), pp. 1481–1488. ISSN: 00431354. DOI: 10.1016/J.WATRES.2004.12.042.
- [18] Francesco Calise et al. "A Review of the State of the Art of Biomethane Production: Recent Advancements and Integration of Renewable Energies". In: *Energies* 2021, Vol. 14, Page 4895 14.16 (Aug. 2021), p. 4895. ISSN: 19961073. DOI: 10.3390/EN14164895. URL: <https://www.mdpi.com/1996-1073/14/16/4895/htm%20https://www.mdpi.com/1996-1073/14/16/4895>.
- [19] Francesco Calise et al. "Concentrating photovoltaic/thermal collectors coupled with an anaerobic digestion process: Dynamic simulation and energy and economic analysis". In: *Journal of Cleaner Production* 311 (Aug. 2021), p. 127363. ISSN: 0959-6526. DOI: 10.1016/J.JCLEPRO.2021.127363.
- [20] Francesco Calise et al. "Modeling of the Anaerobic Digestion of Organic Wastes: Integration of Heat Transfer and Biochemical Aspects". In: *Energies* 2020, Vol. 13, Page 2702 13.11 (May 2020), p. 2702. ISSN: 19961073. DOI: 10.3390/EN13112702. URL: <https://www.mdpi.com/1996-1073/13/11/2702/htm%20https://www.mdpi.com/1996-1073/13/11/2702>.
- [21] Juan M Castano, Jay F Martin, and Richard Ciotola. *Performance of a Small-Scale, Variable Temperature Fixed Dome Digester in a Temperate Climate*. 2014. DOI: 10.3390/en7095701.
- [22] Y Cengel and Transfer Mass Heat. "A practical approach". In: *Second edi* (2003).
- [23] P.S. Ceron Chafra. "Steering Product Formation in High-Pressure Anaerobic Digestion Systems: The role of elevated partial pressure of carbon dioxide (pCO₂)". In: (2022). DOI: 10.4233/UUID:851366E2-88E2-4D9E-8831-35A8DFE450DF. URL: <https://research.tudelft.nl/en/publications/steering-product-formation-in-high-pressure-anaerobic-digestions>.
- [24] Ye Chen, Jay J. Cheng, and Kurt S. Creamer. "Inhibition of anaerobic digestion process: A review". In: *Bioresour. Technol.* 99.10 (July 2008), pp. 4044–4064. ISSN: 09608524. DOI: 10.1016/J.BIORTECH.2007.01.057.
- [25] Shikun Cheng et al. "Development and application of prefabricated biogas digesters in developing countries". In: *Renewable and Sustainable Energy Reviews* 34 (June 2014), pp. 387–400. ISSN: 1364-0321. DOI: 10.1016/J.RSER.2014.03.035.
- [26] Marlies E.R. Christiaens et al. "Anaerobic ureolysis of source-separated urine for NH₃ recovery enables direct removal of divalent ions at the toilet". In: *Water Research* 148 (Jan. 2019), pp. 97–105. ISSN: 0043-1354. DOI: 10.1016/J.WATRES.2018.10.021.
- [27] Samuel Olatunde Dahunsi, Omololu Oluwatobi Fagbiele, and Esther Ojima Yusuf. "Bioenergy technologies adoption in Africa: A review of past and current status". In: *Journal of Cleaner Production* 264 (Aug. 2020), p. 121683. ISSN: 0959-6526. DOI: 10.1016/J.JCLEPRO.2020.121683.
- [28] A. Donoso-Bravo et al. "Influence of temperature on the hydrolysis, acidogenesis and methanogenesis in mesophilic anaerobic digestion: parameter identification and modeling application". In: *Water Science and Technology* 60.1 (July 2009), pp. 9–17. ISSN: 0273-1223. DOI: 10.2166/WST.2009.316. URL: <http://iwaponline.com/wst/article-pdf/60/1/9/448618/9.pdf>.
- [29] Michel Dubois et al. "Colorimetric Method for Determination of Sugars and Related Substances". In: *Analytical Chemistry* 28.3 (1956). ISSN: 15206882. DOI: 10.1021/ac60111a017.
- [30] Jenessa Duncombe. "A Climate Mystery Warns Us to Heed the Unknown". In: *Eos (United States)* 103.6 (2022), p. 19. ISSN: 23249250. DOI: 10.1029/2022E0220207.

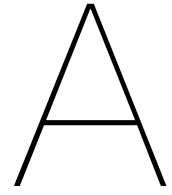
- [31] Aransiola Elizabeth Funmi et al. "Biogas production as energy source and strategy for managing waste and climate change". In: *SN Applied Sciences* 3.1 (Jan. 2021), pp. 1–11. ISSN: 25233971. DOI: 10.1007/s42452-020-03973-8/FIGURES/12. URL: <https://link-springer-com.tudelft.idm.oclc.org/article/10.1007/s42452-020-03973-8>.
- [32] Dilek Erdirencelebi and Gool Mohammad Ebrahimi. "Enhanced sewage sludge treatment via parallel anaerobic digestion at the upper mesophilic level". In: *Journal of Environmental Management* 320 (Oct. 2022). ISSN: 10958630. DOI: 10.1016/J.JENVMAN.2022.115850.
- [33] Yucheng Feng et al. "Parameter analysis of the IWA Anaerobic Digestion Model No. 1 for the anaerobic digestion of blackwater with kitchen refuse". In: *Water Science and Technology* 54.4 (Aug. 2006), pp. 139–147. ISSN: 0273-1223. DOI: 10.2166/WST.2006.535. URL: <http://iwaponline.com/wst/article-pdf/54/4/139/431808/139.pdf>.
- [34] Fernando G. Feroso et al. *Trace Elements in Anaerobic Biotechnologies*. June 2019. ISBN: 9781789060218.
- [35] Adrian Gonzalez. *Standard operation procedures (SOPs) for BMP & related analyses v1*. Tech. rep. Delft: TU Delft Waterlab.
- [36] W Gujer and A J B Zehnder. "Conversion Processes in Anaerobic Digestion". In: *Water Science and Technology* 15.8-9 (Aug. 1983), pp. 127–167. ISSN: 0273-1223. DOI: 10.2166/wst.1983.0164. URL: <https://doi.org/10.2166/wst.1983.0164>.
- [37] Muhammad Usman Hanif et al. "The Effects of Using Pretreated Cotton Gin Trash on the Production of Biogas from Anaerobic Co-Digestion with Cow Manure and Sludge". In: *Energies* 15.2 (Jan. 2022). ISSN: 19961073. DOI: 10.3390/en15020490.
- [38] Kaare Hvid Hansen, Irini Angelidaki, and Birgitte Kiær Ahring. "ANAEROBIC DIGESTION OF SWINE MANURE: INHIBITION BY AMMONIA". In: *Water Research* 32.1 (Jan. 1998), pp. 5–12. ISSN: 0043-1354. DOI: 10.1016/S0043-1354(97)00201-7.
- [39] Amro A.M. Hassanein et al. "Simulation and validation of a model for heating underground biogas digesters by solar energy". In: *Ecological Engineering* 82 (Sept. 2015), pp. 336–344. ISSN: 0925-8574. DOI: 10.1016/J.ECOLENG.2015.05.010.
- [40] Yang He et al. "Wort composition and its impact on the flavour-active higher alcohol and ester formation of beer – a review". In: *Journal of the Institute of Brewing* 120.3 (June 2014), pp. 157–163. ISSN: 2050-0416. DOI: 10.1002/JIB.145. URL: <https://onlinelibrary.wiley.com/doi/full/10.1002/jib.145>
<https://onlinelibrary.wiley.com/doi/abs/10.1002/jib.145>
<https://onlinelibrary.wiley.com/doi/10.1002/jib.145>.
- [41] M. Henze and P. Harremoës. "Anaerobic Treatment of Wastewater in Fixed Film Reactors – A Literature Review". In: *Water Science and Technology* 15.8-9 (Aug. 1983), pp. 1–101. ISSN: 0273-1223. DOI: 10.2166/WST.1983.0161. URL: <http://iwaponline.com/wst/article-pdf/15/8-9/1/95621/1.pdf>.
- [42] Mogens Henze et al. *Biological Wastewater Treatment: Principles, Modeling and Design*. 2019. DOI: 10.2166/9781780408613.
- [43] C. N. Hinshelwood. "The Chemical Kinetics of the Bacterial Cell". In: *Journal of the American Chemical Society* 69.9 (1947). ISSN: 15205126. DOI: 10.1021/ja01201a035.
- [44] Christof Holliger et al. "Towards a standardization of biomethane potential tests". In: *Water Science and Technology* 74.11 (Dec. 2016), pp. 2515–2522. ISSN: 0273-1223. DOI: 10.2166/WST.2016.336. URL: <http://iwaponline.com/wst/article-pdf/74/11/2515/457029/wst074112515.pdf>byTECHNISCHEUNIVERSITEITDELFTuser.
- [45] Rainier Hreiz et al. "Modeling and simulation of heat transfer phenomena in a semi-buried anaerobic digester". In: *Chemical Engineering Research and Design* 119 (2017), pp. 101–116. ISSN: 02638762. DOI: 10.1016/J.CHERD.2017.01.007.
- [46] C. Hubert et al. "Variation of the digester temperature in the annual cycle – using the digester as heat storage". In: *Water Practice and Technology* 14.2 (June 2019), pp. 471–481. ISSN: 1751231X. DOI: 10.2166/WPT.2019.030. URL: <http://iwaponline.com/wpt/article-pdf/14/2/471/639740/wpt0140471.pdf>.

- [47] IEA. "World energy balance 2018: Overview". In: *lea* (2018).
- [48] "IMPLEMENTING THE REPOWER EU ACTION PLAN: INVESTMENT NEEDS, HYDROGEN ACCELERATOR AND ACHIEVING THE BIO-METHANE TARGETS". Brussels, May 2022.
- [49] Ying Jiang et al. "Ammonia inhibition and toxicity in anaerobic digestion: A critical review". In: *Journal of Water Process Engineering* 32 (Dec. 2019), p. 100899. ISSN: 2214-7144. DOI: 10.1016/J.JWPE.2019.100899.
- [50] M. A. Khan et al. "Optimization of process parameters for production of volatile fatty acid, biohydrogen and methane from anaerobic digestion". In: *Bioresource Technology* 219 (Nov. 2016), pp. 738–748. ISSN: 0960-8524. DOI: 10.1016/J.BIORTECH.2016.08.073.
- [51] Jugal Kishor et al. "Solar assisted biogas plants III: Energy balance of fixed dome biogas plants and enhancement of production in winters". In: *International Journal of Energy Research* 12.4 (Oct. 1988), pp. 711–737. ISSN: 1099-114X. DOI: 10.1002/ER.4440120411. URL: <https://onlinelibrary.wiley.com/doi/full/10.1002/er.4440120411>. URL: <https://onlinelibrary.wiley.com/doi/abs/10.1002/er.4440120411>. URL: <https://onlinelibrary.wiley.com/doi/10.1002/er.4440120411>.
- [52] V.N.N. Kishore and S. Dhingra. "A gas regulator for fixed dome biogas plants". In: *Changing villages* 9.1 (1990), pp. 32–39.
- [53] Robbert Kleerebezem et al. "Anaerobic digestion without biogas?" In: *Reviews in Environmental Science and Biotechnology* 14.4 (Dec. 2015), pp. 787–801. ISSN: 15729826. DOI: 10.1007/S11157-015-9374-6/FIGURES/9. URL: <https://link.springer.com/article/10.1007/s11157-015-9374-6>.
- [54] *KNMI - Daggegevens van het weer in Nederland*. URL: <https://www.knmi.nl/nederland-nu/klimatologie/daggegevens>.
- [55] *KNMI - Jaar 2010: Koudste jaar sinds 1996*. URL: <https://www.knmi.nl/nederland-nu/klimatologie/maand-en-seizoensoverzichten/2010/jaar>.
- [56] Adam Kovalovszki et al. "Modeling temperature response in bioenergy production: Novel solution to a common challenge of anaerobic digestion". In: *Applied Energy* 263 (Apr. 2020), p. 114646. ISSN: 0306-2619. DOI: 10.1016/J.APENERGY.2020.114646.
- [57] Setyo Budi Kurniawan et al. "Challenges and opportunities of biocoagulant/bioflocculant application for drinking water and wastewater treatment and its potential for sludge recovery". In: *International Journal of Environmental Research and Public Health* 17.24 (Dec. 2020), pp. 1–33. ISSN: 16604601. DOI: 10.3390/IJERPH17249312.
- [58] Johnny Lee. "Development of a model to determine mass transfer coefficient and oxygen solubility in bioreactors". In: *Heliyon* 3.2 (Feb. 2017). ISSN: 24058440. DOI: 10.1016/J.HELIYON.2017.E00248. URL: [/pmc/articles/PMC5318378/](https://pubmed.ncbi.nlm.nih.gov/318378/). URL: [https://pubmed.ncbi.nlm.nih.gov/318378/](https://pubmed.ncbi.nlm.nih.gov/318378/?report=abstract). URL: <https://www.ncbi.nlm.nih.gov/pmc/articles/PMC5318378/>.
- [59] W. K. Lewis and W. G. Whitman. "Principles of Gas Absorption". In: *Industrial and Engineering Chemistry* 16.12 (1924). ISSN: 00197866. DOI: 10.1021/ie50180a002.
- [60] Qiang Lin et al. "Microorganism-regulated mechanisms of temperature effects on the performance of anaerobic digestion". In: *Microbial Cell Factories* 15.1 (2016), p. 96. ISSN: 1475-2859. DOI: 10.1186/s12934-016-0491-x. URL: <https://doi.org/10.1186/s12934-016-0491-x>.
- [61] Yanfeng Liu et al. "Investigation on the heat loss characteristic of underground household biogas digester using dynamic simulations and experiments". In: *Biosystems Engineering* 163 (Nov. 2017), pp. 116–133. ISSN: 1537-5110. DOI: 10.1016/J.BIOSYSTEMSENG.2017.09.002.
- [62] Jianbo Lu and Xianyi Gao. "Biogas: Potential, challenges, and perspectives in a changing China". In: *Biomass and Bioenergy* 150 (July 2021), p. 106127. ISSN: 0961-9534. DOI: 10.1016/J.BIOMBIOE.2021.106127.
- [63] J. Martí-Herrero. "Reduced hydraulic retention times in low-cost tubular digesters: Two issues". In: *Biomass and Bioenergy* 35.10 (Oct. 2011), pp. 4481–4484. ISSN: 0961-9534. DOI: 10.1016/J.BIOMBIOE.2011.07.020.

- [64] Hamed M. El-Mashad et al. "Effect of temperature and temperature fluctuation on thermophilic anaerobic digestion of cattle manure". In: *Bioresource Technology* 95.2 (Nov. 2004), pp. 191–201. ISSN: 0960-8524. DOI: 10.1016/J.BIORTECH.2003.07.013.
- [65] N R Melbinger, J Donnellon, and Herman R Zablatzky. "Toxic Effects of Ammonia Nitrogen in High-Rate Digestion [with Discussion]". In: *Journal (Water Pollution Control Federation)* 43.8 (Nov. 1971), pp. 1658–1670. ISSN: 00431303. URL: <http://www.jstor.org/stable/25037154>.
- [66] Gérard Merlin et al. "Importance of heat transfer in an anaerobic digestion plant in a continental climate context". In: *Bioresource Technology* 124 (Nov. 2012), pp. 59–67. ISSN: 0960-8524. DOI: 10.1016/J.BIORTECH.2012.08.018.
- [67] W. Metcalf and C. Eddy. *Wastewater Engineering: Treatment and Resource Recovery, Fifth Edition*. 2014.
- [68] J. Moestedt, J. Rönnerberg, and E. Nordell. "The effect of different mesophilic temperatures during anaerobic digestion of sludge on the overall performance of a WWTP in Sweden". In: *Water Science and Technology* 76.12 (Dec. 2017), pp. 3213–3219. ISSN: 0273-1223. DOI: 10.2166/WST.2017.367. URL: <http://iwaponline.com/wst/article-pdf/76/12/3213/241882/wst076123213.pdf>.
- [69] Jan Moestedt, Erik Nordell, and Anna Schnürer. "Comparison of operating strategies for increased biogas production from thin stillage". In: *Journal of Biotechnology* 175.1 (Apr. 2014), pp. 22–30. ISSN: 0168-1656. DOI: 10.1016/J.JBIOTEC.2014.01.030.
- [70] Jacques Monod. "THE GROWTH OF BACTERIAL CULTURES". In: *Annual Review of Microbiology* 3.1 (1949). ISSN: 0066-4227. DOI: 10.1146/annurev.mi.03.100149.002103.
- [71] Jerome Ndam Mungwe et al. "The fixed dome digester: An appropriate design for the context of Sub-Saharan Africa?" In: *Biomass and Bioenergy* 95 (Dec. 2016), pp. 35–44. ISSN: 0961-9534. DOI: 10.1016/J.BIOMBIOE.2016.09.007.
- [72] Jerusha Ngungui. *EAST AFRICA CLIMATIC DATA AND GUIDELINES FOR BIOCLIMATIC ARCHITECTURAL DESIGN*. Tech. rep. Nairobi: UN Habitat, 2016, p. 194. URL: https://unhabitat.org/sites/default/files/2020/06/gh050e_compressed.pdf.
- [73] Sosuke Nishimura and Motoyuki Yoda. "Removal of hydrogen sulfide from an anaerobic biogas using a bio-scrubber". In: *Water Science and Technology* 36.6-7 (Jan. 1997), pp. 349–356. ISSN: 0273-1223. DOI: 10.1016/S0273-1223(97)00542-8.
- [74] *Norsk Klimaservicesenter*. URL: <https://seklima.met.no/observations/>.
- [75] A. Pauss et al. "Liquid-to-Gas mass transfer in anaerobic processes: Inevitable transfer limitations of methane and hydrogen in the biomethanation process". In: *Applied and Environmental Microbiology* 56.6 (1990). ISSN: 00992240. DOI: 10.1128/aem.56.6.1636-1644.1990.
- [76] S G Pavlostathis and E Giraldo-Gomez. "Critical Reviews in Environmental Science and Technology Kinetics of anaerobic treatment: A critical review Kinetics of Anaerobic Treatment: A Critical Review". In: *Critical Reviews in Environmental Control* 21.January 2013 (1991).
- [77] Miriam Peces et al. "Transition of microbial communities and degradation pathways in anaerobic digestion at decreasing retention time". In: *New Biotechnology* 60 (Jan. 2021), pp. 52–61. ISSN: 18764347. DOI: 10.1016/J.NBT.2020.07.005.
- [78] Michael W. Peck et al. "Effects of temperature shock treatments on the stability of anaerobic digesters operated on separated cattle slurry". In: *Water Research* 20.4 (Apr. 1986), pp. 453–462. ISSN: 0043-1354. DOI: 10.1016/0043-1354(86)90193-4.
- [79] Ruizhe Pei et al. "Exploring the Limits of Polyhydroxyalkanoate Production by Municipal Activated Sludge". In: *Environmental Science and Technology* 56.16 (Aug. 2022), pp. 11729–11738. ISSN: 15205851. DOI: 10.1021/ACS.EST.2C03043.
- [80] John T. Pfeffer. "Temperature effects on anaerobic fermentation of domestic refuse". In: *Biotechnology and Bioengineering* 16.6 (June 1974), pp. 771–787. ISSN: 1097-0290. DOI: 10.1002/BIT.260160607. URL: <https://onlinelibrary.wiley.com/doi/full/10.1002/bit.260160607>. <https://onlinelibrary.wiley.com/doi/abs/10.1002/bit.260160607> <https://onlinelibrary.wiley.com/doi/10.1002/bit.260160607>.

- [81] Divya Prakash, Shikha S. Chauhan, and James G. Ferry. "Life on the thermodynamic edge: Respiratory growth of an acetotrophic methanogen". In: *Science Advances* 5.8 (2019). ISSN: 23752548. DOI: 10.1126/sciadv.aaw9059.
- [82] Rameshprabu Ramaraj and Yuwalee Unpaprom. "Effect of temperature on the performance of biogas production from Duckweed". In: *Chemical Science* 1 (Mar. 2016), pp. 58–66.
- [83] Parastoo Rashidian, Javad Mahmoudimehr, and Kazem Atashkari. "An underground anaerobic digester with permissible temperature fluctuations: A parametric study". In: *Cleaner Energy Systems* 2 (July 2022), p. 100007. ISSN: 2772-7831. DOI: 10.1016/J.CLES.2022.100007.
- [84] Salih Rebac et al. "High-rate anaerobic treatment of wastewater under psychrophilic conditions". In: *Journal of Fermentation and Bioengineering* 80.5 (Jan. 1995), pp. 499–506. ISSN: 0922-338X. DOI: 10.1016/0922-338X(96)80926-3.
- [85] C. Rosen and U. Jeppsson. "Aspects on ADM1 Implementation within the BSM2 Framework". In: *Technical report* (2006).
- [86] L. Rosso, J. R. Lobry, and J. P. Flandrois. "An Unexpected Correlation between Cardinal Temperatures of Microbial Growth Highlighted by a New Model". In: *Journal of Theoretical Biology* 162.4 (1993). ISSN: 00225193. DOI: 10.1006/jtbi.1993.1099.
- [87] P Sadrimajd et al. "PyADM1: a Python implementation of Anaerobic Digestion Model No. 1". In: *bioRxiv* (2021).
- [88] Xiaoli Song et al. "Fate of proteins of waste activated sludge during thermal alkali pretreatment in terms of sludge protein recovery". In: *Frontiers of Environmental Science & Engineering* 2019 13:2 13.2 (Mar. 2019), pp. 1–9. ISSN: 2095-221X. DOI: 10.1007/S11783-019-1114-7. URL: <https://link.springer.com/article/10.1007/s11783-019-1114-7>.
- [89] *Storing large scale renewables with basalt stones – pv magazine International*. URL: <https://www.pv-magazine.com/2021/05/04/storing-large-scale-renewables-with-basalt-stones/>.
- [90] Gede Adi Wiguna Sudiarta, Tsuyoshi Imai, and Yung Tse Hung. "Effects of Stepwise Temperature Shifts in Anaerobic Digestion for Treating Municipal Wastewater Sludge: A Genomic Study". In: *International Journal of Environmental Research and Public Health* 19.9 (May 2022). ISSN: 16604601. DOI: 10.3390/IJERPH19095728.
- [91] Meichen Sun et al. "Novel Long-Chain Fatty Acid (LCFA)-Degrading Bacteria and Pathways in Anaerobic Digestion Promoted by Hydrochar as Revealed by Genome-Centric Metatranscriptomics Analysis". In: *Applied and Environmental Microbiology* 88.16 (Aug. 2022). ISSN: 10985336. DOI: 10.1128/AEM.01042-22.
- [92] K. C. Surendra et al. *Biogas as a sustainable energy source for developing countries: Opportunities and challenges*. 2014. DOI: 10.1016/j.rser.2013.12.015.
- [93] W. C. Swinbank. "Long-wave radiation from clear skies". In: *Quarterly Journal of the Royal Meteorological Society* 89.381 (July 1963), pp. 339–348. ISSN: 1477-870X. DOI: 10.1002/QJ.49708938105. URL: <https://onlinelibrary.wiley.com/doi/full/10.1002/qj.49708938105> <https://onlinelibrary.wiley.com/doi/abs/10.1002/qj.49708938105> <https://rmets.onlinelibrary.wiley.com/doi/10.1002/qj.49708938105>.
- [94] Georgina Terradas-III et al. "Thermic model to predict biogas production in unheated fixed-dome digesters buried in the ground". In: *Environmental Science and Technology* 48.6 (Mar. 2014), pp. 3253–3262. ISSN: 15205851. DOI: 10.1021/ES403215W/SUPPL{_}FILE/ES403215W{_}SI{_}001.PDF. URL: <https://pubs.acs.org/doi/abs/10.1021/es403215w>.
- [95] T. Thamsiroj and J. D. Murphy. "Modelling mono-digestion of grass silage in a 2-stage CSTR anaerobic digester using ADM1". In: *Bioresource Technology* 102.2 (2011). ISSN: 09608524. DOI: 10.1016/j.biortech.2010.09.051.
- [96] Jules Van Lier. *Slides from CIE4703-19 Water Treatment: Anaerobic treatment 1*. Tech. rep. Delft: TU Delft, 2021. URL: <https://brightspace.tudelft.nl/d21/le/content/399357/viewContent/2560442/View>.

- [97] Jules B. Van Lier, Salih Rebac, and Gatze Lettinga. "High-rate anaerobic wastewater treatment under psychrophilic and thermophilic conditions". In: *Water Science and Technology* 35.10 (Jan. 1997), pp. 199–206. ISSN: 0273-1223. DOI: 10.1016/S0273-1223(97)00202-3.
- [98] S. Vilms Pedersen et al. "Management and design of biogas digesters: A non-calibrated heat transfer model". In: *Bioresource Technology* 296 (Jan. 2020), p. 122264. ISSN: 0960-8524. DOI: 10.1016/J.BIORTECH.2019.122264.
- [99] Yvonne Vögeli et al. *Anaerobic Digestion of Biowaste in Developing Countries - Practical Information and Case Studies*. Jan. 2014. ISBN: 978-3-906484-58-7. DOI: 10.13140/2.1.2663.1045.
- [100] Darko Vrecko et al. "Benchmark Simulation Model No 2 in Matlab-Simulink: towards plant-wide WWTP control strategy evaluation". In: *Water Science and Technology* 54.8 (Oct. 2006), pp. 65–72. ISSN: 0273-1223. DOI: 10.2166/WST.2006.773. URL: <http://iwaponline.com/wst/article-pdf/54/8/65/431513/65.pdf>.
- [101] Henry Wasajja et al. "Improvement of biogas quality and quantity for small-scale biogas-electricity generation application in off-grid settings: A field-based study". In: *Energies* 14.11 (June 2021), p. 3088. ISSN: 19961073. DOI: 10.3390/EN14113088/S1. URL: <https://www.mdpi.com/1996-1073/14/11/3088/html>
<https://www.mdpi.com/1996-1073/14/11/3088>.
- [102] Sören Weinrich and Michael Nelles. "Systematic simplification of the Anaerobic Digestion Model No. 1 (ADM1) – Model development and stoichiometric analysis". In: *Bioresource Technology* 333 (2021). ISSN: 18732976. DOI: 10.1016/j.biortech.2021.125124.
- [103] World Bioenergy Association. *Global Bioenergy Statistics 2020*. Tech. rep. 2020.
- [104] *World Radiation Data Center*. URL: <http://wrdc.mgo.rssi.ru/>.
- [105] Sihuang Xie et al. "Anaerobic co-digestion: A critical review of mathematical modelling for performance optimization". In: *Bioresource Technology* 222 (Dec. 2016), pp. 498–512. ISSN: 0960-8524. DOI: 10.1016/J.BIORTECH.2016.10.015.
- [106] Bao Shan Xing and Xiaochang C. Wang. "High-rate mesophilic co-digestion with food waste and waste activated sludge through a low-magnitude increasing loading regime: Performance and microorganism characteristics". In: *Science of The Total Environment* 777 (July 2021), p. 146210. ISSN: 0048-9697. DOI: 10.1016/J.SCITOTENV.2021.146210.
- [107] Bojie Yan et al. "Spatial-temporal distribution of biogas production from agricultural waste per capita in rural China and its correlation with ground temperature". In: *Science of The Total Environment* 817 (Apr. 2022), p. 152987. ISSN: 0048-9697. DOI: 10.1016/J.SCITOTENV.2022.152987.
- [108] Li Yan et al. "Hydrogen sulfide formation control and microbial competition in batch anaerobic digestion of slaughterhouse wastewater sludge: Effect of initial sludge pH". In: *Bioresource Technology* 259 (July 2018), pp. 67–74. ISSN: 0960-8524. DOI: 10.1016/J.BIORTECH.2018.03.011.
- [109] Orhan Yenigün and Burak Demirel. "Ammonia inhibition in anaerobic digestion: A review". In: *Process Biochemistry* 48.5-6 (May 2013), pp. 901–911. ISSN: 1359-5113. DOI: 10.1016/J.PROCBIO.2013.04.012.
- [110] A. S.M. Younus Bhuiyan Sabbir et al. "Effects of Seasonal Temperature Variation on Slurry Temperature and Biogas Composition of a Commercial Fixed-Dome Anaerobic Digester Used in Bangladesh". In: *Sustainability* 2021, Vol. 13, Page 11096 13.19 (Oct. 2021), p. 11096. ISSN: 20711050. DOI: 10.3390/SU131911096. URL: <https://www.mdpi.com/2071-1050/13/19/11096/html>
<https://www.mdpi.com/2071-1050/13/19/11096>.



ADM1 Petersen matrix

	1	2	3	4	5	6	7
	S_su	S_aa	S_fa	S_va	S_bu	S_pro	S_ac
1	Disintegraton	X_c					
2	Hydrolysis	X_ch					
3	Hydrolysis	X_pr					
4	Hydrolysis	X_li	f_fa_li				
5	Acidogenesis	S_su			(1-Y_su) * f_bu_su	(1-Y_su) * f_pro_su	(1-Y_su) * f_ac_su
6	Acidogenesis	S_aa	-1	(1-Y_aa) f_va_aa	(1-Y_aa) * f_bu_aa	(1-Y_aa) * f_pro_aa	(1-Y_aa) * f_ac_aa
7	Acidogenesis	S_fa	-1			(1-Y_aa) * 0,7	
8	Acetogenesis	S_va		-1		(1-Y_c4) * 0,54	(1-Y_c4) * 0,31
9	Acetogenesis	S_bu			-1		(1-Y_c4) * 0,8
10	Acetogenesis	S_pro				-1	(1-Y_c4) * 0,57
11	Methanogenesis	S_ac					-1
12	Methanogenesis	S_h2					
13	Decay	X_su					
14	Decay	X_aa					
15	Decay	X_fa					
16	Decay	X_c4					
17	Decay	X_pro					
18	Decay	X_ac					
19	Decay	X_h2					
20	Dissociation	S_va					
21	Dissociation	S_bu					
22	Dissociation	S_pro					
23	Dissociation	S_ac					
24	Dissociation	S_IC					
25	Dissociation	S_IN					
26	Phase transition	S_h2					
27	Phase transition	S_ch4					
28	Phase transition	S_co2					

	8	9	10	11	12	13
	S_h2	S_ch4	S_IC	S_IN	S_I	X_c
1	Disintegraton X_c		s_1	(N_xc - f_xl_xc * N_l - f_sl_xc * N_l - f_pr_xc * N_aa)	f_sl_xc	-1
2	Hydrolysis X_ch		s_2			
3	Hydrolysis X_pr		s_3			
4	Hydrolysis X_li		s_4			
5	Acidogenesis S_su		s_5	-Y_su * N_bac		
6	Acidogenesis S_aa		s_6	N_aa - Y_aa * N_bac		
7	Acidogenesis S_fa		s_7	-Y_fa * N_bac		
8	Acetogenesis S_va		s_8	-Y_c4 * N_bac		
9	Acetogenesis S_bu		s_9	-Y_c4 * N_bac		
10	Acetogenesis S_pro		s_10	-Y_pro * N_bac		
11	Methanogenesis S_ac		s_11	-Y_ac * N_bac		
12	Methanogenesis S_h2	1 - Y_h2	s_12	-Y_h2 * N_bac		
13	Decay X_su		s_13	N_bac - N_xc		1
14	Decay X_aa		s_13	N_bac - N_xc		1
15	Decay X_fa		s_13	N_bac - N_xc		1
16	Decay X_c4		s_13	N_bac - N_xc		1
17	Decay X_pro		s_13	N_bac - N_xc		1
18	Decay X_ac		s_13	N_bac - N_xc		1
19	Decay X_h2		s_13	N_bac - N_xc		1
20	Dissociation S_va					
21	Dissociation S_bu					
22	Dissociation S_pro					
23	Dissociation S_ac					
24	Dissociation S_IC					
25	Dissociation S_IN					
26	Phase transition S_h2	-1				
27	Phase transition S_ch4	-1				
28	Phase transition S_co2		-1			

B

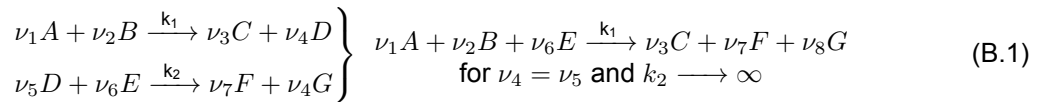
Simplifications

In order to relieve the model of complexities in terms of computational burden and number of parameters, simplifications of the model have been made according to the method proposed in the article of Weinrich and Nelles [102]. In contrast with this method which uses concentrations in kg m^{-3} , here the states of the ADM1 will be kept in kg COD m^{-3} basis.

This simplification method is based on the same assumption as the DAE implementation, that from the perspective of slower reactions, fast reactions are instantaneous. If reactions are consecutive, they can be represented by their sum reaction, with the reaction rate taken from the slowest step. A generalized case is shown in (B.1). This method has been used to simplify the ADM1 in a systematic way, which is summarised in Figure B.1 [102].

In the first simplification, the hydrogenotrophic methanogenesis step is relinquished. With this simplification, now each time hydrogen or hydrogenotrophic methanogens would have been produced, it is converted to methane, inorganic carbon, inorganic nitrogen, and complex matter instead. Hydrogen inhibition is omitted from the model as well. This first simplification is called R1. In the next simplification, in addition to the R1 simplification, the acidogenesis reactions are left out of the conversion matrix as well. In the new conversion pathway, hydrolysis results in the production of VFAs, acetate, methane, inorganic carbon, inorganic nitrogen and complex matter. This version is then called R2. In R3, the same method is applied to omit VFAs. Here, carbohydrates, proteins and lipids are immediately converted to acetate, methane, inorganic carbon and nitrogen and complex matter. In the last version, R4, Hydrolysis results in the immediate production of methane and carbon dioxide. In this model, pH inhibition, free ammonia inhibition and inorganic nitrogen inhibition are left out of the model as well.

The resulting Gujer-Petersen matrices can be found in the Github link in Appendix C Both the influent and initial conditions are converted with these matrices for each simplification, to ensure all COD is still converted. The resulting models are used for simulation of the BSM2, to test the influence of simplification on biogas production. For this, the model will simulate digestion at 35°C for 200 days to reach steady state, and final biogas production will be compared.



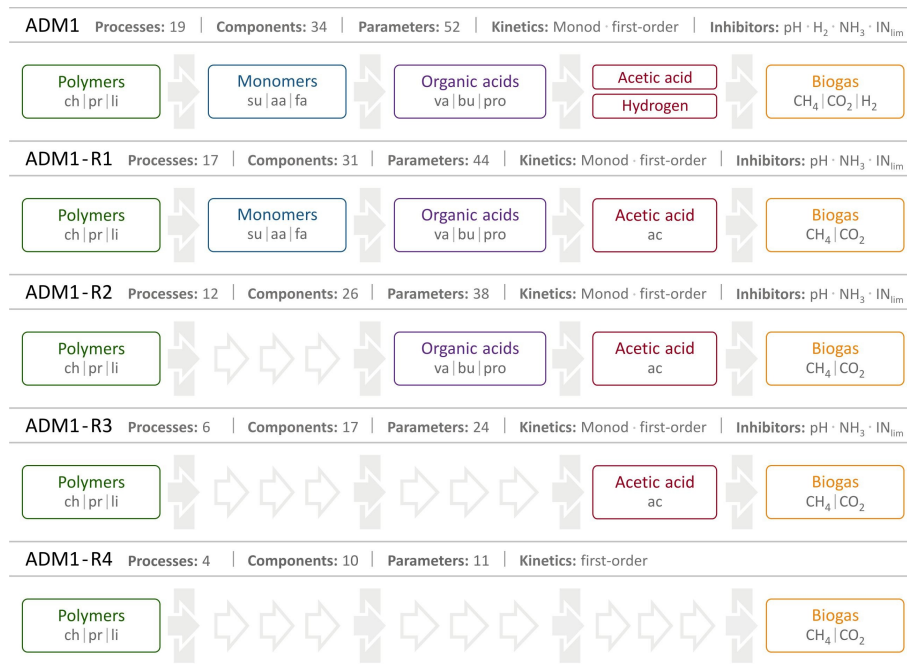


Figure B.1: Systemic simplification of the ADM1, method and figure taken from Weinrich and Nelles [102]

The simplifications of the ADM1 according to the method of Weinrich and Nelles [102] gave 5 models. These have been compared to the BSM2 using the DAE implementation with the Radau solver, and the results are shown in Figure B.2

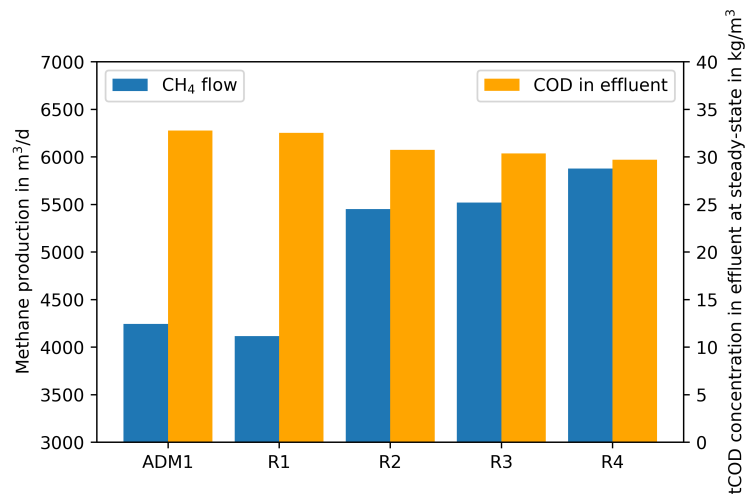
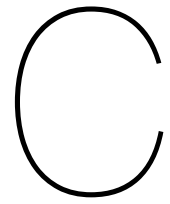


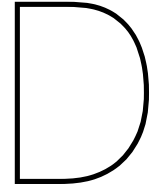
Figure B.2: Yearly methane productions and COD effluent concentrations on simulation with the BSM2 initial and influent values of different simplifications.

Figure B.2 shows that the difference in methane production and effluent COD is quite small between the original ADM1 and the R1 simplification. However, in simplifications R2, R3 and R4, the amount of methane produced is increased by around 50 % and effluent COD concentrations lower as well. This increase comes from the shorter degradation pathway, allowing for fuller digestion for a given HRT. In order to correct for these differences, it is therefore recommended to lower rate coefficients. A lower rate coefficient can account for the time needed for both its own as the removed conversion in the simplification. However, calibration of these rate coefficients was deemed outside the scope of this study. If successive research finds these parameters, a simple yet powerful model could be created for simulation of the anaerobic digestion process.



Code metadata

Code version used in this thesis	1.0
Python version	3.8.8
Link to code repository	https://gitlab.tudelft.nl/amoradvandi/adm1-ht
Support email	S.H.Heegstra@student.tudelft.nl



Biochemical fractionation for high sCOD substrate

As the results of the biochemical fractionation method deviated from expected values, a critical reconsideration of the used equations has been done. It was found that the used equations are not fitted for substrates that mostly consists of sCOD, like the wort and the MNR influent and effluent. Therefore, a proposal is done for new equations for such substrates. The proposal is the replacement of equations 3.14 till 3.19 with equations D.1 till D.6. This fractionation assumes equal ratios and biodegradability of macro nutrients between the particulate and soluble fraction of the substrate. If clarification about the difference in between the particulate and soluble fractions is desired as well, then the macro nutrient tests should be done twice after substrate filtration, once for the filtrate and once for the residue. This is advisable for substrates with between 20 and 80 % soluble COD. For other fractions, the original equations of Arnell et al. [7] or the equations as depicted here can be used, respectively.

$$S_{su} = C_{ch} f_d \frac{sCOD}{tCOD} \quad (D.1)$$

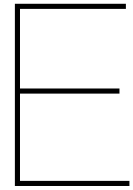
$$S_{aa} = C_{pr} f_d \frac{sCOD}{tCOD} \quad (D.2)$$

$$S_{fa} = sCOD f_d - S_{su} - S_{aa} - tVFA \quad (D.3)$$

$$X_{ch} = S_{su} \frac{(pCOD f_d)}{sCOD f_d} \quad (D.4)$$

$$X_{pr} = S_{aa} \frac{(pCOD f_d)}{sCOD f_d} \quad (D.5)$$

$$X_{li} = pCOD f_d - X_{ch} - X_{pr} \quad (D.6)$$



Other considerations for La Trappe

- It is known that a sulphur containing coagulant is used in the DAF system before the belt-thickener, and that sulphur is present in the detergents used for bottle cleaning. This sulphur therefore ends up in the WAS, and will be introduced to the digester. Sulphur will reduce methane production and hydrogen sulfide in the biogas can corrode equipment [108]. solutions will need to be found to prevent or deal with this. For example, the coagulant used in the DAF system can be replaced with a bio coagulant [57], or sulphate can be scrubbed after anaerobic digestion [73].
- In the simulations, the operation and effluent concentrations of the WWTP at La Trappe were assumed to be steady over time. However, it is known that a weekly discharge of the cheese factory effluent is present in the same system. This can be an asset, if nitrogen is limited in the digestion if, for example, low amounts of WAS is available. However, it could also be a liability, if high levels of free ammonia are already present in the digester when only WAS and urine are available. The co-digestion with this source should therefore be investigated.
- It was assumed in the simulation that the bulk liquid in the digester is completely mixed at all times. The settling of suspended solids in the digester is ignored and temperature gradients over digester depth are assumed to be non-existing. However, these phenomena will occur in the digester and will have negative effects on the biogas production. This can be prevented by installing a mixer in the digester. Because the model could not quantify the effect of such a mixer, no recommendations are given on its installment, but consideration is recommended.